





Recent development for application of functionalized Graphene for CO₂ capture: A review

Raed Muslim Mhaibes^{1,*} , Abdul Amir H. Kadhum² , Taif Abdulhasan³,
Mustafa Mudhafar^{4,5} , Qais R. Lahhob⁶ , Guang Shu^{7,*} 

¹Department of Biochemistry, College of Medicine, Missan University, Missan, Iraq.

²College of Medicine, University of Al-Ameed, Karbala, Iraq.

³Radiology Techniques Department, College of Health and Medical Techniques, Al-mustaqbal University, Babylon, Iraq.

⁴Department of Medical Physics, Faculty of Medical Applied Sciences, University of Karbala, Karbala, Iraq.

⁵Department of Anesthesia Techniques and Intensive Care, Al-Taff University College, Karbala, Iraq.

⁶Collage of Pharmacy, National University of Science and Technology, Dhi Qar, Iraq.

⁷College of Chemistry and Chemical Engineering, China University of Petroleum, Beijing, China.

*Corresponding authors: Raed Muslim Mhaibes: raadmuslim7@gmail.com, raid.mcm@uomisan.edu.iq

Guang Shu: guangshu163@gmail.com

Review Paper

Received:

13 December 2024

Revised:

12 March 2025

Accepted:

15 March 2025

Published online:

16 March 2025

© 2025 The Author(s). Published by the OICCP Press under the terms of the [Creative Commons Attribution License](#), which permits use, distribution and reproduction in any medium, provided the original work is properly cited.

Abstract:

The rising levels of carbon dioxide (CO₂) in the atmosphere present a serious challenge to global climate stability, highlighting the urgent need for effective carbon capture technologies. Among the various materials investigated for CO₂ capture, functionalized graphene has shown considerable promise due to its remarkable characteristics, such as a high surface area, robust mechanical properties, and adjustable chemical functionalities. This review article offers a thorough examination of the latest developments in the use of functionalized graphene for CO₂ capture, focusing on its improved adsorption capacity, selectivity, and reusability. We explore innovative methods of functionalization, the combination of functionalized graphene with advanced materials like metal-organic frameworks (MOFs) and zeolites, and the critical role of environmental and economic sustainability in the advancement of these materials. Additionally, we stress the importance of real-world applications and pilot studies to evaluate the practical feasibility of functionalized graphene in industrial contexts. By consolidating current research and outlining future pathways, this paper seeks to aid ongoing initiatives aimed at combating climate change through effective CO₂ capture methods, ultimately facilitating the shift towards a sustainable low-carbon economy.

Keywords: CO₂ capture; Graphene; Functionalization; Catalyst; Environmental chemistry

1. Introduction

The rising levels of carbon dioxide (CO₂) in the atmosphere, largely credited to human activities like the burning of fossil fuels, deforestation, and various industrial operations, have emerged as a major factor in climate change [1]. As a powerful greenhouse gas, CO₂ is instrumental in the planet's warming, resulting in detrimental environmental consequences such as increased sea levels, severe weather patterns, and disruptions to natural ecosystems [2, 3]. This urgency for effective mitigation strategies has led to a growing interest in carbon capture and storage (CCS) technologies. These approaches focus on capturing and storing CO₂ emis-

sions at their source, thereby preventing their release into the atmosphere and their contribution to global warming [4, 5]. Figure 1 represents a closed loop aimed at reducing atmospheric CO₂ levels while promoting the creation of useful products through innovative technologies. The significance of CO₂ capture goes beyond merely combating climate change; it also supports the shift towards a more sustainable energy landscape [6]. By incorporating CO₂ capture technologies into current industrial practices and energy generation systems, we can greatly diminish emissions while ensuring energy production and economic viability [7, 8]. Furthermore, innovations in CO₂ utilization, which involve transforming captured CO₂ into valuable

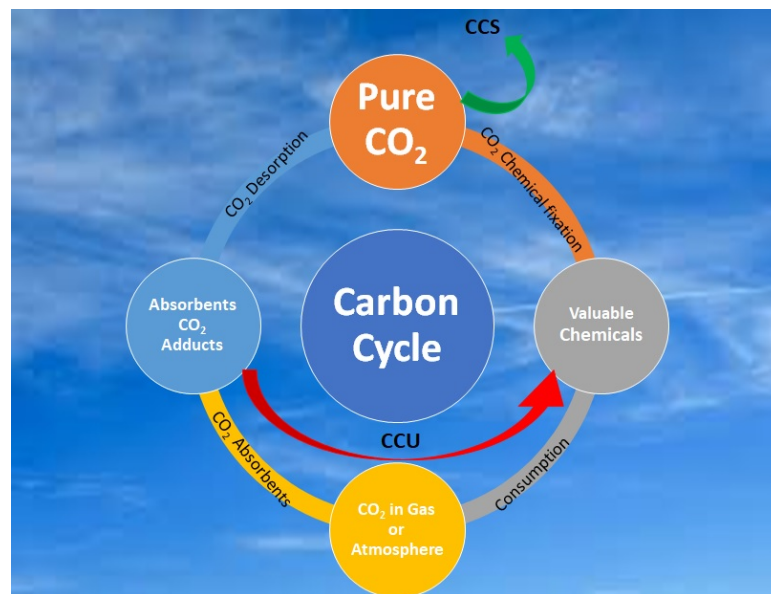


Figure 1. Carbon cycle and role of CO₂ capture.

products like fuels, chemicals, and construction materials, offer additional avenues for resource recovery and economic growth [9–11]. As global initiatives to reach net-zero emissions gain momentum, CO₂ capture and storage will be essential in achieving climate objectives and promoting a sustainable, low-carbon economy [12].

Background of CO₂ capture technology

Carbon capture technology has emerged as a viable approach to mitigate atmospheric carbon emissions [13–15]. This innovative solution addresses a significant challenge confronting the world: the increase in global temperatures. Carbon capture, utilization, and storage (CCUS) involves the extraction of CO₂ from diverse sources, including power generation facilities, industrial plants, and natural gas processing sites [17]. Once captured, the CO₂ can be transported and securely stored in underground geological formations. Numerous methods exist for capturing carbon and tackling the issue of global climate change, with the ten most effective strategies outlined below [18, 19] I) *Direct Air Capture (DAC)*: DAC technology employs air filtration systems to extract CO₂ directly from the atmosphere. Once the CO₂ is captured, it is concentrated and subsequently transported for either conversion or storage into valuable target products. Although still in its nascent phase and associated with high costs, DAC presents significant promise for reducing atmospheric carbon emissions as research and development progress [20]. II) *Carbon Capture at Power Plants*: This technology focuses on capturing carbon emissions produced by power plants prior to their release into the atmosphere. The captured CO₂ is compressed and then either stored or utilized for enhanced oil recovery. Despite certain limitations, this method is now the most prevalent form of carbon capture technology, and its widespread implementation can play a crucial role in lowering carbon emissions [21]. III) *Enhanced Rock Weathering (ERW)*: Enhanced Rock Weathering (ERW) involves the application of rocks, and crushed silicate minerals such as glauconite, to

soil and basalt. This process accelerates the natural weathering that typically occurs over extensive time frames, thereby increasing the amount of CO₂ sequestered in the soil. A key advantage of this approach is its efficiency and cost-effectiveness, as it also contributes to improved soil fertility [22]. IV) *Aqueous Amine-Based CO₂R Capture*: This approach utilizes amines to capture CO₂ from industrial method before it is emitted into the air. The CO₂ is subsequently isolated from the amine and moved for either reuse or storage. While this approach is well-established, it does face challenges, involving significant energy utilization and high operational costs [23, 24]. V) *Membrane Gas Separation*: Membrane gas separation method employs permeable substances to isolate CO₂ from other gases. Its operation at low pressures and temperatures makes it both economically viable, and energy-efficient. Although still largely experimental, this technology shows significant potential for the CO₂ capture, separation, and storage of CO₂ [25]. VI) *Carbon Capture and Conversion*: This approach focuses on the capture CO₂ and providing of CO₂ into valuable products, including fuels, industrial chemicals, and polymers. While it is still in the early steps of development, carbon capture and conversion represent a sustainable method for minimizing carbon emissions while generating useful materials [26]. VII) *Bioenergy with Carbon Capture and Storage (BECCS)*: BECCS captures CO₂ produced during biomass energy generation and stores it effectively. This method not only mitigates emissions but also provide electricity, resulting in a carbon-negative outcome. As a low-carbon energy source, BECCS has the potential to significantly aid in the decarbonization of the economy [27]. VIII) *Chemical Looping*: This method utilizes particles of metal in a reaction with CO₂. The metals serve as catalysts, facilitating the separation of CO₂ from the fuel. Following this, the captured CO₂ is stored while the fuel remains available for further combustion. Although still in the experimental phase, chemical looping technology displays promise in decreasing carbon emissions from industries that heavily

depend on fossil fuels [28]. IX) *Cryogenic Carbon Capture (CCC)*: CCC is an emerging carbon capture method that utilizes cryogenic cooling to extract and eliminate CO₂ from gas streams. It offers a higher extraction rate compared to traditional systems and allows for the storage of CO₂ at a reduced volume. While its applications are currently limited, the technology has significant potential for reducing carbon emissions as it continues to develop [29]. X) *Carbon Capture Utilizing Nanotechnology*: This approach uses nanomaterials, like carbon nanotubes, to effectively store, and capture CO₂ at significantly lower pressures compared to traditional methods [30]. It requires fewer resources and energy while generating less waste than other carbon capture methods. Although the application of nanotechnology in carbon capture is still in the experimental phase, it shows considerable potential for efficiency, and scalability. Each of these methods presents unique challenges and advantages, making them more or less suitable for various applications. Nonetheless, they share a common goal: to serve as vital tools in mitigating the emission and concentration of greenhouse gases, which pose a significant threat to humanity's long-term survival.

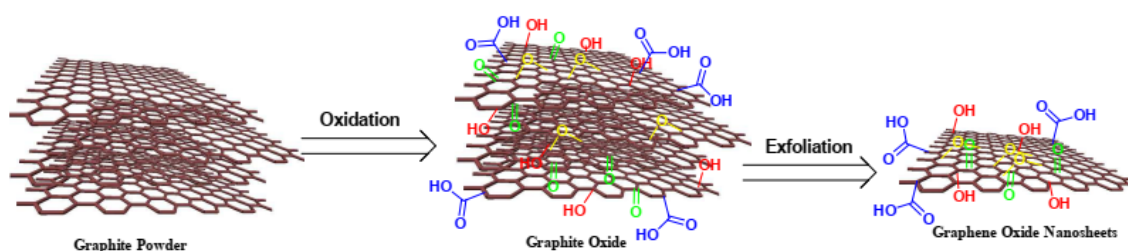
Recent developments in CO₂ capture technology have become essential in combating climate change, particularly through the creation of various catalytic materials that improve the efficiency of CO₂ absorption and conversion processes. Traditional CO₂ capture techniques, which often depend on chemical absorption with amines, are increasingly being enhanced or replaced by advanced catalysts capable of selectively transforming CO₂ into worthwhile products such as chemicals, polymers and fuels, [31–33]. These catalysts, which may include metal-organic frameworks (MOFs) [34], zeolites [35], and bio-inspired materials [36], exhibit superior performance in selectivity, reaction rates, and energy efficiency, positioning them as promising solutions for lowering atmospheric CO₂ concentrations. The investigation of novel catalytic methods not only seeks to enhance CO₂ capture efficiency but also plays a significant role in fostering a circular carbon economy. By optimizing the use of captured CO₂, these innovations convert a detrimental waste product into valuable resources, addressing both environmental and economic issues. Furthermore, ongoing research in this area aims to improve the stability and scalability of these catalytic systems for industrial applications [37–39]. As countries work towards achieving ambitious climate goals, leveraging these cutting-edge catalytic techniques will be crucial for enabling large-scale CO₂ capture and conversion, ultimately aiding global decarbonization

initiatives. In recent years, several significant review articles pertaining to CO₂ capture technology have been examined [40–45].

Functionalized graphene for CO₂ capture

Monolayer graphene, often referred to as pure graphene, can be understood as a single layer of graphite that has been successfully isolated and consists exclusively of sp^2 hybridized carbon atoms [46, 47]. Its structure resembles a network of interconnected benzene rings. Consequently, a graphene sheet serves as the essential building block of graphite. The sp^2 bonding present in graphene contributes significantly to its advantageous physicochemical properties, rendering it a preferred material for a wide range of applications [48–50]. Nevertheless, a significant limitation to the broader adoption of graphene lies in the challenges associated with its synthesis. Due to its atomic thickness, developing a synthesis method that yields defect-free graphene has proven to be a formidable task for researchers over the years. Oxygenated functionalities are incorporated into the graphite structure as illustrated in Scheme 1 [16].

Functionalized graphene presents a highly effective solution for CO₂ capture, attributed to its substantial surface area, remarkable adsorption capabilities, and adjustable chemical characteristics [51–53]. The advantages of employing functionalized graphene for CO₂ capture are as follows: I) *Enhanced Adsorption Capacity*: The extensive surface area of graphene facilitates the capture of significant amounts of CO₂, positioning it as a powerful material for lowering greenhouse gas levels. II) *Targeted Adsorption*: Through functionalization, graphene's ability to selectively adsorb CO₂ over other gases is improved, thereby increasing the efficiency of capture methods and broadening its applicability. III) *Reusability*: Functionalized graphene can frequently be regenerated for multiple cycles of CO₂ capture, offering a sustainable alternative with reduced long-term operational expenses. IV) *Adaptability*: The introduction of various functional groups allows for the customization of graphene's properties, enabling it to be optimized for specific capture scenarios, such as extracting CO₂ from industrial emissions or the atmosphere. V) *Lightweight and Durable*: The combination of mechanical strength and lightweight properties of graphene materials allows for seamless integration into existing systems without significant weight addition or the need for extensive alterations. The application of functionalized graphene for CO₂ capture merges efficiency with adaptability, representing a promising strategy for addressing climate change and fostering sustainability. Figure 2



Scheme 1. Depiction of graphite, graphite oxide, and graphene oxide [Royal Society of Chemistry, copyright 2017, with permission] [16].

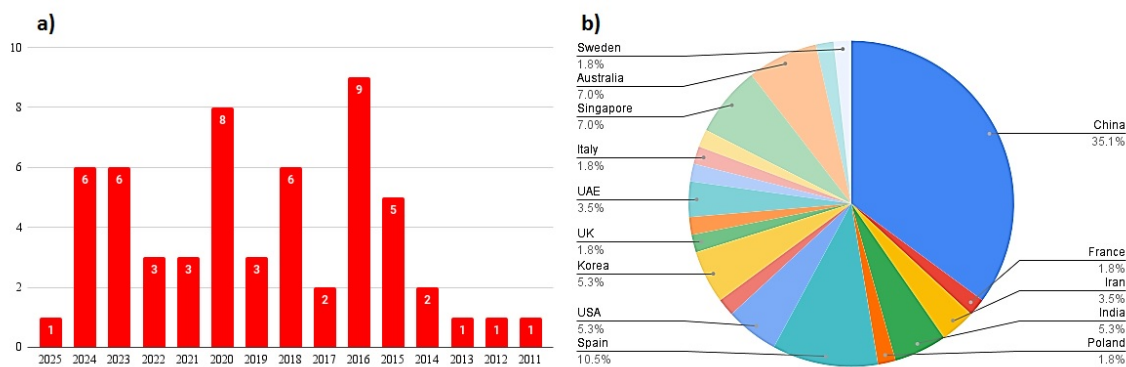


Figure 2. Meta-analysis of published original research paper (a) Number of published papers between 2025-2011 (b) distribution of published papers in different countries.

shows more information regarding to the number of published papers between 2025 – 2011 and distribution of published papers in different countries.

Literature review on functionalized graphene for CO₂ adsorption

The distinctive attributes of atomically thin graphene sheets, such as their chemical stability, highly specific surface area, exceptional selectivity, and adjustable adsorption properties, render them a highly promising material for CO₂ capture applications [55–57]. The process of CO₂ adsorption can take place through multiple mechanisms, notably physisorption and chemisorption [59, 60]. Physisorption is characterized by its reversible nature and dependence on temperature and pressure conditions [61, 62]. This mechanism involves relatively weak interactions between CO₂ molecules and the graphene surface, primarily mediated by van der Waals forces [63–66]. Additionally, the affinity for CO₂ in physisorption can be affected by the surface area and porosity of the adsorbent material. Chemisorption, in contrast, entails a chemical interaction between CO₂ and the molecules that have been introduced onto the graphene surface via various modification techniques. The interaction between CO₂ molecules that are chemisorbed on the graphene surface tends to be more robust and less reversible than that of physisorbed CO₂. Researchers are currently investigating a range of approaches to leverage the capabilities of graphene

and functionalized graphene, which encompasses the creation of surface-microporous graphene [51, 52, 68, 69].

In 2025, Navik et al. introduced a sustainable and rapid one-step N₂/H₂ plasma treatment method aimed at producing graphene-based sorbent materials with improved CO₂ adsorption capabilities [54] (figure 3). This plasma treatment effectively enriches amine species, enhances surface area, and optimizes textural characteristics. The CO₂ adsorption capacity was found to increase from 1.6 to 3.3 mmol/g for flue gas capture and from 0.14 to 1.3 mmol/g for direct air capture (DAC). Notably, the electrothermal properties of the plasma-modified aerogels were improved significantly, resulting in faster heating rates and an almost 5-fold decrease in energy consumption compared to conventional external heating sorbent regeneration methods. The modified aerogels showed selectivity enhancements of 42 and 87 after plasma treatment times of 5 and 10 minutes, respectively. Moreover, the plasma-treated aerogels showed high stability, where only a 17% to 19% capacity loss was observed after 40 cycles of adsorption and desorption. Treatment of adsorbent materials with N₂/H₂ plasma treatment is expected to reduce energy costs and help mitigate adverse impacts on the world economy due to global climate change.

In 2024, Khadiri et al. successfully synthesized highly porous xerogel beads of CS@HKUST-1 through an in-situ growth approach under mild conditions [58]. It emphasized the manipulation of the molar ratio of n(NH₂) to n(Cu) (fig-

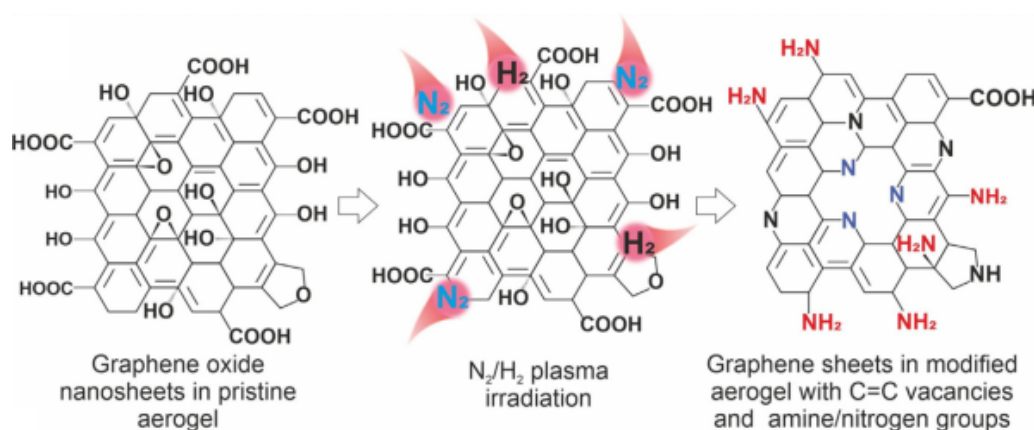


Figure 3. Rapid one-step N₂/H₂ plasma treatment method using graphene-based sorbent materials [Elsevier, copyright 2025, with permission] [54].



Figure 4. CS@HKUST-1[n(NH₂):n(Cu)] xerogels. From left to right: CS@HKUST- 1[2:1], [1:1], [1:2], and [1:3]. [Elsevier copyright 2024, with permission] [58].

ure 4) and the synthesis temperature, since both parameters played a crucial role in determining the specific surface area and crystalline integrity of the synthesized materials. It was observed that lower temperatures were favorable to obtain a pure HKUST-1 phase embedded in the CS matrix, which enhanced the surface area. Due to the moisture sensitivity of HKUST-1, graphene oxide was incorporated under optimal conditions to generate highly porous CS-GO@HKUST-1 composites with surface areas as high as 878 m²/g and significantly enhanced water stability compared to unmodified HKUST-1 and CS@HKUST-1. Investigations of nitrogen adsorption showed that 45% of the original textural properties were maintained after a two-day immersion of CS-GO@HKUST-1 in water, whereas the microporous structure of CS@HKUST-1 fully collapsed with a 94% reduction in SBET after just one day. In addition to improving the chemical stability, graphene oxide also had a beneficial effect on the mechanical stability of the beads. The CO₂ sorption performance of the composites was evaluated and an average uptake of 2.68 mmol/g at 298 K and 1 bar was obtained for CS@HKUST-1 beads, which showed stable performances over more than 10 cycles of adsorption-desorption. Further comparative studies on CO₂ sorption in humid conditions should be performed to understand thoroughly the role of graphene oxide in the stabilization of HKUST-1 framework. In 2024, Safaei et al. examined how different graphite oxidation conditions influence the hierarchical porous structure of graphene aerogel for CO₂ adsorption [72]. The researchers found that a graphene aerogel, which exhibited high meso and micro surface areas, as well as the highest Sm/ST ratio

(micro surface area divided by the sum of micro and meso surface area) of 33%, was synthesized by using a large amount of H₂SO₄ in the oxidation process. This configuration gave an optimum CO₂ adsorption capacity of 1.72 mmol/g. Furthermore, the higher H₂O₂ concentrations favored the formation of macropores in the aerogel matrix and, as a consequence, improved the Sm/ST ratio as well as the CO₂ adsorption capacity. In contrast, higher KMnO₄ concentration led to a lower Sm/ST ratio, fewer macropores, and reduced CO₂ adsorption capacity to 1.04 mmol/g.

In 2024, Yang et al. introduced ultra-thin mixed-matrix membranes (MMMs) made from polyether-block-amide (Pebax) that incorporated graphene oxide (GO) [67]. They emphasized controlling the interlayer channels to improve the separation performance of CO₂ from N₂. They systematically investigated different membrane preparation parameters, such as the lateral size of GO nanosheets, the usage amount of GO, and thermal reduction conditions like temperature and time. The results indicated that the well-regulated interlayer channels of GO nanosheets promote fast CO₂-selective transport by coupling the effects of size sieving and preferential adsorption. The GO/Pebax ultra-thin MMMs showed a very high CO₂/N₂ selectivity of 72 and a high CO₂ permeance of 400 GPU (1 GPU = 106 cm³(STP)•cm²•s⁻¹•cmHg⁻¹), which represents a good candidate for CO₂-capture applications (figure 5).

In 2024, Jha et al. developed a monolithic adsorbent based on graphene oxide through a self-assembly method (figure 6), followed by reduction with oxalic acid at various mass ratios and activation via UV treatment [70]. The mod-

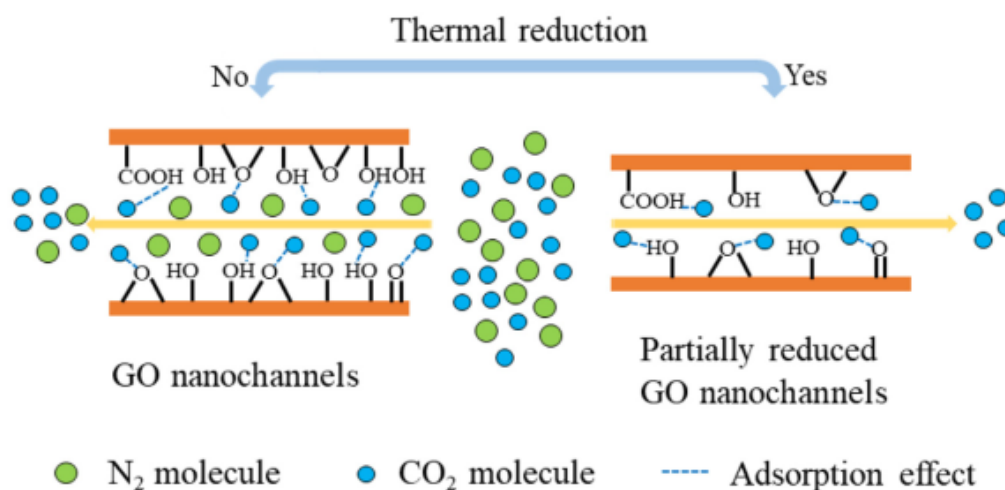


Figure 5. The suggested mechanism CO₂ separation on the GO nanochannels [Elsevier copyright 2024, with permission] [67].

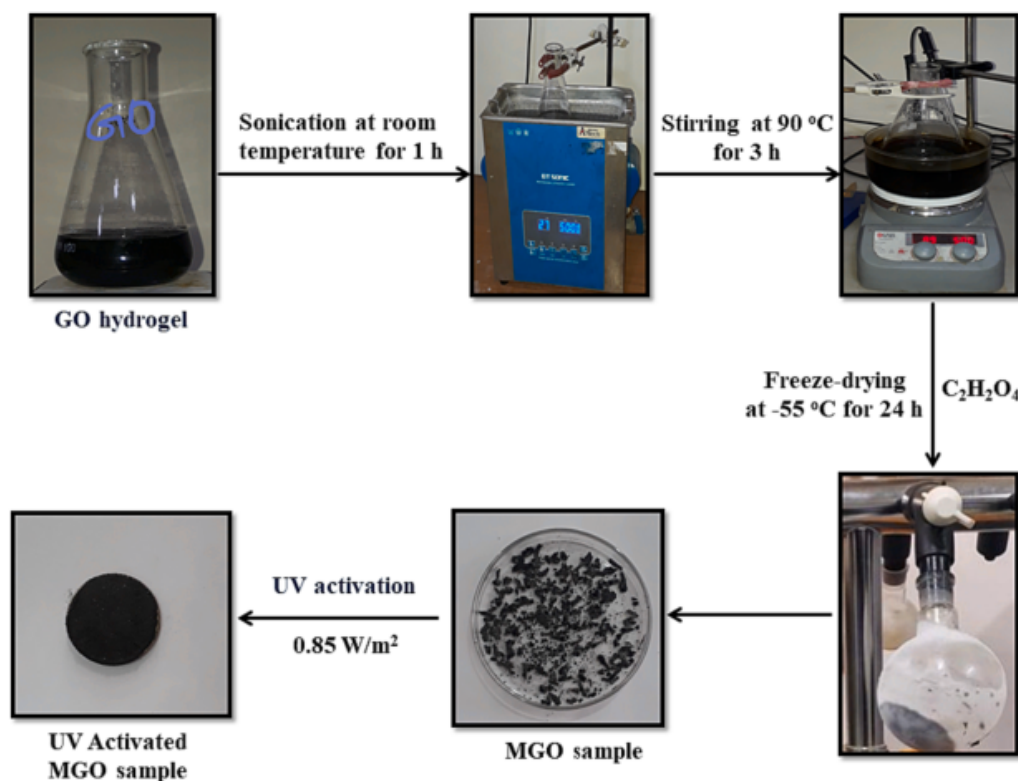


Figure 6. The chemical approach of the monolithic graphene oxide-based adsorbents. [Elsevier copyright 2024, with permission] [70].

ified adsorbent displayed a remarkable dynamic capacity of 1.65 mmol/g at 25 °C for CO₂ capture and this may be attributed to its high BET surface area of 577.3 m²/g. During desorption, the observation of a fixed volumetric flow rate revealed that lowering the pressure led to an increase in the consumption of the desorbing gas (N₂) of almost 50% over the course of regeneration. Numerous characterizations were conducted, demonstrating 98.8% regenerability, high CO₂/N₂ selectivity, rapid kinetics, and perfect agreement with both the Freundlich isotherm model and the pseudo-second-order kinetic model. Thermodynamical analyses pointed out that the adsorption sites were heterogeneous and the adsorption process was endothermic with $\Delta H^0 + 13.1154139$ kJ/mol, which underlines some particular characteristics of chemisorption.

In 2024, Zhang et al. highlighted the potential of graphene oxide (GO) membranes for selective CO₂ adsorption over N₂, attributed to their carboxyl groups, which makes them suitable for capturing CO₂ from flue gases [71]. However, insufficient carboxyl content, the flexibility of nanosheets, and dense layering of materials restrict their N₂/CO₂ selectivity, pressure resistance, and permeability. In this study, a new strategy is presented by incorporating a unique sub-nanometer framework structure in graphene oxide membranes through in-situ synthesis of ZIF-8 nanocrystals. This approach simultaneously infiltrated the precursors of zinc nitrate and 2-methylimidazole to both sides of the membranes, which remarkably improved the CO₂ capture capacity as well as pressure stability for the resultant ZIF-8@GO composite membranes (figure 7). Moreover, additional cross-

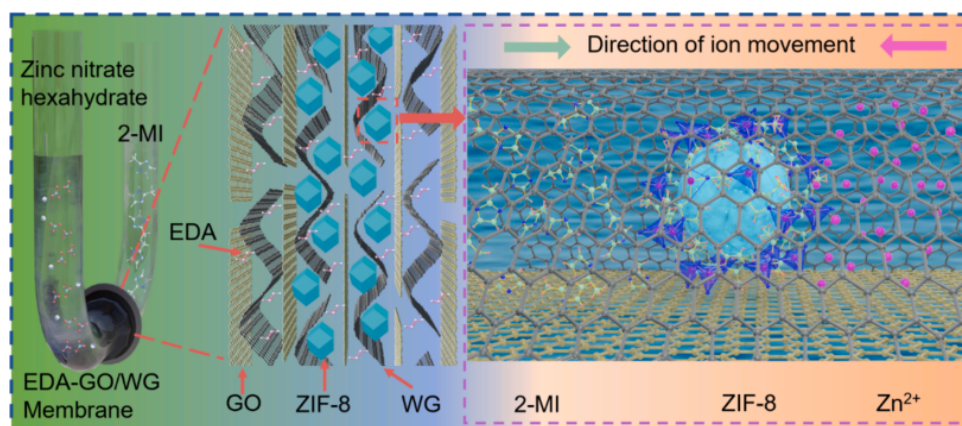


Figure 7. porous ZIF-8@EDA-GO/WG membrane [Elsevier copyright 2024, with permission] [71].

linking with carboxylated wrinkled graphene (WG) and ethylenediamine (EDA) further enhance the CO₂ capture property and provide reinforced porous frameworks to enhance the permeability. Experimental data show that the ZIF-8@EDA-GO/WG composite membranes have excellent permeability, selectivity, and pressure stability. The permeability reaches 1850 GPU at a gas pressure of 0.2 MPa, along with theoretical selectivity for N₂/CO₂ single-gas and separation factors for mixed gases of 18.3 and 32.3, respectively; these values are far better than those of the traditional GO membranes (3 GPU, 1.1, and 1.2). Under high air pressure conditions-1.2 MPa-the composite membranes still retain a theoretical selectivity of 13.4. This approach toward the design of CO₂ capture membranes not only realizes the development of efficient membranes but also plays a part in cutting down CO₂ emissions from flue gases to battle global warming.

In 2024, Saha et al. conducted a study examining the interfacial characteristics of graphene and nickel nanoparticles (Ni-NP) for applications in water splitting and CO₂ capture [73]. The composition of the composite was characterized by techniques such as Raman spectroscopy, which provided information on characteristic features attributed to nickel and graphene. Further proof for the existence of Ni-NP and adsorption of hydroxyl ions during catalysis was given by UV-vis spectroscopy and analysis by FT-IR spectroscopy. The electrochemical properties were further investigated using scanning electrochemical microscopy, which clarified the role of Ni-NP in redox reactions and the enhancement of interfacial current response at applied potentials. It was found that oxygen vacancies significantly dominated CO₂ adsorption and photocatalytic reduction on the graphene/Ni(OH)₂ interface. Photocurrent measurements and in-situ transmittance evaluations at various wavelengths and potentials revealed a wavelength-dependent photo-response, evidencing the existence of interfacial plasmonic effects. This result explained the photo-induced processes under anodic and cathodic sweeps. A dramatic increase in photocurrent from -5.7 to -11 mA/cm² was observed as a result of CO₂ reduction. Numerical simulations by using COMSOL, which combined electromagnetic theory with photo-electrochemical analysis, further confirmed the experimental results and revealed the importance of localized surface plasmon resonance for high catalytic activity, especially in the 200 – 350 nm illumination range. With the increase in particle size, the catalytic efficiency was shifted to longer wavelengths. In summary, the present research gives important insight into the influence of material characteristics and illumination conditions on the efficacy of graphene/Ni-NP composites, illustrating their prospective utility in catalytic processes and energy transformation applications.

In 2023, Yao et al. highlighted the significant challenges posed by rising CO₂ emissions from fossil fuel combustion, prompting extensive research into CO₂ capture technologies [75]. A big challenge remains in the way of developing membranes with high mechanical properties and high CO₂ adsorption capacity. Herein, a new in situ anodic electrodeposition method is developed for inducing

the growth of HKUST-1 metal-organic frameworks (MOFs) within the two-dimensional (2D) nanochannels of graphene oxide (GO). A tripartite mechanism for MOFs' constrained growth during the electrodeposition has been proposed. By a novel layer-by-layer confinement structural growth approach, MOFs@GO composite membranes with a hierarchical pore structure were successfully prepared. Notably, these membranes showed a CO₂ adsorption capacity of 194.1 cm³/g and an ideal CO₂/N₂ adsorption selectivity of 276.5 at 273 K and atmospheric pressure, owing to the synergistic interaction between nanoconfined HKUST-1 and GO. The electrodeposition method exposes more metal active sites because of the hierarchical porous structures, which enhances CO₂ adsorption performance. Moreover, the incorporation of HKUST-1 into GO nanochannels led to increases of 50.6% in hardness and 138.13% in elastic modulus compared to the pristine GO membrane. This approach presents a promising strategy in the development of high-performance CO₂ capture membrane systems under standard temperature and pressure conditions and might be more applicable to the synthesis of other MOFs@GO composite membranes, including Cu-BDC@GO and Cu-BDCNH₂@GO, due to their fitness for large-scale industrial uses.

In 2023, Barbarin et al. highlighted the significant challenges associated with the separation of CO₂ from N₂ in post-combustion CO₂ capture processes [74]. This difficulty arises mainly from the low concentration of CO₂ (3 – 15%) relative to N₂ (70%). The issue is particularly evident in carbon-based adsorbents, which typically demonstrate low selectivity. This study introduces an effective approach to enhance the selectivity of composite aerogels composed of reduced graphene oxide (rGO) and functionalized polymer particles (figure 8). The CO₂/N₂ selectivity of such aerogels is determined by two crucial factors: surface chemistry, which enhances CO₂ capture sites, and well-controlled microporosity, which generates a molecular sieve effect. Both have been altered in situ in the synthesis process. The resulting aerogels exhibit a dramatic increase in their CO₂ adsorption capacity and a considerable decrease in N₂ adsorption at 25 °C and 1 atm, leading to over tenfold increase in selectivity compared with the starting material. This represents the highest reported level of selectivity for carbon-based adsorbents to date. Detailed characterization of the aerogel surfaces shows that the revised synthesis method leads to an increase in surface oxygen functional groups and a rise in the fractions of micropores (<2 nm) and small mesopores (<5 nm). In addition, profound alterations in the surface topography of the aerogels were noted. The reference materials presented a surface with curved wrinkles around 100 nm in diameter and consequently, the selectivity values between 50 – 100. The newly synthesized aerogels, on the other hand, display better oxidation, that makes them stiffer but less flexible, much alike crumpled paper. The modification, combined with the improved functionalization and increased microporosity, has rendered the aerogels to be mainly N₂-phobic with selectivity values in the range of 470 – 621. This observation gives experimental evidence to the theoretically predicted correlation between the elas-

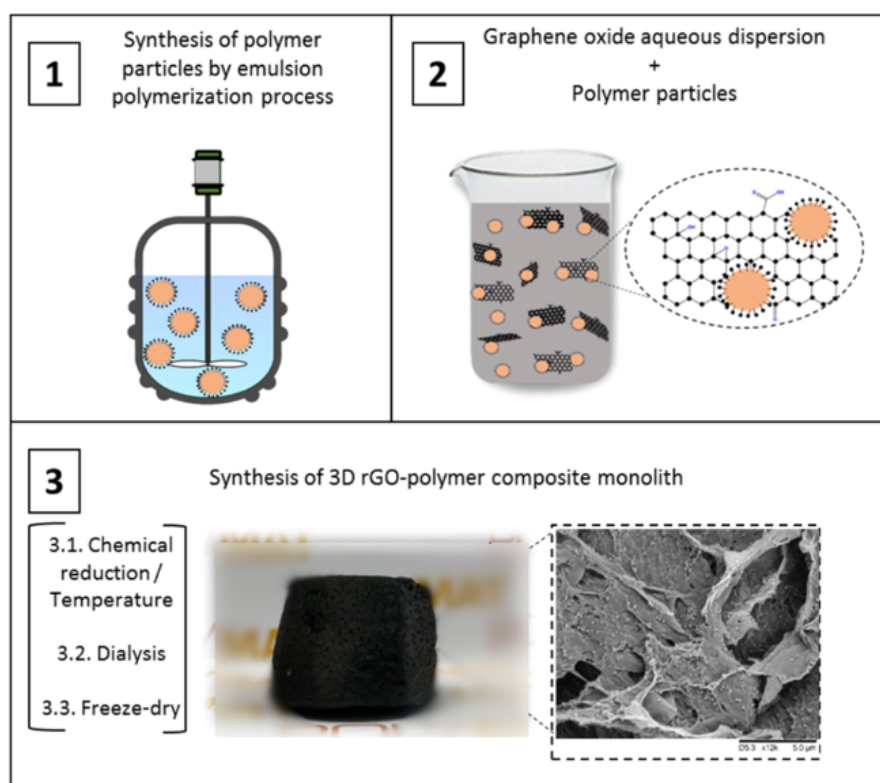


Figure 8. Synthetic route for reduced graphene oxide and functionalized polymer particles [American Chemical Society copyright 2023, with permission] [74].

ticity of graphene-based adsorbents and their effectiveness of selectivity for CO_2/N_2 . It presents a new look toward the concept of N_2 -phobicity. The high performances obtained, which show a CO_2 adsorption capacity of almost 2 mmol/g and excellent selectivity of 620, highlight these composites as very promising candidates for the most favorable CCS applications in the domain of post-combustion technology. In 2023, Pruna et al. introduced innovative dendrimer-modified graphene oxide (GO) aerogels utilizing generation 3.0 poly(amidoamine) (PAMAM) dendrimers through a synthesis method that combines hydrothermal processing with freeze-casting and subsequent lyophilization [76]. Some properties of modified aerogels were evaluated with changes in concentration of dendrimer and incorporation of carbon nanotubes (CNT) in different ratios. Aerogel properties were characterized with the following techniques: SEM, FTIR, Raman spectroscopy, and XPS. The results indicated there was a corresponding relationship between nitrogen content and PAMAM/CNT ratio. The optimum values have been proven. Increasing the concentration of dendrimer at an appropriate PAMAM/CNT ratio improved the CO_2 adsorption capacity of these modified aerogels reaching a maximum of 2.23 mmol/g at a PAMAM/CNT ratio of 0.6/0.12 (mg/mL). These data suggest that CNTs can improve the degree of functionalization and reduction of PAMAM-modified GO aerogels for proper CO_2 capture. In 2023, Liu et al. highlighted the significant role of gas adsorbents in mitigating CO_2 emissions, with GO emerging as a promising two-dimensional material for CO_2 capture due to its high theoretical surface area and the presence of numerous oxygen-containing functional groups on its

nanosheet structure [80]. However, currently, the performance of gas adsorption is quite far from optimal levels because of aggregation and restacking of GO nanosheets which hinder access to the adsorption sites. To overcome this, the researchers developed an 'ionic-crosslinking induced dynamic assembly coupled ice-templating' (IDAI) technique to fabricate a porous three-dimensional GO framework for CO_2 capture. Ionic crosslinking effectively diminishes the aggregation and restacking of GO nanosheets during fabrication of this methodology. The final structure of the 3D GO microstructure can be optimized by variation of the dynamic assembly process using different concentrations of GO. The optimized porous 3D GO adsorbent demonstrated a CO_2 adsorption capacity of 2.24 mmol/g under ambient temperature and pressure with an attractive operational stability due to the strong ionic crosslinking. The technique is amenable to an array of multivalent cations creating a versatile platform for tailoring GO microstructures.

In 2023, Gu et al. highlighted the challenges posed by water molecules in carbon dioxide capture efforts aimed at mitigating global warming. Water can interfere with CO_2 adsorption in various porous sorbents and may also cause irreversible damage to their structures [81]. This research concludes that porous graphene membranes are highly selective and energy efficient as evidenced by their experimental and theoretical work for CO_2 membrane filtration. Information derived from recent studies indicates that water molecules with 2 to 3 layers coats a graphene surface. It is indeed significant for separation processes, as water vapor is usually found in flue gas and in surrounding ambi-

ent air. However, previous theoretical attempts have largely ignored considering water in CO₂ filtration cases. Herein, we present an outcome of an all-atom molecular dynamics simulation showing how a thin layer of adsorbed water molecules on porous graphene affects CO₂ capture and separation from nitrogen. Results reveal that the topology with regard to pore termination-hydrophobic or hydrophilic-can modify the water solvation shell thickness at the pore edge, intensifying selectivity towards CO₂ with respect to N₂, even with pores of significantly larger radius (5 – 15 Å) than CO₂ and N₂. This yields a previously unidentified sieving mechanism at the pore edge, with previous theoretical studies arguing that sieving could only occur in pores of size comparable to the gas molecules themselves. Interestingly, we found that gas transport scales with R1, where R represents the effective pore radius adjusted for the thickness of the water solvation shell, rather than the typical R2 scaling of macroscopic pores.

In 2023, Roy et al. developed a highly effective fabrication method for creating super-expanded freestanding 3D reduced graphene oxide foams (SE-rGO) characterized by an exceptional porous structure and stable geometry (figure 9), which are ideal for capturing CO₂ from the atmosphere and converting it into fuel [77]. Using a template-assisted method, the exfoliation of graphene layers was induced by salicylic acid to prepare 3D SE-rGO foam. The foam was, thereafter, improved for physical and functional properties by thin coating with a polydopamine (pDA). Such structural and morphological characteristics were studied using SEM, XRD, XPS, and TGA. The foam possesses multifunctional properties due to its unique 3D porous design and an appreciably high specific surface area of 767 m²/g, with carbon dioxide adsorption capacity of 4.17 mmol/g and good catalytic support in the hydrogenation of this greenhouse gas into formate. Palladium nanoparticles loaded over the foam exhibited better catalytic activity than the foam alone. Thus, the coated foam achieved 24.3% maximum yield at 120 °C for hydrogenating CO₂ into formate. Therefore, the

present study found that this graphene foam is capable of both CO₂ capture and hydrogenation processes and could act as a good versatile option.

In 2022, Barbarin et al. emphasized the importance of developing efficient adsorbents for the selective capture of CO₂, aiming to minimize secondary pollution and maintain a low carbon footprint [78]. This work has described a technique that is both versatile and robust for generating functionalized 3D porous graphene/polymer monolithic structures via an entirely aqueous self-assembly process (figure 10). During this process, immersion functionalization with waterborne polymer particles occurs spontaneously with functionalized graphene. These are real composites that can manage genetic properties by varying process parameters. The incorporation of polymer particles into the graphene framework significantly enhances the textural features, increasing the number of micropores, because they act as spacers between reduced graphene oxide (rGO) platelets, resulting in increased microporosity, which greatly enhances the performance (especially, selectivity) of CO₂ over N₂ in adsorption and could turn out into a promising alternative technology in post-formation CO₂ capture.

In 2022, Zhao et al. investigated the hybridization of metal-organic frameworks (MOFs) with graphene oxide (GO) to enhance the CO₂ adsorption capabilities of MOFs [79]. However, the precise mechanisms that lead to this improvement are not so well understood. This investigation would thus provide a full analogy that can be used to elucidate CO₂ adsorption and separation processes on GO/CuBTC and GO/UTSA-16, (figure 11) which can facilitate the synthesis of these materials effectively. Here, molecular models emulating the experimentally available hybrid materials were developed and analyzed through molecular simulations. On validation of the above models with existing experimental results, a detailed investigation on the influence of different structural variables was carried out to determine the best hybridization strategy for this application in a predictive way. These findings elucidated that the interface formed between

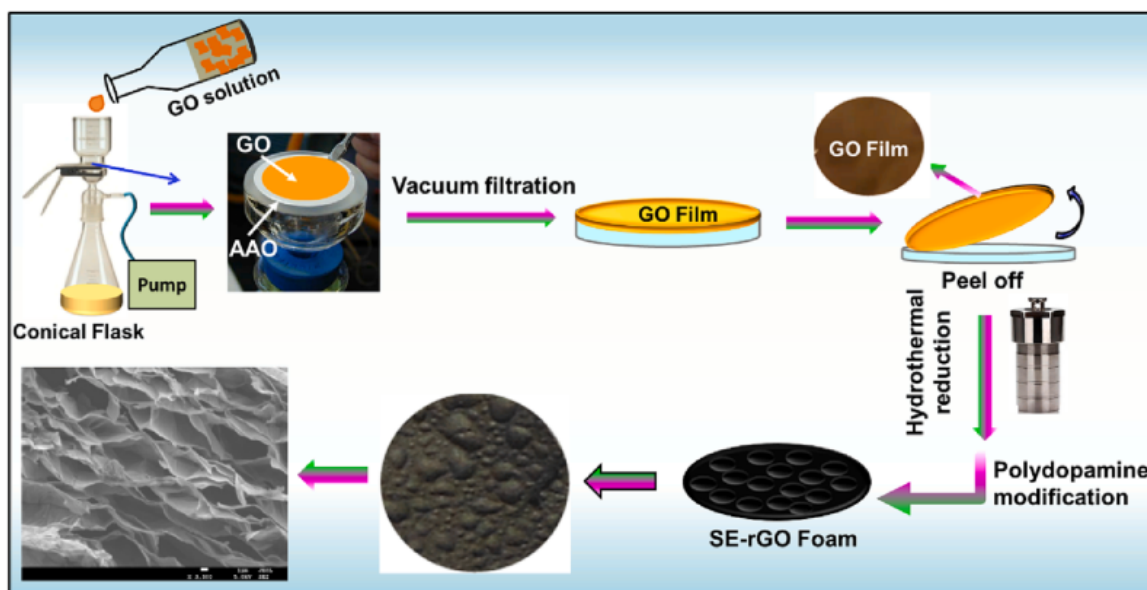


Figure 9. Preparation of 3D SE-rGO foam [Elsevier copyright 2023, with permission] [77].

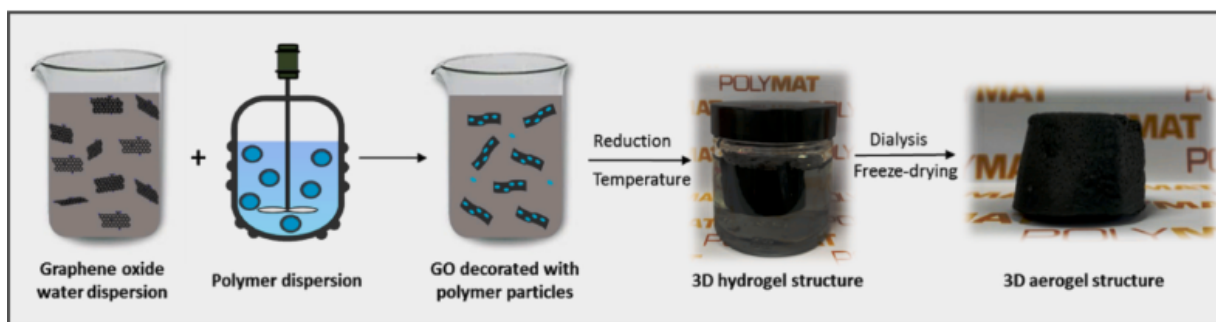


Figure 10. Preparation method of the 3D rGO-polymer monolith composite [Elsevier copyright 2022, with permission] [78].

GO and MOFs caused very strong interaction with CO_2 , which along with reduced pore size improved significantly the adsorption performance at low pressures. In addition, performance for promising hybrid GO/MOF structures on CO_2 separation from nitrogen was predicted by means of Grand Canonical Monte Carlo (GCMC) simulations that considered binary mixture (15 CO_2 :85 N_2) under temperature swing adsorption (TSA) process. Among the different materials and different compositions studied, GO/CuBTC with maximum GO content (65% wt) and without GO stack-

ing gave the most satisfactory results in key performance parameters: CO_2/N_2 adsorption selectivity (120 at 313 K), working capacity (1.794 mmol/g at a desorption temperature of 443 K), and specific energy consumption (0.534 GJ/tonne- CO_2), which is at a par with conventional amine scrubbing methods.

In 2022, Hu et al. highlighted the ongoing global challenge posed by greenhouse gas emissions, emphasizing the need for prioritizing their reduction or control. One effective solution to this issue is the application of mem-

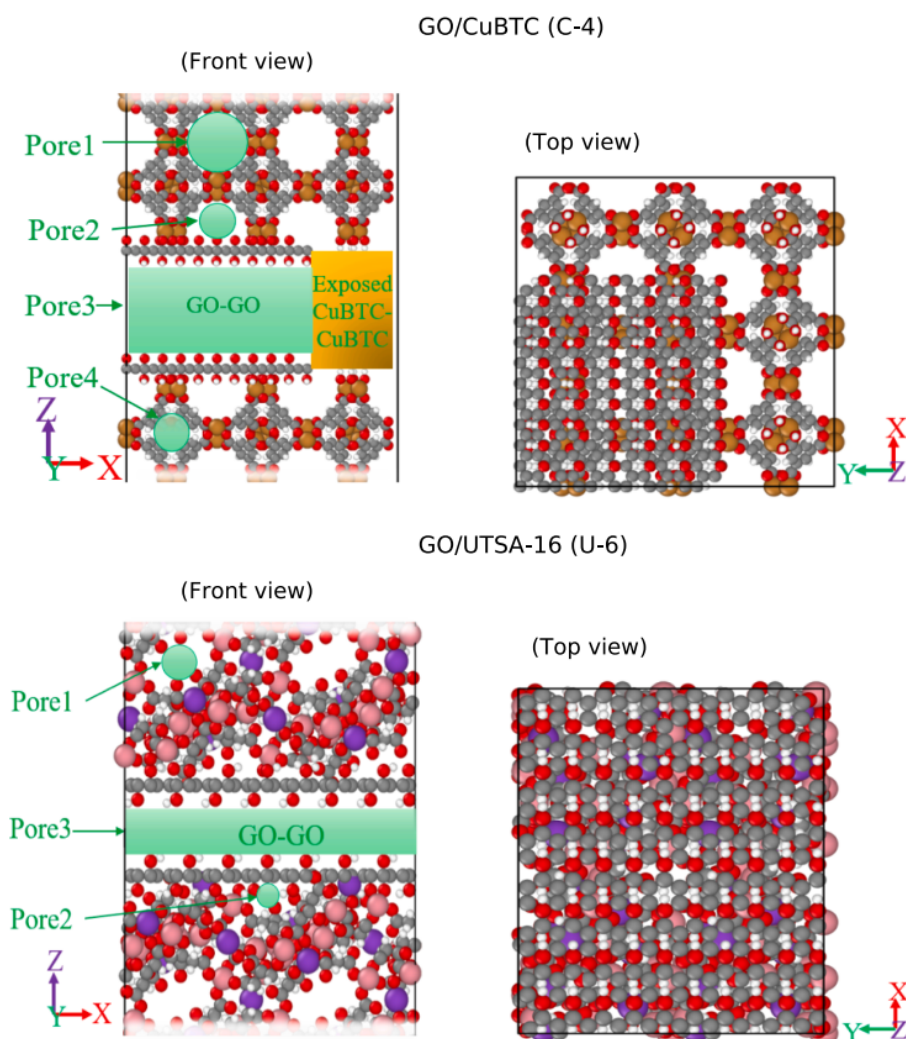


Figure 11. GO/CuBTC and GO/UTSA-16 structures [Elsevier copyright 2022, with permission] [79].

brane separation technology [86]. Mixed matrix composite membrane was developed using poly (dimethylsiloxane) (PDMS)-Pebax MH1657 (Pebax)-graphene oxide modified with 3-(aminopropyl)triethoxysilane (APTES) on polysulfone (PSf) substrate. Hydrophilicity of intermediate layer was improved by UV/O₃ treatments. Varied concentrations of Pebax and APTES-GO were used to study their combination effect on the capture of CO₂. The membrane containing 1 wt% GO showed optimum gas separation efficiency with 54.5 GPU CO₂ permeability and 36.9 CO₂/N₂ selectivity obtained at 35 °C and 0.1 MPa. Further improvement of separation efficiency was realized by using APTES-functionalized GO (aGO). The mixed matrix composite membrane with an addition of 1 wt% aGO increased the CO₂ permeance to 208.9 GPU, with a CO₂/N₂ selectivity of 40 at 35 °C and 0.7 MPa. Amine groups enhanced CO₂ adsorption and selective permeability while improving the stability of the membrane to enable it to work under higher pressure. This work serves to enhance the overall understanding of the functionality of each layer in a gas separation mixed matrix composite membrane.

In 2021, Wang et al. introduced the Mg/DOBDC MOF, which consists of magnesium (II) ions connected by 2,5-dioxido-1,4-benzenedicarboxylate (DOBDC) ligands, as a precursor for creating a new composite material combining Mg/DOBDC MOF and GO, referred to as Mg/DOBDC MOF@GO. The study provided an in-depth analysis of the CO₂ capture capabilities of this newly synthesized Mg/DOBDC MOF@GO composite [82]. The researchers carefully studied how the preparation method, the solvent used for GO, and the GO ratio in the composite affected the results. They also looked closely at the structural changes in the Mg/DOBDC MOF when GO was added. The investigation included an analysis of cyclability, kinetic behavior, and the mechanisms of adsorption. The Mg/DOBDC MOF@GO_w-30, which included 30 mL of GO, reached a maximum CO₂ uptake of 8.60 mmol/g at 0.1 MPa and

25 °C, nearly doubling the capacity of the original Mg/DOBDC MOF (figure 12). This paper not only describes the synthesis and use of the MOF@GO composite for CO₂ capture but also provides a detailed understanding of the adsorption kinetics and mechanisms related to both the MOF and the MOF@GO composite, offering valuable insights for future research.

In 2021, Shen et al. developed a distinctive 3D boron and nitrogen co-doped carbon nanomaterial (B/N-CN) through the carbonization of a blend consisting of orthoboric acid, soybean oil, and melamine [83] (figure 13). The resulting B/N-CN consists of boron and nitrogen co-doped graphene-like carbon nanosheets (BCN) along with hexagonal boron nitride (h-BN) domains, featuring a hierarchically porous structure. This architecture includes erythrocyte-shaped macropores, narrow mesopores, and numerous micropores. The B/N-CN demonstrates superior CO₂ selective capture capabilities compared to the non-boron-doped variant (N-CN). The improved CO₂ uptake and CO₂/N₂ selectivity of B/N-CN can be linked to the abundance of ultramicropores within the hierarchically porous framework and the favorable electrostatic interactions between CO₂ and the adsorption sites on both the BCN nanosheets and h-BN domains.

In 2021, Xia et al. developed porous graphene materials (PGMs) through the activation of thermally exfoliated graphite oxide using CO₂ and KOH [87]. The PGMs activated with CO₂ (CPGMs) have a three-dimensional structure with a hierarchical arrangement of pores, while those activated with KOH (KPGMs) feature a two-dimensional sheet-like structure filled with numerous micropores and small mesopores. By adjusting the activation parameters, we can effectively modify their specific surface areas and pore volumes over a wide range. Furthermore, the synthesized PGMs exhibit varied surface chemistries; CPGMs are rich in quinone and carbonyl functional groups, whereas KPGMs are high in hydroxyl groups. Gas adsorption tests

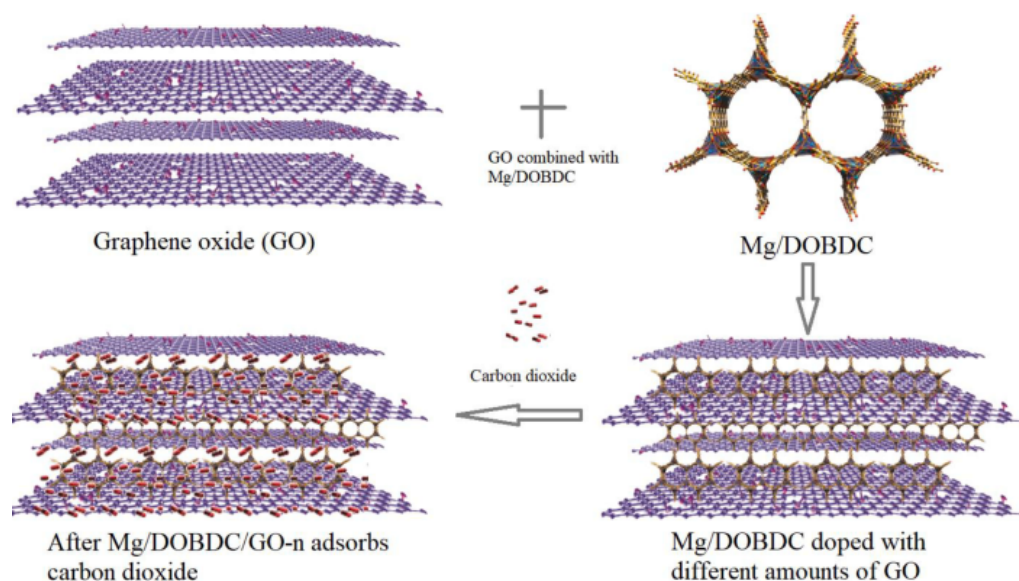


Figure 12. Preparation Mg/DOBDC/GO-n and mechanism of CO₂ adsorption [Elsevier copyright 2021, with permission] [82].

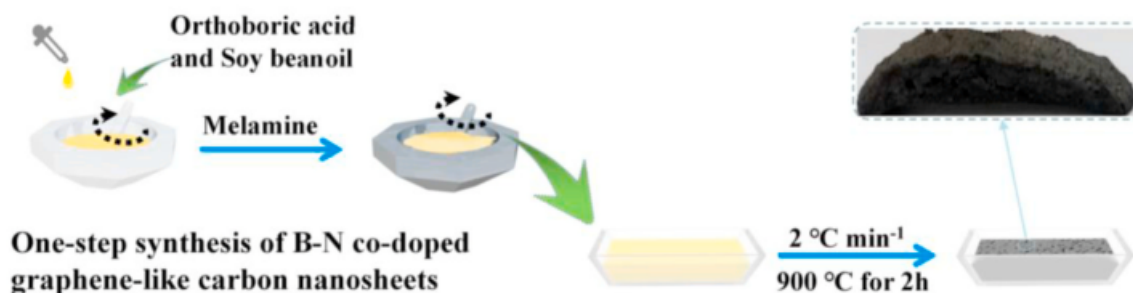


Figure 13. The chemical process for B/N-CNs [Elsevier copyright 2021, with permission] [83].

indicate that the uptake of CO₂ and H₂ by the PGMs is affected by both their pore structure and surface chemistry. Notably, KPGMs-7 achieves the highest CO₂ uptake of 17.87 wt% (4.06 mmol/g) at 273 K and 1 bar, along with an H₂ uptake of 2.41 wt% (11.88 mmol/g) at 77 K and 1 bar (figure 14).

In 2020, Politakos et al. introduced monolithic nanocarbon-based CO₂ solid sorbents that exhibit rapid mass transport, ease of handling, minimal pressure drop, and stable cyclic operation due to their unique interconnected three-dimensional pore network [84]. This study employed a straightforward water-based method to produce graphene-based monoliths by allowing graphene oxide nanoplatelets to spontaneously reduce and self-assemble at mild temperatures (45 – 90 °C). By varying the reaction temperature and the amount of reducing agent (ascorbic acid, AsA), the porous structure of the monoliths was tailored, leading to a range of monoliths with different CO₂ adsorption capacities. The monolith created at the highest temperature with the least AsA exhibited the best specific surface area, porosity, and level of functionalization. As a result, this monolith achieved an impressive CO₂ capture performance of 2.1 mmol/g at 25 °C and 1 atm, placing it among the top performers for CO₂ sorption when compared to similar and untreated materials (figure 15). Its selectivity for CO₂

over N₂ at 25 °C and atmospheric pressure was recorded at 53, showcasing strong potential for real-world applications. However, the monolith did see a decrease in capacity during cyclic operations, likely due to the collapse of smaller pores. This challenge was mitigated by adding a small amount of polymer particles during the one-step synthesis, which significantly improved stability over five adsorption/desorption cycles.

In 2020, Politakos et al. highlighted the progress of polymer composite materials featuring a hierarchical porous structure across various application domains, attributed to their remarkable physico-chemical characteristics [85]. The process of synthesizing these materials is notably energy-intensive and harmful to the environment. This study introduces a novel water-based method for creating monolithic 3D reduced graphene oxide (rGO) composite structures, reinforced with poly (methyl methacrylate) polymer nanoparticles that have been modified with epoxy groups (figure 16). The synthesis utilizes a reduction-induced self-assembly technique carried out under mild conditions. By fine-tuning the reaction parameters and the quantity of polymer used, we were able to alter the textural properties and surface chemistry of the monoliths. Furthermore, the incorporation of the polymer improves the solvent resistance of the composites by forming crosslinks between the polymer and

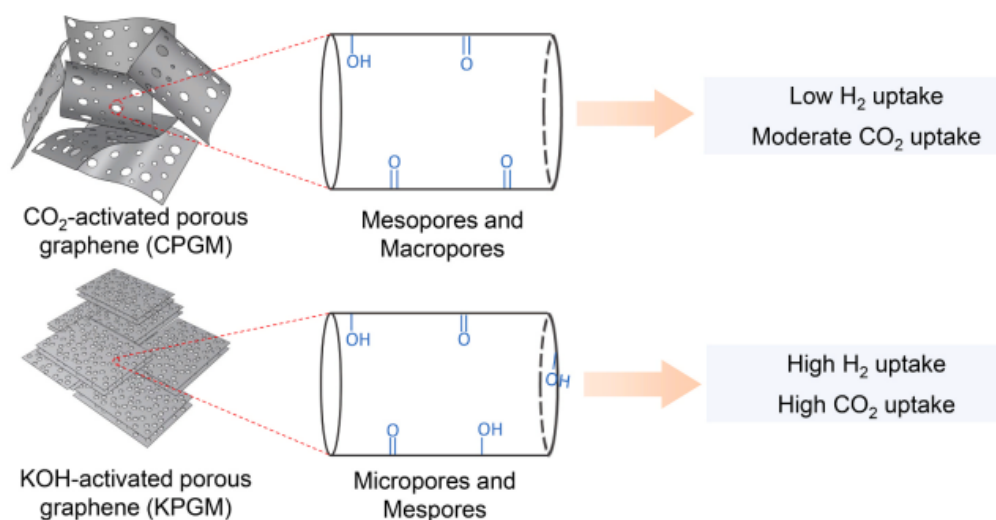


Figure 14. The chemical process for B/N-CNs [Elsevier copyright 2021, with permission] [83].

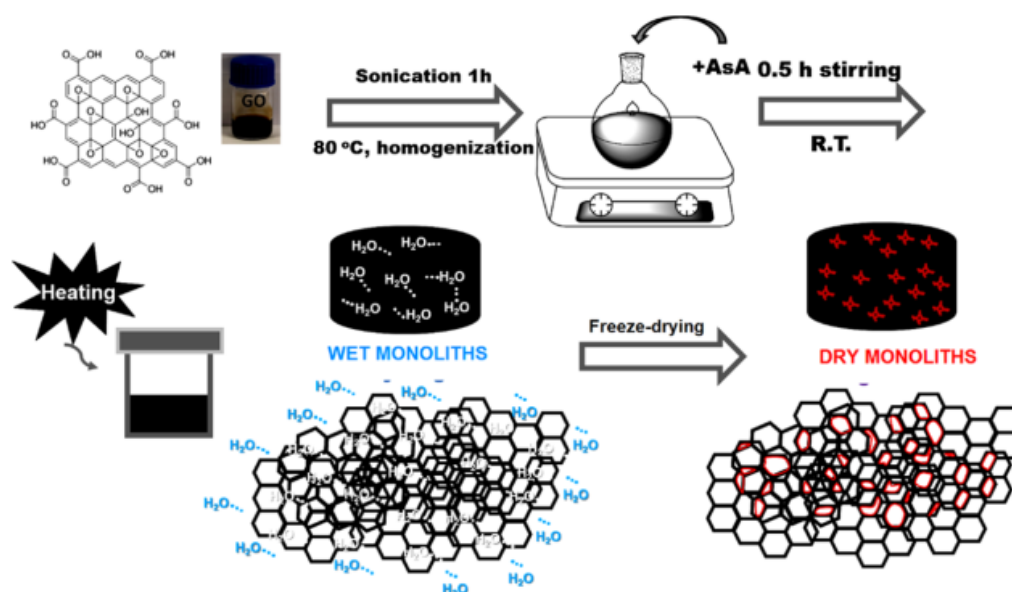


Figure 15. The schematic preparation of graphene-based monoliths [American Chemical Society copyright 2020, with permission] [84].

rGO. They evaluated the monolithic composites for their capacity to selectively capture CO₂. A crucial balance between specific surface area and the level of functionalization was found to be vital for achieving high CO₂ capacity and CO₂/N₂ selectivity. The amount of polymer used affects the textural properties; decreasing the polymer quantity leads to an increase in specific surface area and functional groups, which in turn enhances CO₂ capture capacity, with maximum values observed between 3.56 and 3.85 mmol/g at 1 atm and 25 °C.

In 2020, Varghese et al. emphasized the urgent need for the development of innovative and more effective materials to capture CO₂ from diverse sources, addressing the escalating effects of climate change linked to rising atmospheric CO₂ levels [88]. This study examined the development and evaluation of a UV-irradiated graphene oxide foam (UV-GOF) for CO₂ adsorption. We conducted a detailed analysis of the structural, morphological, and surface properties of both the graphene oxide foam (GOF) and the UV-GOF adsorbents, using methylene blue dye adsorption as a reliable method to determine their specific surface area. The CO₂ adsorption performance was assessed based on various factors, includ-

ing capacity, selectivity, regenerability, kinetics, isosteric heat of sorption, and hydrophilicity. The results indicated that UV treatment, along with the resulting changes in the structure and surface of the GOF, had a significant impact on adsorption performance, allowing us to identify optimal conditions. Remarkably, a 30-fold increase in selectivity was observed at 100 mbar after a 5-hour UV treatment, which also led to a sevenfold increase in CO₂ capacity. The UV treatment of graphene-based adsorbents shows promise for enhancing carbon capture efficiency, indicating its potential as a straightforward and cost-effective pretreatment technology for large-scale industrial applications.

In 2020, Wang et al. demonstrated that the controllable, highly selective, and reversible capture of CO₂ through the application of an electric field is a promising approach to mitigate the greenhouse effect [64]. This research represents the first use of penta-graphene (PG) nanosheets as an effective adsorbent for CO₂ adsorption and separation from H₂ and CH₄, utilizing density functional theory. The results showed that the binding strength of CO₂ on PG nanosheets could be significantly improved by applying an electric field. As the electric field strength increased from 0.025 to 0.030

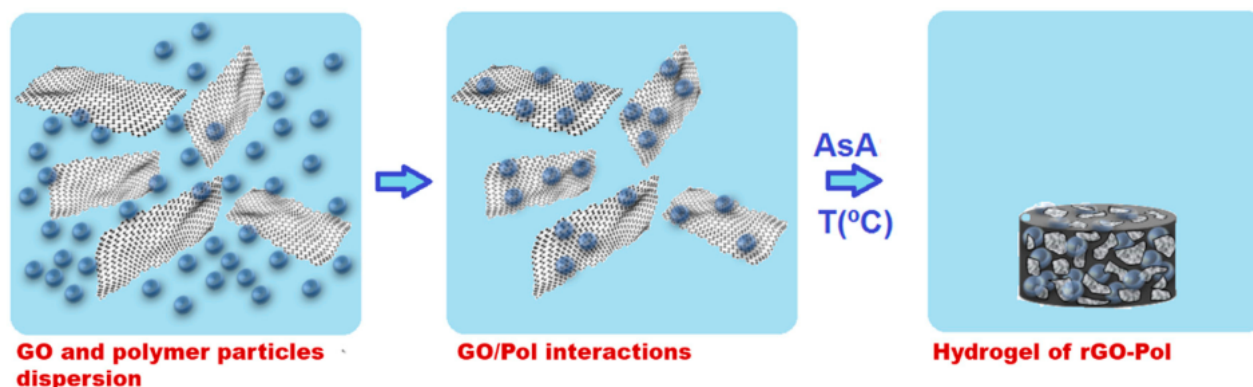


Figure 16. The procedure for reduced graphene oxide/polymer monolithic [MDPI publisher copyright 2020] [85].

a.u., the adsorbed CO₂ transitioned from physisorption to chemisorption. Additionally, the adsorption and desorption of CO₂ on PG nanosheets could be effectively controlled by switching the electric field between 0.030 and 0.040 a.u. The interactions between H₂/CH₄ and PG nanosheets were relatively weak, with only a minor increase as the electric field strengthened, indicating that CO₂ could be efficiently separated from these gases in a dynamically adjustable electric field. This study highlighted the potential of PG nanosheets as a high-performance material for controllable CO₂ capture, regeneration, and separation in the presence of an electric field.

In 2020, Shang et al. highlighted the importance of easily regenerable adsorbents for CO₂ capture. They introduced a novel synthesis method for creating CuBTC and its graphene oxide composites (CuBTC@GO) as adsorbents, utilizing a mixed solvent approach at 323 K for the first time [89]. The use of N,N-Dimethylformamide was essential for promoting the crystallization of CuBTC at lower temperatures by improving nucleation. The newly synthesized CuBTC displayed a significantly larger surface area and total pore volume compared to those made using traditional methods. As a result, the produced CuBTC achieved a CO₂ adsorption capacity of 8.02 mmol/g at 273 K and 1 bar, which was 17–90% greater than the CO₂ capacity of CuBTC created through conventional techniques (figure 17). The development of CuBTC@GO composites further enhanced CO₂ adsorption capacity, mainly due to increased porosity and dispersion forces. In binary breakthrough tests, CuBTC@1%GO demonstrated better CO₂/N₂ selectivity than CuBTC, making it beneficial for real-world gas separation applications. The partition coefficients for both CuBTC and the CuBTC@GO composite were evaluated at different breakthrough levels (5%, 10%, and 100%) with an inlet CO₂ partial pressure of 0.15 bar, showing that CuBTC@1%GO consistently had higher partition coefficient values at all levels. Regenerability tests revealed that the CO₂ adsorption reversibility for the CuBTC@1%GO composite remained above 90%, while CuBTC's reversibility dropped below 74% after five cycles of adsorption and desorption. Therefore, the CuBTC@GO composite stands out as a promising option for CO₂ capture, providing both high adsorption capacity and excellent regeneration capabilities.

In 2020, Xia et al. demonstrated that reduced-graphene-oxide (rGO) aerogels serve as highly effective, multifunc-

tional, and porous supports for nanoparticles derived from hydrotalcite, such as MgAl-mixed-metal-oxides (MgAl-MMO), in two key sorption applications [90]. The MgAl-MMO nanoparticles supported by aerogels showed significant improvements in adsorptive desulfurization performance compared to unsupported nanoparticle powders (figure 18). These enhancements included a remarkable increase in organosulfur uptake capacity (over 100%), a more than 30-fold improvement in sorption kinetics, and nanoparticle regeneration stability that was over three times greater. Similar enhancements in organosulfur capacity were observed for aerogel-supported NiAl- and CuAl-metal-nanoparticles. Importantly, the electrical conductivity of the rGO aerogel network adds a new level of functionality, enabling precise and stable temperature control of the nanoparticles through direct electrical heating of the graphitic support. This support-mediated resistive heating allows for thermal recycling of nanoparticles at significantly higher heating rates (over 700 °C/min) and results in a substantial reduction in energy consumption compared to traditional external heating methods. For the first time, the CO₂ adsorption capabilities of MgAl-MMO/rGO hybrid aerogels were assessed under elevated temperature and high CO₂ pressure conditions, which are relevant to pre-combustion carbon capture and hydrogen production technologies. The total CO₂ capacity of the aerogel-supported MgAl-MMO nanoparticles was more than double that of their unsupported counterparts, reaching 2.36 mmol•CO₂ g⁻¹ ads (at pCO₂ = 8 bar, T = 300 °C), thus exceeding the performance of other high-pressure CO₂ adsorbents.

In 2020, Heo et al. explored carbon capture and storage (CCS), a method aimed at capturing carbon dioxide (CO₂) emitted from fossil fuel combustion. As CO₂ significantly contributes to global warming, its removal post-combustion is essential [91]. This study aims to develop a CO₂ capture membrane that integrates tertiary-amine-stabilized gold nanoparticles (Au NPs), graphene oxide (GO), and polyelectrolytes. It is essential to achieve high CO₂ capture efficiency while also ensuring high gas permeance in the membrane. The multilayer films were created using an automated spray-assisted layer-by-layer (LbL) technique. The polar nature of the polyelectrolytes played a key role in facilitating the CO₂ capture process with tertiary amines. Moreover, the randomly oriented and loosely arranged GO layers not only helped in positioning the Au NPs within

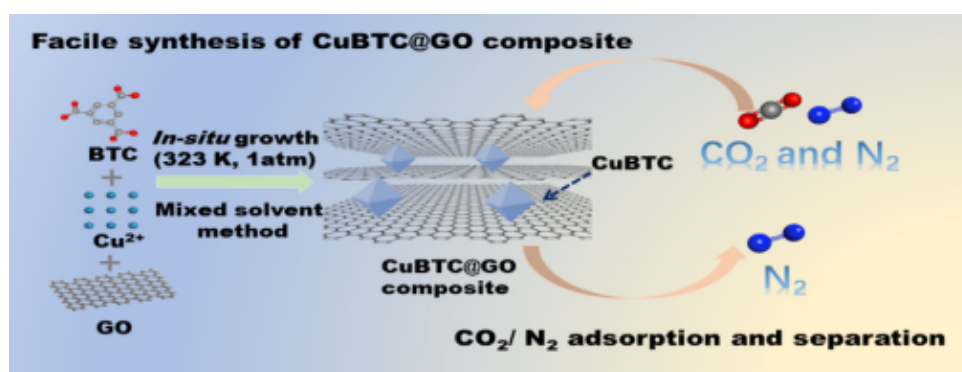


Figure 17. Preparation of graphene oxide composites (CuBTC@GO) as adsorbents for CO₂ [Elsevier copyright 2020, with permission] [89].

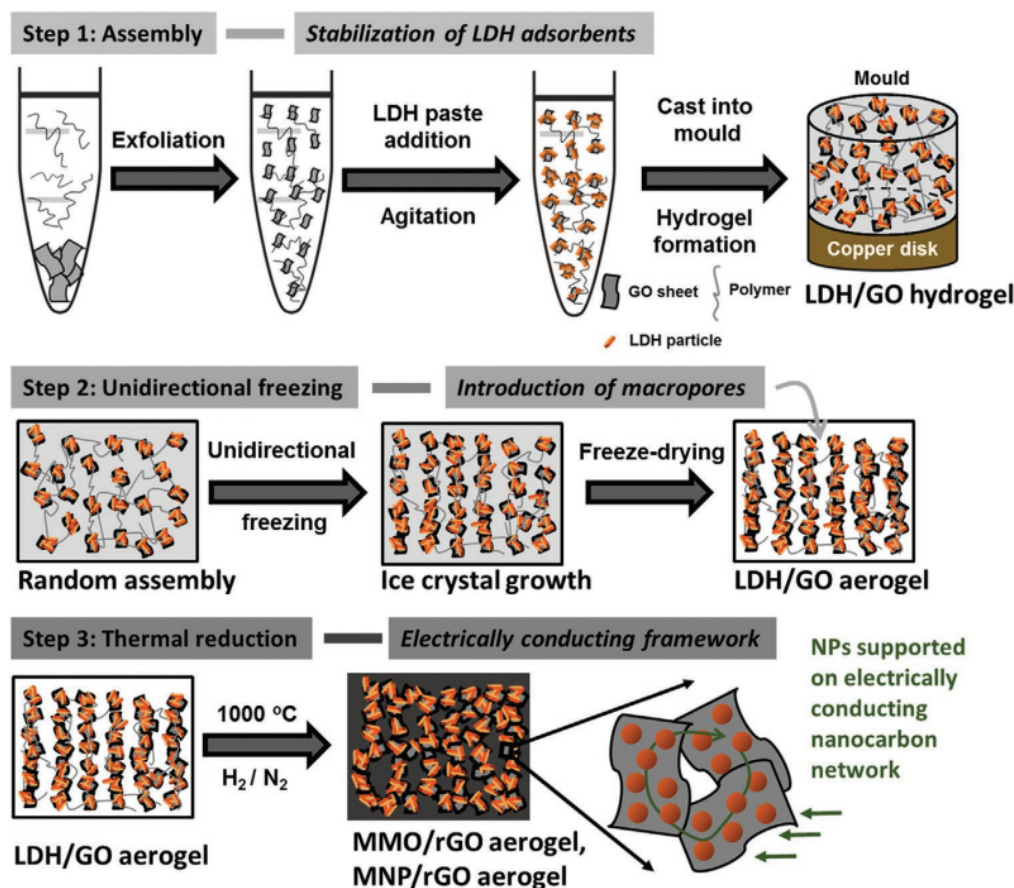


Figure 18. Synthetic procedure for the fabrication of electrically conducting, high-weight loading sorbent-nanoparticle/rGO hybrid aerogel. MMO = mixed-metal-oxide; MNP = metal nanoparticle.[Wiley publisher copyright 2020, with permission]. [90].

the polyelectrolyte matrix but also maintained the permeance of nitrogen (N_2). As a result, a CO_2 adsorptive multilayer nanocoating was successfully developed, achieving a CO_2/N_2 selectivity of 48.48 while keeping an N_2 permeance of 1204.25 GPU (figure 19).

In 2020, Thomou et al. presented a straightforward and efficient synthetic method for producing highly porous heterostructures with customized properties through the silylation of organically modified graphene oxide [94]. The study explored three different silica precursors, each featuring unique structural characteristics (such as alkyl or phenyl groups), to create high-yield silica networks that serve as supports between the organo-modified graphene oxide layers. The thermal decomposition process effectively eliminates organic molecules, leading to porous heterostructures with remarkably high surface areas ($\geq 500 \text{ m}^2/\text{g}$), which makes them ideal for a range of applications, including catalysis, absorption, and as fillers in polymer nanocomposites. The final hybrid materials underwent comprehensive characterization using methods like X-ray diffraction, Fourier transform infrared spectroscopy, X-ray photoelectron spectroscopy, thermogravimetric analysis, scanning electron microscopy, and porosity evaluations. To showcase their potential, the heterostructure with the highest surface area was chosen to assess its CO_2 adsorption capabilities. In 2019, Pruna et al. developed ethylenediamine-modified graphene oxide-based three-dimensional aerogels using

a one-step hydrothermal method [97]. They explored how different oxidation conditions and the type of starting graphite material affected the results using various analytical techniques such as elemental analysis, XPS, Raman spectroscopy, and SEM. They assessed the CO_2 adsorption capabilities of the modified aerogels. The results showed that the distribution of oxygen functional groups and the properties of the graphene oxide, shaped by the oxidation conditions and the type of graphite, led to unique nitrogen doping configurations in the modified aerogels. This resulted in a better surface utilization factor for CO_2 capture. Notably, the aerogel made from expanded graphite exhibited exceptional performance, achieving a CO_2 adsorption capacity of 1.18 mmol/g at 1 bar and 298 K, which is twice that of the unmodified aerogel, underscoring the significant potential of this approach for enhancing CO_2 capture efficiency.

In 2019, Zhou et al. developed ultrathin hollow fiber membranes of ethylenediamine (EDA)-functionalized GO using a previously established deposition technique aimed at achieving high-efficiency CO_2 capture from flue gas (figure 20) [92]. The process involved uniformly depositing single-layered graphene oxide (SLGO) sheets onto the inner surface of poly (ether sulfone) (PES) hollow fibers. EDA was incorporated into the SLGO interlayer nanochannels through chemical grafting, acting as an effective CO_2 -philic agent. To analyze the morphology and structure of the GO

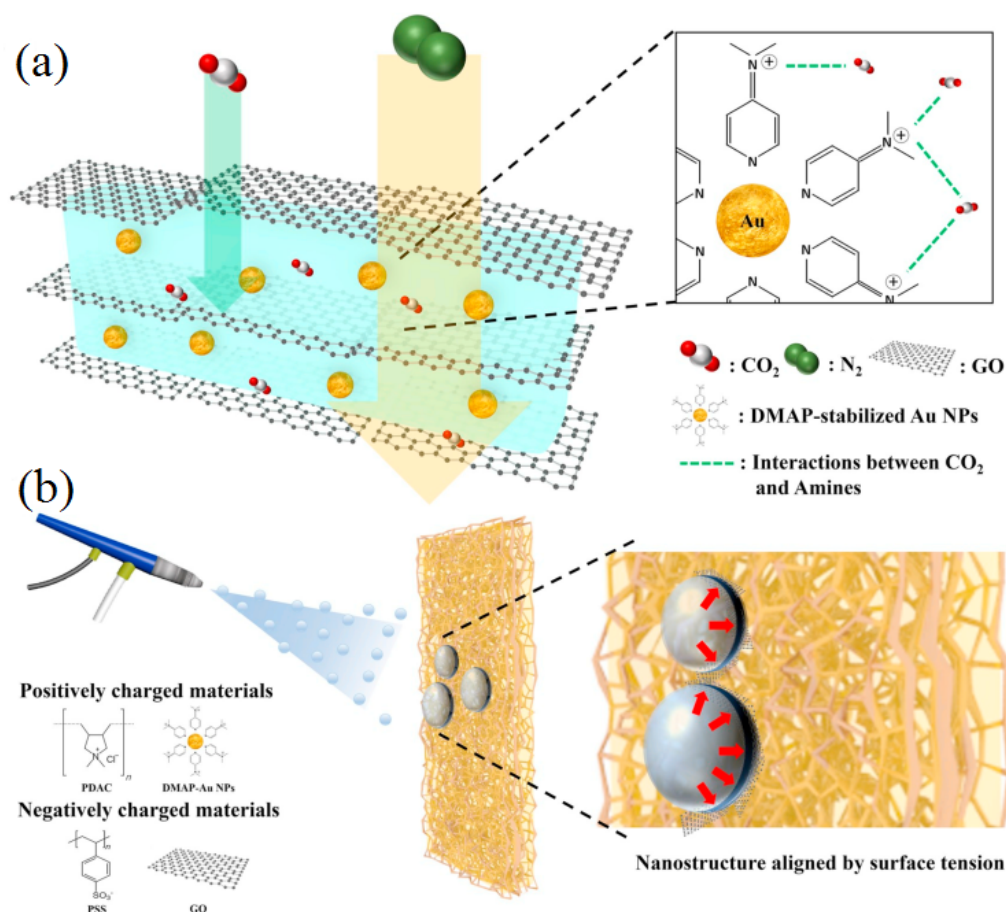


Figure 19. Schematic illustration of the structure of the multilayer film (a) and spray-assisted layer-by-layer self-assembly method (b). [Elsevier publisher copyright 2020, with permission] [91].

and GO-EDA hollow fiber membranes, various characterization techniques were used, including FESEM, Raman Spectroscopy, XPS, Attenuated Total Reflectance-Fourier Transform Infrared Spectroscopy (ATR-FTIR), and XRD. The permeation of a mixed gas (15 vol% CO₂/85 vol% N₂) was tested under wet conditions, resulting in impressive CO₂ separation performance with a CO₂ permeance of 660 GPU and a CO₂/N₂ selectivity exceeding 500 at 75 °C. This study, along with previous research, suggests that

amine-functionalization of GO-based membranes could be a promising strategy to enhance the CO₂ capture capabilities of ultrathin GO-based membranes.

In 2019, Nazari-Kudahi et al. conducted a study that introduced an adsorption performance indicator to assess the effectiveness of CO₂ capture in thermal power plants using a mesoporous graphene oxide/TiO₂ nanocomposite [98]. The research started with the synthesis and characterization of the adsorbent, using N₂ adsorption-desorption tech-

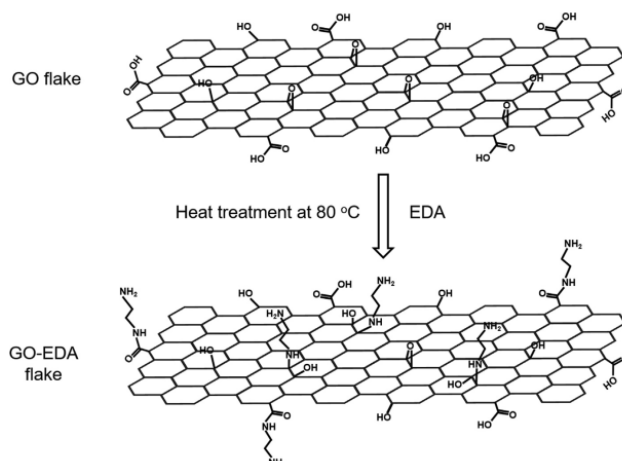


Figure 20. Proposed structure of GO-EDA sheets after amine functionalization. [Elsevier copyright 2019, with permission] [92].

niques (BET and BJH methods), XRD, FE-SEM, and FT-IR spectroscopy. After that, the study measured pure single-component adsorption isotherms at 298 K and applied the Ideal Adsorbed Solution Theory (IAST) with direct search minimization to assess the selectivity of the synthesized nanocomposite for CO₂ compared to N₂. This analysis also aimed to estimate CO₂ adsorption capacity in binary gas mixtures of CO₂: N₂ at molar ratios of 5:95, 10:90, and 15:85. Ultimately, the results were validated through breakthrough experiments carried out in a fixed-bed column, which were then used to calculate the Adsorption Performance Indicator (API) for evaluating CO₂ separation from N₂ in the Pressure Swing Adsorption (PSA) process across different types of thermal power plants.

In 2018, Qin et al. highlighted the importance of developing advanced materials and innovative technologies for effective CO₂ capture and gas separation, which can significantly mitigate the effects of global climate change [99]. This study conducts a detailed investigation using density functional theory to explore how N₂, CH₄, H₂, and CO₂ are adsorbed on a graphene-like C₃N monolayer. Their results show that all four gas molecules are physisorbed on the neutral C₃N monolayer. Importantly, the interaction between CO₂ and C₃N can be significantly improved through electrochemical methods, such as applying a negative charge or an external electric field. In contrast, the adsorption of N₂, CH₄, and H₂ on the C₃N monolayer is only slightly influenced by these methods. Moreover, CO₂ is likely to spontaneously desorb from the C₃N monolayer once the additional charge or electric field is removed. These results indicate that the processes of CO₂ capture, regeneration, and separation on the C₃N monolayer can be effectively managed by adjusting the charge state or electric field during adsorption. Additionally, as a newly synthesized two-dimensional material (see PNAS, 2016, 113, 7414 – 7419), C₃N has an exceptionally narrow band gap of 0.39 eV, which supports the practical use of negative charge or electric field through electrochemical techniques.

In 2018, He and Wang highlighted hydrate-based CO₂ capture and sequestration (CCS) as a promising approach for atmospheric CO₂ control [93]. The rapid formation and high storage capacity of CO₂ hydrates are essential for the effective implementation of this technology. While sodium dodecyl sulfate (SDS) has been identified as the most effective promoter for methane hydrate formation, its efficacy

in promoting CO₂ hydrate formation is notably limited. Consequently, the development of specialized and efficient promoters for CO₂ hydrate formation is vital for advancing hydrate-based CCS. In this research, graphene nanosheets were utilized as carriers, onto which –SO₃ groups (analogous to the hydrophilic group of SDS) and silver nanoparticles measuring approximately 2–5 nm were grafted, resulting in a novel promoter referred to as Ag@SGO (figure 21). This new promoter addresses the shortcomings of SDS and enhances its promotion efficiency. When 1 mmol/L (0.288 g/L) SDS was employed as the promoter, CO₂ hydrate formation extended beyond 1000 minutes, with gas consumption reaching only 2.90 ± 0.22 mmol/mL of water at that time, indicating significantly poorer promotion compared to methane hydrate formation, which was completed within a few hours and achieved gas consumption of 6 – 7 mmol/mL of water. In contrast, the application of Ag@SGO at a concentration of 0.25 g/L resulted in the majority of CO₂ hydrate formation occurring within 200 – 250 minutes, with gas consumption reaching 7.62 ± 0.16 mmol/mL of water at 1000 minutes, nearly 2.6 times greater than that with SDS. This demonstrates that the graphene-supported –SO₃ groups and nano-silver developed in this study provide highly effective promotion of CO₂ hydrate formation, indicating their significant potential for industrial applications in hydrate-based CCS.

In 2018, Huang et al. highlighted the challenges associated with the development of mixed matrix membranes (MMMs), particularly regarding the dispersion of fillers and the creation of defect-free membranes featuring an ultra-thin selective layer [95]. Graphene oxide-based MMMs have emerged as promising candidates for gas separation applications. The low filler content and the tendency of extended GO lamellae to align perpendicularly to the membrane surface, and consequently to the gas flow direction, facilitate the creation of thin film composite membranes (TFC). In this study, facilitated transport MMMs were developed by integrating ionic liquid functionalized graphene oxide (GO-IL) into poly (ether-block-amide) (Pebax 1657). The ionic liquid 1-(3-aminopropyl)-3-methylimidazolium bromide was reacted with graphene oxide sheets, which enhanced the solubility of CO₂ and the CO₂/gas selectivity of the MMMs (figure 22). Additionally, hydrogen bonding interactions between the ionic liquid and the amide groups in Pebax ensured a uniform dispersion of GO-IL. Gas per-

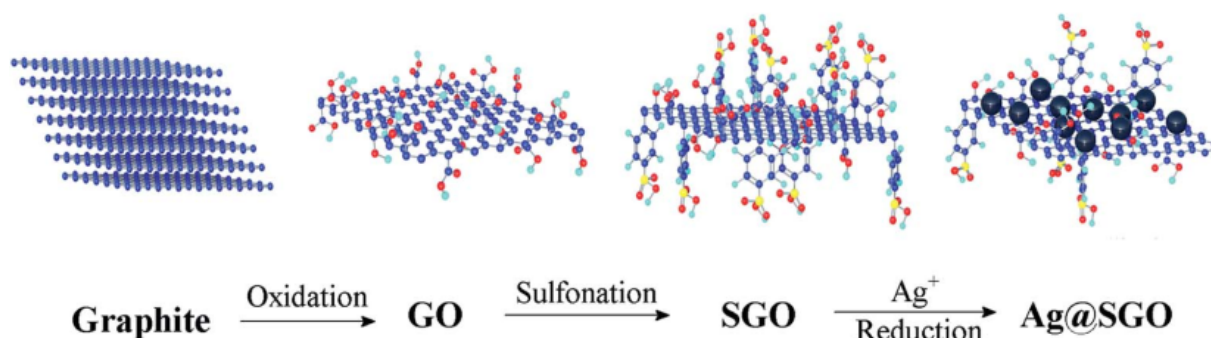


Figure 21. The chemical procedure for the preparation of Ag@SGO [Royal Society of Chemistry, copyright 2018, with permission] [93].

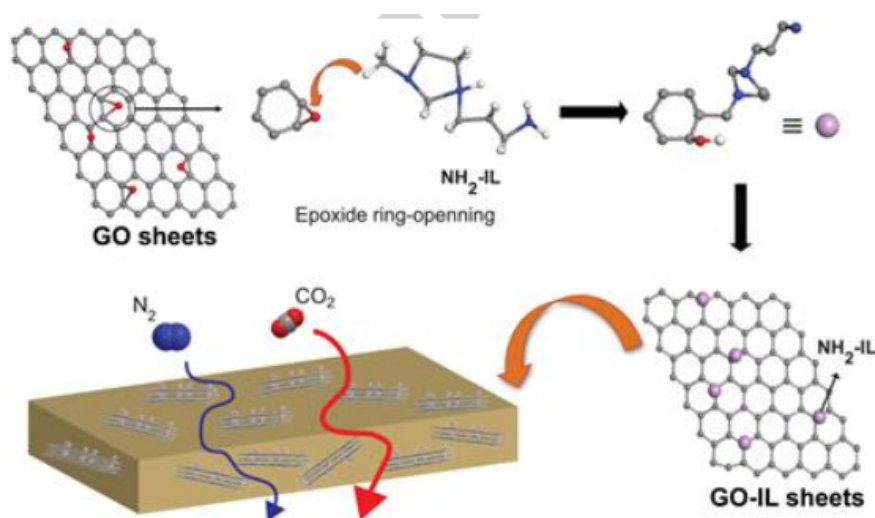


Figure 22. The diagram gas transport through the GO-IL based membrane [Elsevier copyright 2018, with permission] [95],[91].

meability tests for pure gases (H_2 , CO_2 , O_2 , N_2 , CH_4) and mixed gases (CO_2/H_2 , CO_2/N_2) were conducted at 25 °C and 4 bar. The results demonstrated a significant improvement of over 90% in CO_2/N_2 selectivity and a 50% increase in CO_2 permeability for the GO-IL MMMs compared to the pure Pebax membrane. The resulting TFC membranes exhibited a high CO_2 permeance of up to 900 GPU ($10^{-6} \text{ cm}^3 \text{ (STP) cm}^{-2} \text{ s}^{-1} \text{ cmHg}^{-1}$) and CO_2/N_2 and CO_2/H_2 selectivities of approximately 45 and 5.8, respectively. This study emphasizes the critical role of GO-IL nanosheets in designing highly selective thin film membranes, paving the way for the practical application of mixed matrix membranes.

In 2018, Sarfraz and Ba-Shammakh developed high-performance mixed-matrix membranes (MMMs) aimed at mitigating global warming by capturing and sequestering CO_2 from flue gas produced by fossil fuel combustion [96]. A variety of mixed matrix membranes (MMMs) were developed by combining the glassy polymer Ultrason S 6010 (US) with nanosheets of graphene oxide (GO) and nanocrystals of zeolitic imidazolate frameworks (ZIF-300) in various ratios. The solution-casting technique was utilized to fabri-

cate these MMMs, aiming to enhance their ability to capture CO_2 from a CO_2 -rich gas mixture (figure 23). The resulting composite membranes showed improved adhesion at the interface between the filler and the polymer, a uniform distribution of nanofillers, and a thermally stable matrix structure. Due to the synergistic effects of the incorporated nanofillers, the membranes exhibited increased CO_2 permeability and CO_2/N_2 permselectivity, as demonstrated by gas sorption and permeation tests. When compared to the neat Ultrason membrane, the MMMs with 30 wt% ZIF-300 nanocrystals and 1 wt% GO nanosheets displayed significant enhancements in both CO_2 permeability and CO_2/N_2 ideal selectivity. Key features of the developed MMMs include their structural and thermal stability, along with improved gas separation performance.

In 2018, Park et al. investigated the use of nanomaterials, including zeolites and metal-organic frameworks, for the capture and sequestration of CO_2 [101]. While these nanomaterials hold great promise, their effectiveness has been limited by poor selectivity for flue gases and a restricted ability to capture at low pressures. To investigate how mechanical strain affects CO_2 capture efficiency, first-principle

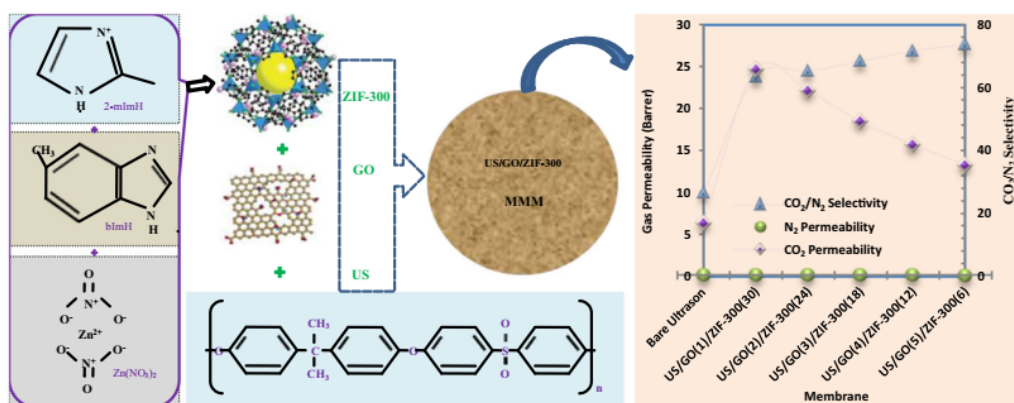


Figure 23. Efficient CO_2 -capture membranes: graphene oxide- and MOF-integrated Ultrason membranes [Springer publisher, copyright 2018, with permission] [96]

density-functional theory calculations were performed on porphyrin-like graphene modified with transition metals. The research indicated that Sc- and V-decorated porphyrin-like graphenes could selectively capture CO₂ from gas mixtures at low CO₂ pressures when under compressive strain, and then release the gas under tensile strain at room temperature. The interaction between CO₂ and these transition metals was mainly due to the Dewar interaction, which involves the hybridization of the metal d orbitals with the π orbitals of CO₂. These results offer a new approach to improving CO₂ capture by applying mechanical strain to nanomaterials.

In 2018, Rea et al. developed innovative composite (mixed matrix) membranes utilizing a permeable glassy polymer, Poly (2,6-dimethyl-1,4-phenylene oxide) (PPO), combined with varying amounts of few-layer graphene to evaluate their effectiveness in gas separation and CO₂ capture [102]. The study investigated how the permeability, selectivity, and diffusivity of different gases were affected by varying levels of graphene loading, which ranged from 0.3 to 15 wt%, at temperatures of 35 and 65 °C. Membranes with lower amounts of graphene showed improved permeability and He/CO₂ selectivity compared to pure PPO, which was attributed to the positive impact of the nanofillers on the polymer's structure. In contrast, higher graphene concentrations led to a reduction in permeability due to the increased tortuosity that gas molecules encountered within the membrane. Furthermore, graphene played a crucial role in reducing the increase in permeability with temperature, acting as a “stabilizer” for the polymer matrix. This stabilizing effect lessened the temperature-related decline in size selectivity for He/N₂ and CO₂/N₂, while also boosting the temperature-driven increase in selectivity for He/CO₂. The results suggest that, similar to other graphene-based mixed matrix glassy membranes, the ideal graphene concentration in the polymer should be kept below 1 wt%. At this concentration, the morphology of the nanoscopic filler enhances the arrangement of glassy chains, leading to improvements in both permeability and selectivity, and increasing membrane selectivity at higher temperatures. These findings indicate that even small amounts of graphene added to polymers can greatly enhance their permselectivity and stabilize

their performance.

In 2017, Li and Zeng emphasized the importance of developing efficient and cost-effective solid sorbents for carbon capture and storage [100]. This study presents a new type of high-performance CO₂ adsorbent called rGO@MgO/C, developed through the careful integration of reduced graphene oxide (rGO), amorphous carbon, and MgO nanocrystallites. The optimized rGO@MgO/C nanocomposite shows remarkable CO₂ capture capacity, reaching up to 31.5 wt% at 27 °C and 1 bar of CO₂, and 22.5 wt% under simulated flue gas conditions (figure 24). It also features a fast sorption rate and impressive durability throughout the process. Notably, its CO₂ capture ability exceeds that of all previously reported MgO-based sorbents. The outstanding performance of the rGO@MgO/C nanocomposite is due to its hierarchical structure and unique physicochemical properties, which include a sheet-on-sheet sandwich-like configuration, ultrathin nanosheets with numerous nanopores, a large surface area, and well-dispersed ultrafine MgO nanocrystallites (about 3 nm in size). The rGO sheet and the in-situ generated amorphous carbon serve as dual carbon supports, preventing the agglomeration of MgO nanocrystallites. Additionally, the CO₂ uptake capacity at intermediate temperatures (e.g., 350 °C) can be increased by more than three times with the application of alkali metal salt promotion treatment. This research offers a simple and effective method for designing advanced graphene-based functional nanocomposites with carefully engineered compositions and structures for potential applications in gas storage and separation.

In 2017, Zhou et al. highlighted that among the existing CO₂ capture technologies, membrane gas separation offers several inherent advantages compared to traditional methods [103]. The ongoing challenge is to create gas separation membranes that can deliver both high CO₂ permeance and strong CO₂/N₂ selectivity, especially in humid conditions. This study introduces the development of hollow fiber membranes made from layered graphene oxide (GO) that are less than 20 nm thick. These membranes feature a grafted, brush-like CO₂-attracting agent placed between the GO layers. They are produced using a simple coating method, which allows for effective CO₂/N₂ separation even in wet

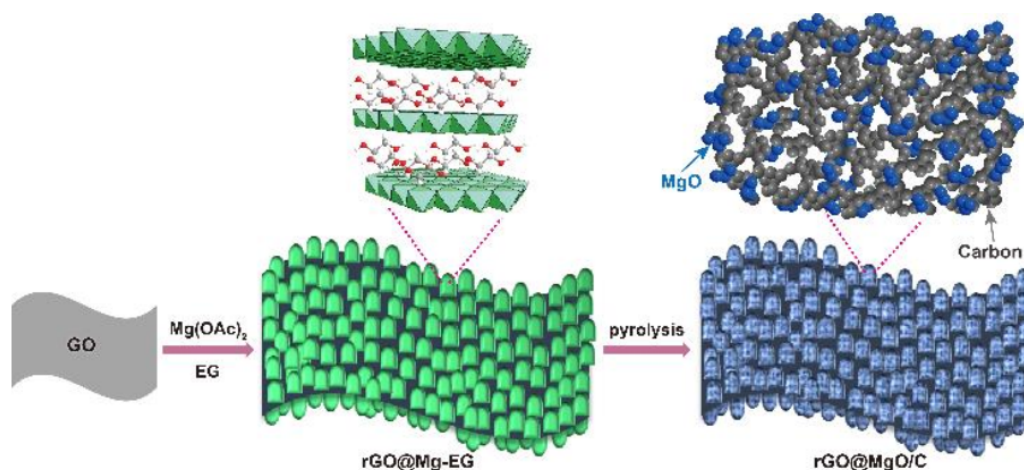


Figure 24. The chemical route for sandwich-like rGO@MgO/C nanocomposite [American Chemical Society, copyright 2017, with permission] [100].

environments. Piperazine serves as a highly effective CO₂-attracting agent, chemically bonded as a carrier-brush within the GO nanochannels. The resulting membrane shows exceptional separation performance under simulated flue gas conditions, achieving a CO₂ permeance of 1,020 GPU and a CO₂/N₂ selectivity of 680, highlighting its considerable potential for CO₂ capture from flue gas. This innovative structure of the GO-based membrane, combined with the straightforward coating technique, is expected to propel the advancement of ultrathin GO-based membranes for CO₂ capture applications (figure 25).

In 2016, Tan et al. proposed hexagonal boron nitride (h-BN) as a sorbent material for charge-induced switchable CO₂ capture [104]. The wide bandgap of h-BN poses a challenge for the injection of the necessary charge. In this study, we employ first-principle calculations to show that in-plane h-BN/graphene (P-BN/G) heterostructures, consisting of alternating strips of h-BN and graphene, can act as an effective material platform for voltage-induced charging of h-BN strips, facilitating switchable CO₂ capture. Our results reveal that a significant amount of negative charge can be injected into the h-BN strips of the P-BN/G structure, enabling easy control over CO₂ capture and release by adjusting the charge states of the P-BN/G system. At peak CO₂ capture coverage, the negatively charged P-BN/G heterostructures can achieve CO₂ capture capacities of up to $2.27 \times 10^{14} \text{ cm}^{-2}$, which is twice the capacity that can be reached with stacked h-BN/graphene (S-BN/G) nanosheets. In 2016, Karunakaran et al. emphasized the necessity for advanced membrane systems that exhibit both high flux and

adequate selectivity for industrial gas separation applications [105]. To attain these characteristics, it is essential for the membrane material to be as thin as feasible, incorporating selective sieving channels while ensuring long-term stability. This objective can be realized by developing a three-component material that combines an ionic liquid with graphene oxide, which is then coated with a highly permeable yet low-selective polymer. Utilizing a straightforward dip coating method, we successfully fabricated ultrathin graphene oxide (GO)/ionic liquid membranes that are highly selective for CO₂ on a porous ultrafiltration substrate. The resulting ultrathin composite membranes, formed from the GO/ionic liquid complex, demonstrate exceptional permeability (with a CO₂ flux of 37 GPU) and selectivity (CO₂/N₂ selectivity of 130), exceeding the upper limits typically observed in ionic liquid membranes for CO₂/N₂ separation. Furthermore, these membranes exhibited stability during a 120-hour testing period.

In 2016, Dai et al. developed mixed matrix membranes (MMMs) utilizing imidazole functionalized graphene oxide (ImGO), an inorganic material with CO₂ affinity, combined with poly (ether-b-amide) (PEBAX) for the purpose of CO₂ capture [106]. The MMM containing 0.8 wt.% ImGO demonstrated the highest CO₂ separation efficiency, achieving a CO₂/N₂ selectivity of 105.5 alongside a CO₂ permeability of 76.2 Barrer (where 1 Barrer = $10^{-10} \text{ cm}^3 \text{ (STP) cm}^{-2} \text{ s}^{-1} \text{ cmHg}^{-1}$), exceeding the Robeson Upper Bound established in 2008. The selectivity for CO₂/N₂ in the MMM increased by 46.0% compared to the pristine PEBAX, attributed to the interaction between CO₂ and the

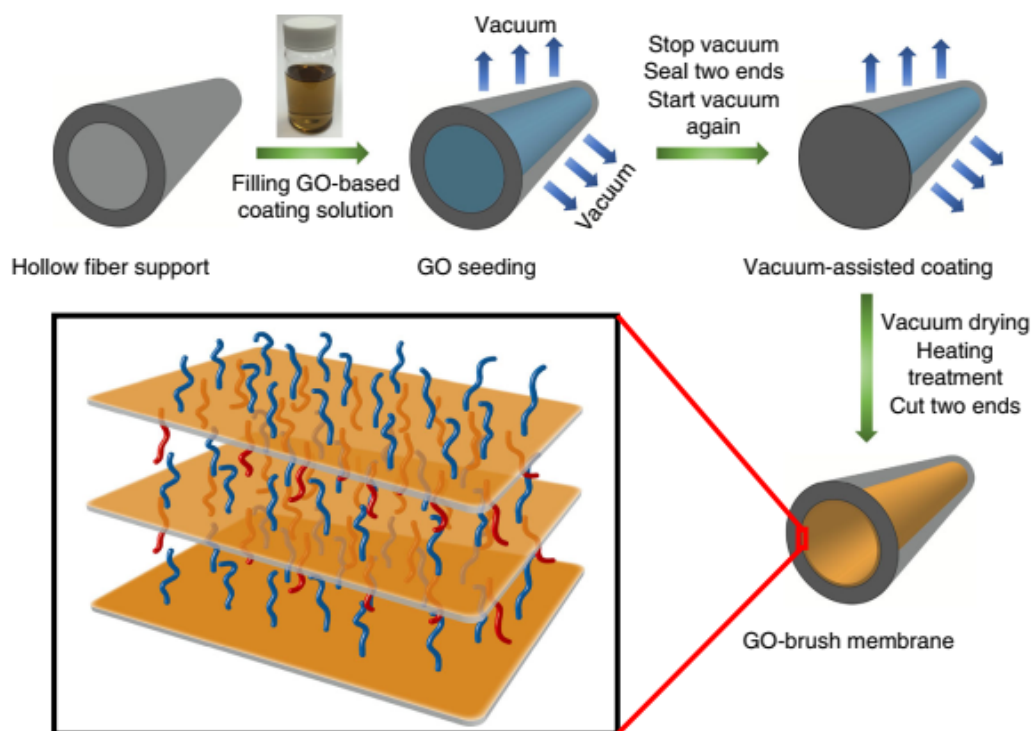


Figure 25. Fabrication process and structure diagram of the ultrathin GO-based hollow fiber membranes with brush-like CO₂-philic agent. The blue brushes denote the grafted agents on the top surface of GO, and the red brushes denote the grafted agents on the bottom surface of GO. The brushes can be appropriate CO₂-philic agents that are able to chemically bond with the GO surface by reacting with oxygen-functional groups [Springer nature copyright 2017, with permission] [103].

imidazole groups. As feed pressure rises, CO₂ permeability significantly improves due to its enhanced solubility within the polymer matrix and the resulting plasticization effect. The MMMs are particularly effective in separating CO₂ from N₂ at lower temperatures, as the apparent activation energy for N₂ permeation in ImGO/PEBAX MMMs is considerably higher than that for CO₂. The glass transition temperature (T_g) of the MMMs gradually increases, reflecting the restricted mobility of the polymer chains caused by the presence of ImGO (figure 26), which also creates a more rigid interface between the polymer and the filler. The mechanical properties of the membranes have been notably improved due to the incorporation of ImGO sheets, which facilitate hydrogen bonding. With significant enhancements in CO₂ separation performance, the ImGO/PEBAX MMMs show great potential for applications in CO₂ capture technologies.

In 2016, Haque et al. proposed that capturing and storing CO₂ could serve as a viable method for mitigating global greenhouse gas emissions [107]. In recent years, significant research has been dedicated to developing highly efficient materials for capturing CO₂. A variety of porous materials, such as zeolites, porous carbons, nitrogen/boron-doped porous carbons, and metal-organic frameworks (MOFs), have been investigated for this purpose. This study specifically examines the CO₂ capture capabilities of innovative hybrid materials called graphene-organic frameworks (GOFs). These GOFs were synthesized under mild conditions using a solvothermal method, with graphene oxide (GO) serving as the base material and benzene 1,4-diboronic acid acting as the organic linker. Remarkably, the resulting GOF exhibits a substantial surface area of 506 m²/g, which is about 11 times greater than that of GO alone (46 m²/g). This indicates that the organic modification of the GO surface effectively promotes the development of a porous structure. Our synthetic approach is notably simple and quick compared to many previously reported methods. Furthermore, the synthesized GOF demonstrates a significantly high CO₂ capacity, exceeding that of other porous materials and previously documented carbon-based materials, along

with excellent CO₂/N₂ selectivity.

In 2016, Wang et al. emphasized the critical need to mitigate greenhouse gas emissions by effectively separating CO₂ from flue gases produced by power plants that utilize carbon-based fossil fuels [109]. They found that N₂-selective membranes present a more advantageous option for systems with low CO₂ concentrations compared to CO₂-selective membranes. Through density functional theory (DFT) calculations and molecular dynamics (MD) simulations, this study demonstrated that the poly (triazine imide) (PTI) membrane can efficiently separate N₂ from CO₂, achieving a selectivity of 273 and an N₂ permeance of 106 GPU, which surpasses the performance of most traditional membranes. Additionally, the study indicated that the presence of H₂O has a minimal effect on the gas separation efficiency of the PTI membrane. This ultrathin N₂-selective membrane, which is available for experimental use, holds promise for practical applications in post-combustion CO₂ capture.

In 2016, Dong et al. developed a novel fixed carrier composite membrane through interfacial polymerization, utilizing graphene oxide nanosheets (GO), hyperbranched polyethylenimine (HPEI), and trimesoyl chloride (TMC) on a polysulfone membrane. The successful interfacial polymerization was validated using techniques such as SEM, ATR-FTIR, TEM, XPS, DSC, and water contact angle measurements [108]. Subsequent gas separation experiments with a CO₂/N₂ (10:90 v:v) mixture demonstrated that the incorporation of GO significantly enhanced both CO₂ permeance and CO₂/N₂ selectivity. The maximum CO₂ permeance achieved in this study was 9.7 GPU, with a selectivity exceeding 80. Additional gas separation tests conducted under varying feed gas humidity indicated that facilitated transport was the primary mechanism for gas separation through the membrane (figure 27). The inclusion of GO in the membrane exhibited a synergistic effect with the gas carriers, where surface defects functioned as molecular sieves, and the interlayer provided fixed flow channels that maintained a high-water content microenvironment, thereby enhancing the reactivity between CO₂ and amino-based carriers. Furthermore, the composite membrane demonstrated excellent stability.

In 2016, Liu et al. presented a one-step method for synthesizing nitrogen-doped graphene-based materials (GMCs) that feature high nitrogen content and adjustable nitrogen sites [111]. The unique layered architecture and the presence of numerous meso-macropores in these GMCs enhance the accessibility of nitrogen functionalities to CO₂ while simultaneously hindering N₂ adsorption. As a result, the produced GMCs exhibit remarkable capabilities in the selective adsorption of CO₂. The synthetic approach outlined in this study paves the way for the straightforward and cost-efficient production of highly macroporous graphene-based nanomaterials with customizable nitrogen sites, which are expected to have a wide range of potential applications.

In 2016, Chowdhury et al. developed three-dimensional (3D) crumpled graphene-based porous adsorbents characterized by highly interconnected networks [68]. This was achieved through a straightforward one-step physical activation process utilizing reduced graphene oxide (RGO)

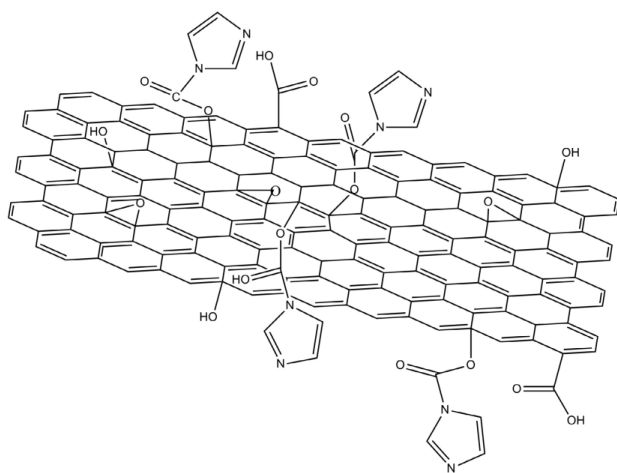


Figure 26. The chemical structure of ImGO [Elsevier copyright 2016, with permission] [106].

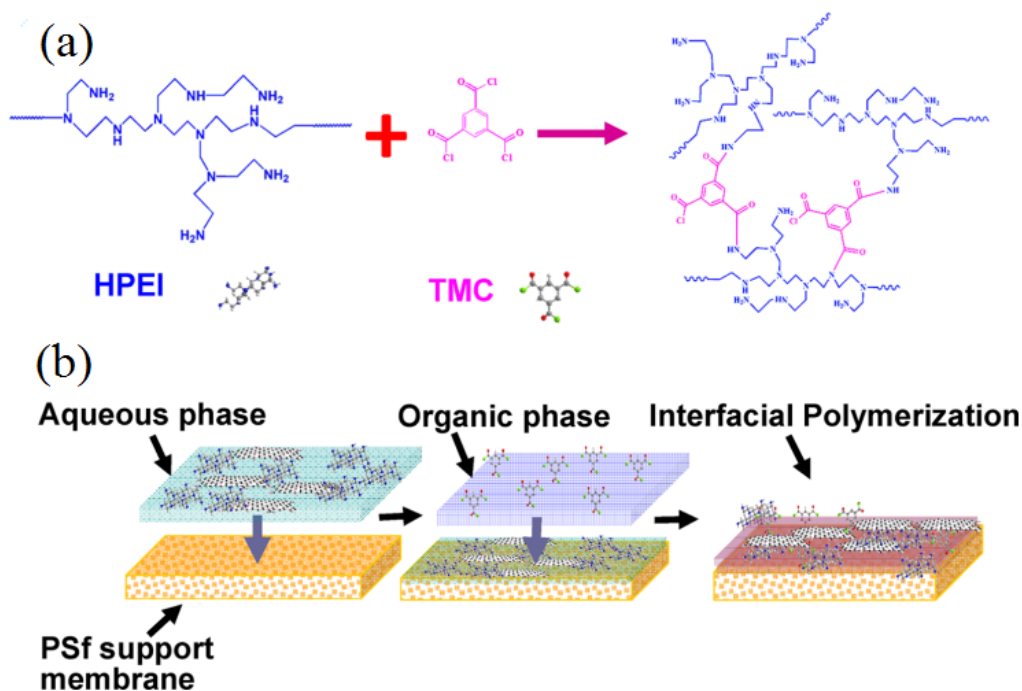


Figure 27. (a) the reaction between HPEI and TMC and (b) the fabrication process for the HPEI/GO-TMC composite membrane [American Chemical Society copyright 2016, with permission] [108].

as the precursor, aimed at separating carbon dioxide (CO_2) from post-combustion flue gas mixtures. These materials exhibit a substantial surface area exceeding $1300 \text{ m}^2/\text{g}$, a high pore volume surpassing $1 \text{ cm}^3/\text{g}$, and a well-defined bimodal microporous-mesoporous structure. As a result, they demonstrate rapid, stable, reversible, and significant CO_2 uptake of 2.45 mmol/g at 25°C and 1 bar. Notably, the selectivity for CO_2 over nitrogen (N_2) is among the highest at partial pressures pertinent to CO_2 capture from post-combustion power plants that utilize either coal or natural gas. Additionally, the isosteric heat of adsorption measured at only -27.42 kJ/mol at zero coverage indicates that the regeneration of the adsorbent is straightforward and requires minimal energy, potentially lowering the costs associated with carbon capture and sequestration (figure 28). In 2016, Bhanja et al. developed a novel imine-functionalized graphene oxide (IFGO) through post-synthetic modifications [110]. This process involved the co-condensation of 3-aminopropyltriethoxysilane with the hydroxyl and epoxy functional groups present on the graphene oxide basal plane. This was followed by a Schiff base condensation reaction with 2,6-diformyl-4-methylphenol and

the covalent attachment of copper (II) to form Cu-IFGO (figure 29). The characterization of the materials was conducted using various techniques, including powder X-ray diffraction, N_2 sorption analysis, FT-IR, FE-SEM, HR-TEM, and TGA/DTA analysis. The IFGO demonstrated a significant CO_2 storage capacity of 8.10 mmol/g (35.64 wt%) at 273 K and 2.10 mmol/g (9.24 wt%) at 298 K under pressures of up to 3 bar, indicating its potential for environmental remediation applications. Additionally, Cu-IFGO exhibited remarkable catalytic activity in microwave-assisted one-pot three-component C–S coupling reactions involving a variety of aryl halides, thiourea, and benzyl bromide in an aqueous medium, yielding aryl thioether products with a maximum yield of 86%, which are derivatives of natural products. The presence of imine and hydroxyl groups in the functionalized graphene oxide allowed for strong chelation of Cu(II) at the graphene oxide surface, preventing leaching during the coupling reaction. Consequently, there was only a minimal decrease in product yield even after six reaction cycles, highlighting the sustainability of this Cu(II) -grafted catalyst.

In 2015, Rao et al. conducted a study focused on the effi-

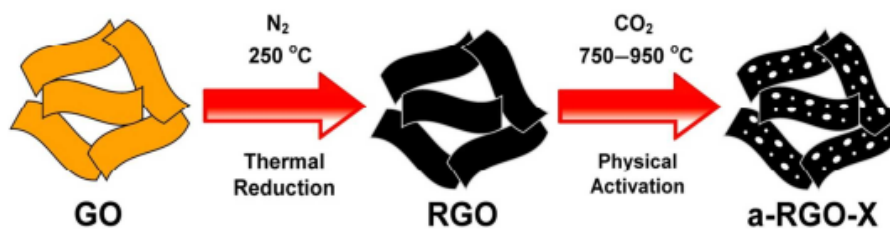


Figure 28. the major steps involved in the preparation of a-RGO-X [American Chemical Society copyright 2016, with permission] [68].

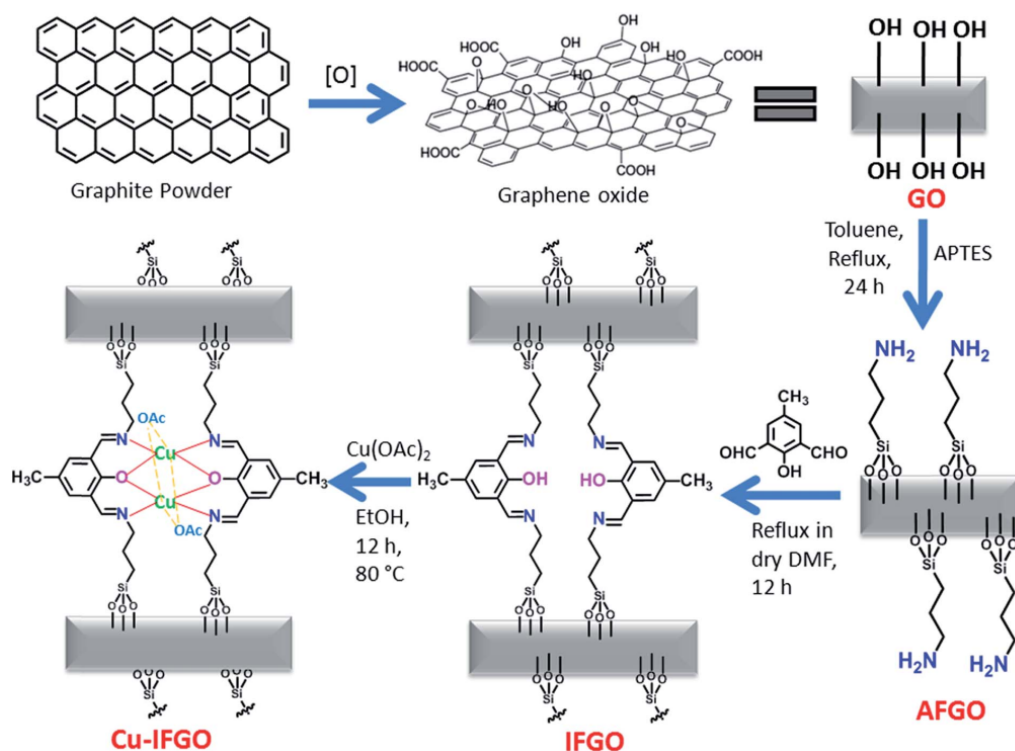


Figure 29. The chemical process for the preparation of Cu-IFGO [Royal Society of Chemistry copyright 2016, with permission] [110].

cient capture of CO_2 using two-dimensional (2D) nanostructures, aiming to contribute to atmospheric cleaning and the purification of emissions from fuel engines [112]. This research involved comprehensive first-principles calculations grounded in density functional theory (DFT) to explore the interaction between CO_2 and a newly synthesized ZnO monolayer (ZnO-ML) in its pure, defected, and functionalized states. A series of detailed calculations identified the most favorable binding configurations for the CO_2 gas molecule on the ZnO-ML. The findings revealed that substituting one oxygen atom with boron, carbon, or nitrogen in the ZnO monolayer significantly enhanced CO_2 adsorption. Our results indicate that the presence of foreign atoms such as B, C, and N leads to improved CO_2 adsorption on the ZnO-ML. The increased adsorption energy of CO_2 on ZnO suggests that the ZnO-ML holds potential as a viable candidate for future CO_2 capture applications.

In 2015, Liu et al. developed covalently bonded CO_2 adsorbents through the acid-catalyzed ring-opening polymerization of aziridine on the basal surfaces of three-dimensional hydroxylated graphene (HG) [113]. The resulting materials feature elevated surface areas, robust covalent interactions between polyethyleneimine (PEI) and graphene, and excellent thermal conductivity. The HG-PEI nanocomposites demonstrate significant amine loading (exceeding $10.03 \text{ mmol N g}^{-1}$) and impressive adsorption capacity (reaching up to $4.13 \text{ mmol } CO_2 \text{ g}^{-1}$ in simulated ambient air at 1 atm of dry CO_2), along with strong stability at both low (100°C) and high desorption temperatures (135°C). This combination indicates that the overall CO_2 capture process is both promising and sustainable.

In 2015, Tawfik et al. emphasized the importance of identi-

fying stable systems with a high capacity for CO_2 adsorption in the context of CO_2 capture and storage technologies [114]. We conducted an extensive first-principles investigation to assess the CO_2 capture capabilities of 16 representative metal-doped graphene systems, where the metal dopants are stabilized by both single and double vacancies. The maximum number of CO_2 molecules that can be adsorbed was evaluated based on criteria related to adsorption energy and bond distances. Generally, while double vacancies provide stronger binding for metal dopants compared to single vacancies, single-vacancy graphene with metal dopants demonstrates superior sorption properties, with each of the Ca, Sc, and Y dopants capable of binding up to 5 CO_2 molecules. The process of CO_2 capture involves significant charge transfer between the CO_2 molecule and the dopant-vacancy complexes, with defective graphene serving as a charge reservoir for the binding of CO_2 molecules. Some systems are predicted to lead to the formation of a bent CO_2 anion. However, Ca-doped single- and double-vacancy graphene systems tend to readily form metal oxides upon reaction with CO_2 , making them less suitable for repeated CO_2 capture.

In 2015, Chowdhury et al. focused on the creation of effective adsorbents characterized by high adsorption capacity and selectivity for the separation of CO_2 from flue gas streams, which are significant contributors to global warming [116]. This research introduced a series of mesoporous titanium dioxide/graphene oxide (TiO_2/GO) nanocomposites, synthesized through a straightforward colloidal blending method, with varying mass ratios of GO to TiO_2 . This study marks the first systematic investigation of these materials as potential CO_2 adsorbents. The synthesized com-

posites underwent characterization using diffraction, spectroscopy, and microscopy techniques. The pure component adsorption isotherms for CO₂ were evaluated at temperatures of 0, 25, and 50 °C, with pressures reaching up to 100 kPa. The analysis indicated that the CO₂ adsorption isotherms aligned well with the temperature-dependent Toth model, while the adsorption kinetics were effectively described by the Avrami model. The TiO₂/GO composites demonstrated a CO₂ uptake capacity of 1.88 mmol/g at room temperature, significantly surpassing that of many conventional adsorbents. Additionally, TiO₂/GO exhibited a low heat of adsorption and exceptional CO₂/N₂ selectivity, highlighting its potential for CO₂ capture from dry flue gas. In 2015, Shen et al. conducted a study in which they developed a facilitated transport mixed matrix membrane using a surface coating technique [117]. The polymer matrix consisted of polyvinyl amine (PVAm) and chitosan (Cs), which were applied to a porous polysulfone (PS) substrate. Additionally, graphene oxide (GO) modified with hyperbranched polyethylenimine (HPEI-GO) was incorporated as nanofillers. Gas separation experiments utilizing a CO₂/N₂ (10:90 v:v) mixture indicated that the inclusion of GO enhanced the selectivity for CO₂ over N₂. The membrane containing 2.0 wt% HPEI-GO achieved a maximum CO₂ permeance of 36 GPU, while the optimal selectivity of 107 was observed in the membrane with 3.0 wt% HPEI-GO. The presence of GO facilitated the formation of transport channels for CO₂ and contributed to the membranes' long-term stability. Additional gas separation tests conducted at varying relative humidity levels confirmed that facilitated transport was the primary mechanism for gas separation in the membrane. Stability assessments indicated that the membrane maintained its performance over time. CO₂ transport through the membrane primarily occurred via the facilitated transport mechanism, supplemented by the solution-diffusion mechanism, whereas N₂ transport relied

solely on the solution-diffusion mechanism (figure 30).

In 2014, Parshetti et al. highlighted the critical necessity for addressing climate change through the implementation of CO₂ reduction technologies [118]. This study introduces an innovative approach for the synthesis of porous graphene-like nanosheets (PGLNS) derived from the lignocellulosic fibers of oil palm empty fruit bunches (EFB) utilizing a thermal graphitization method aimed at enhancing CO₂ capture efficiency. A comprehensive array of microscopic and spectroscopic techniques was employed to elucidate the morphological and structural properties of the PGLNS, which exhibited a d-spacing of approximately 0.35 nm and a pore size of less than 1 nm, derived from EFB biomass. The PGLNS demonstrated remarkable efficacy as adsorbents for post-combustion CO₂ capture, achieving a maximum CO₂ uptake of 2.43 mmol/g at 25 °C and 1 bar pressure, significantly surpassing the performance of other competitive CO₂ adsorbents, such as zeolite, activated carbon, and certain metal-organic frameworks. The selectivity of the PGLNS for CO₂ over N₂ (SCO₂/N₂ = 18.7), calculated from single-component isotherms relevant to post-combustion scenarios, also exceeded that of most previously documented adsorbents. Furthermore, the notably low isosteric heat of adsorption (~ 21 kJ/mol) indicated the feasibility of CO₂ desorption and the regeneration of PGLNS for repeated applications with minimal energy costs.

In 2014, Shen et al. developed graphene oxide (GO) nanosheets that were designed to form layered structures featuring rapid and selective transport channels for gas separation (figure 31) [119]. These GO laminates, characterized by molecular-sieving interlayer spaces and direct diffusion pathways, provided the resulting membranes with remarkable CO₂ permeation capabilities (CO₂ permeability: 100 Barrer, CO₂/N₂ selectivity: 91) and exceptional operational stability exceeding 6000 minutes, making them highly appealing for practical CO₂ capture applications. Membranes

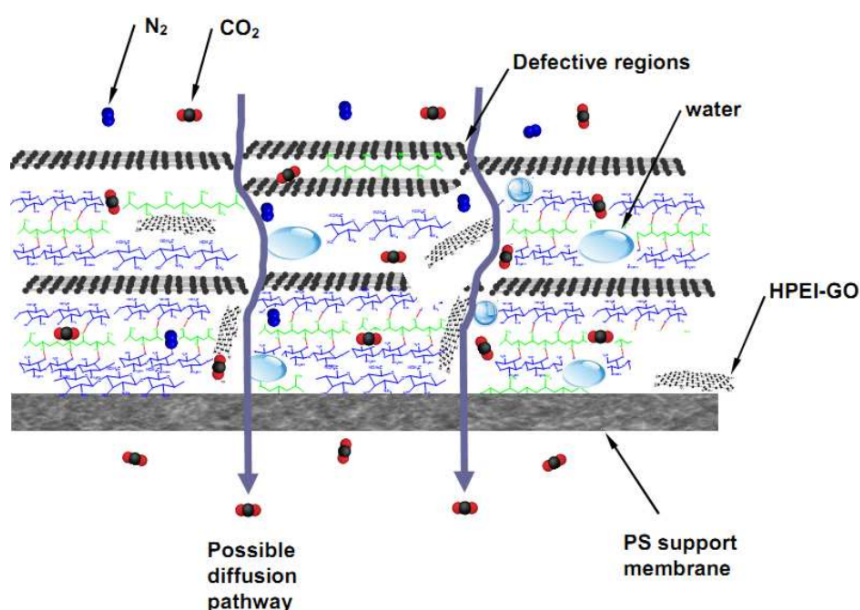


Figure 30. (a) the reaction between HPEI and TMC and (b) the fabrication process for the HPEI/GO-TMC composite membrane [American Chemical Society copyright 2016, with permission] [108].

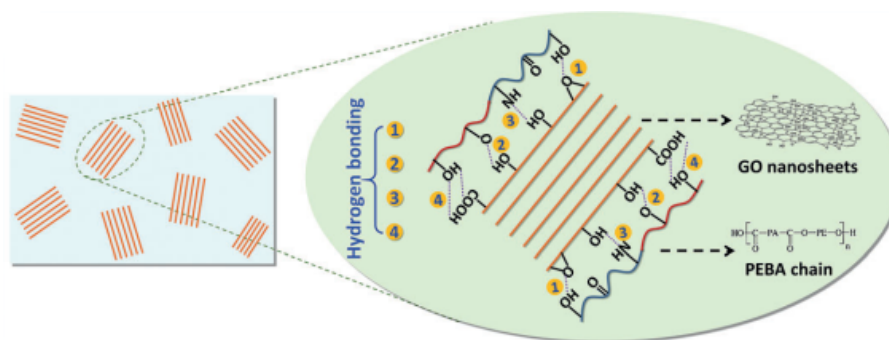


Figure 31. Schematic representation of the assembly of GO nanosheets in polymeric environment based on hydrogen bonds formed between different groups on GO and the PEBA chain [Wiley publisher copyright 2014, with permission] [115].

designed with rapid and selective CO₂ transport channels utilizing graphene oxide (GO) laminates have been developed through the establishment of hydrogen bonding between GO and a polymer. This interaction facilitates the assembly of GO nanosheets into multi-layered stacks, characterized by molecular-sieving interlayer spacing and direct diffusion pathways. The resulting membrane demonstrates remarkable preferential CO₂ permeation properties, achieving an exceptionally high and stable CO₂/N₂ separation performance that surpasses the current limits of advanced membranes. By meticulously managing the polymer environment, further enhancements in performance can be realized by increasing the number of gas-transport channels formed by uniformly distributed GO stacks within the membrane. With significant benefits in terms of ease of fabrication and structural integrity, the GO-based membrane presented here holds considerable promise for effective CO₂ capture applications.

In 2013, Alhwaige et al. highlighted the ongoing extensive research aimed at the development and design of innovative porous materials for clean energy and environmental applications, particularly in mitigating CO₂ emissions [120]. This study focuses on the preparation of hybrid monolith aerogels composed of chitosan (CTS), a biopolymer that is environmentally friendly, combined with varying amounts of graphene oxide (GO) through a freeze-drying process. The CO₂ sorption capabilities of these aerogels are thoroughly examined. Characterization techniques employed include X-ray diffraction (XRD), scanning electron microscopy (SEM), thermogravimetric analysis (TGA), and nitrogen adsorption–desorption measurements. The research investigates the uniform distribution of GO within CTS, particularly at concentrations where particle agglomeration occurs. The influence of GO on the specific surface area of the aerogels and their CO₂ capture efficiency is analyzed, revealing an increase in performance with higher GO content. Notably, the BET surface area significantly rises from 153 to 415 m²/g with the incorporation of 20 wt% GO into the CTS matrix. Additionally, the CO₂ adsorption capacity at 25 °C improves from 1.92 to 4.15 mol/kg with the same GO addition. The results from adsorption–desorption cycles demonstrate the stability of the hybrid aerogels during extended cyclic operations, indicating their promising potential for CO₂ capture applications.

In 2012, Chandra et al. demonstrated that nitrogen-doped

porous carbon, created through the chemical activation of polypyrrole-functionalized graphene sheets, exhibits a selective adsorption capacity of CO₂ at 4.3 mmol/g compared to 0.27 mmol/g for N₂ at 298 K [121]. The material's potential for large-scale production and easy regeneration enhances its applicability in industrial settings.

In 2011, Jiao et al. conducted first-principle calculations on a hexagonal boron nitride (g-BN) monolayer with a boron-atom vacancy, revealing its potential for capturing and activating carbon dioxide [122]. Their findings indicate that CO₂ can decompose to form an oxygen molecule through an intermediate chemisorption state on the defected g-BN sheet. The study confirmed three stationary states and two transition states along the reaction pathway through minimum energy pathway searches and frequency analysis. The calculated energy barriers for this catalytic reaction, after enthalpy correction, suggest that the reaction is likely to occur efficiently at room temperature. Table 1 represents a literature review on the reviewed the original research paper in this review. The name of country referred to the first country of affiliation.

Future directions, opportunities, challenges of functionalized graphene for CO₂ capture

Functionalized graphene holds significant promise as a next-generation material for CO₂ capture, offering a tunable platform to address the pressing need for efficient and sustainable carbon sequestration technologies [51, 89, 123]. However, despite recent advancements, several critical issues remain that need to be addressed before its widespread implementation can be realized [124, 125]. These challenges span the functionalization methods themselves, a comprehensive understanding of the underlying CO₂ capture mechanisms, and the practical aspects of application in real-world scenarios. Overcoming these hurdles will unlock the vast potential of functionalized graphene, paving the way for its integration into diverse CO₂ capture systems [114].

One of the primary challenges lies in the functionalization methods employed to modify graphene's surface [126]. While numerous techniques, including covalent and non-covalent functionalization, have been explored to enhance CO₂ adsorption capacity, each method presents its own set of limitations [54, 97]. Covalent functionalization, which involves the formation of chemical bonds between functional

Table 1. A literature review on the included paper in this review.

Entry	Year	Country	Author	Functionalized Graphene	Results	Ref.
1	2025	China	R. Navik et al.	N ₂ /H ₂ plasma treatment graphene-sorbent	<ul style="list-style-type: none"> Capacity from 1.6 to 3.3 mmol/g. The range for DAC from 0.14 to 1.3 mmol/g. Selectivity of 42 and 87 was increased following plasma for 5 and 10 min. 	[54]
2	2024	Fnce	Y. Khadiri et al.	CS-GO@HKUST-1 xerogel graphene-sorbent	<ul style="list-style-type: none"> SBET reaching 923 m² g⁻¹. HKUST-1 exhibited stability for 2 days when in an aqueous at RT. The MOF and CS@HKUST-1 experienced considerable degradation within a 1 day. 	[58]
4	2024	China	F. Yang et al.	ultra-thin Pebax MMMs incorporated by GO	<ul style="list-style-type: none"> The graphene display elevated meso and micro surface areas. H₂SO₄ during the graphene oxidation process resulted in an enhanced CO₂ adsorption capacity GO/Pebax demonstrated a CO₂/N₂ The CO₂ permeance is measured at 400 GPU, as 106 cm³ (STP) cm² s⁻¹ cmHg⁻¹. 	[67]
5	2024	India	R. K. Jha et al.	monolithic graphene oxide	<ul style="list-style-type: none"> Dynamic capacity for CO₂ capture is 1.65 mmol g⁻¹ at RT. Regenerability is 98.8%, 	[70]
6	2024	China	L. Zhang et al.	ZIF-8@GO	<ul style="list-style-type: none"> Pressure of 0.2 MPa, attains a 1850 GPU, exhibiting selectivity for N₂/CO₂ for mixed gases of 18.3 and 32.3. Air pressure (1.2 MPa), exhibit a theoretical selectivity of 13.4. 	[71]
7	2024	Poland	S. Saha et al.	graphene and nickel nano particle	<ul style="list-style-type: none"> A enhancement in photocurrent was observed, rising from -5.7 to -11 mA/cm² as a result of the CO₂ reduction process. 	[73]
8	2023	China	B. Yao et al.	MOFs@GO composite	<ul style="list-style-type: none"> CO₂ adsorption 194.1 cm³/g, an ideal selectivity CO₂ over N₂ of 276.5, at 273 K. HKUST-1 into GO results in enhancements of 50.6% and 138.13%. 	[75]
9	2023	Spain	Barbarin et al.	reduced graphene oxide (rGO) and functionalized polymer particles	<ul style="list-style-type: none"> CO₂ adsorption capacity in N₂ adsorption at 25 °C and pressure of 1 atm. Aerogels exhibit a degree of nitrogen phobicity, with selectivity values between 470 and 621. A CO₂ adsorption approaching 2 mmol/g along with an selectivity of 620. 	[74]
10	2023	Spain	I. Pruna et al.	dendrimer-modified graphene oxide (GO) aerogels	<ul style="list-style-type: none"> Measurement is 2.23 mmol.g⁻¹ at a PAMAM/CNT ratio of 0.6/0.12 (mg mL⁻¹). 	[76]
11	2023	China	Z. Liu et al.	GO nanosheets	<ul style="list-style-type: none"> A porous GO adsorbent demonstrates a CO₂ adsorption capacity of 2.24 mmol/g. Method demonstrates the broad applicability of various multivalent cations. 	[80]
12	2023	China	Z. Gu et al.	porous graphene	<ul style="list-style-type: none"> The preference for CO₂ over (N₂) is evident, The role of H₂O often overlooked in earlier theoretical CO₂ filtration. 	[81]
13	2023	India	S. Roy et al.	super-expanded freestanding 3D reduced graphene oxide foams	<ul style="list-style-type: none"> Foam exhibited a specific surface area of 767 m²/g, particularly its elevated CO₂ adsorption 4.17 mmol/g. The process of hydrogenating CO₂ to produce formate achieved a maximum yield of 24.3% at a temperature of 120 °C. 	[77]
14	2022	Spain	Barbarin et al.	graphene/polymer monolithic	<ul style="list-style-type: none"> The increased of micropores is attributed to the role of polymer particles, which as spacers among (rGO) platelets. The increased microporosity has enhanced performance, in selectivity of CO₂ adsorption relative to N₂. 	[78]
15	2022	UAE	H. Zhao et al.	hybrid graphene oxide/MOFs	<ul style="list-style-type: none"> GO/MOF were predicted based on CO₂ adsorption for separating CO₂ from nitrogen. Formulation of GO/CuBTC exhibiting highest (GO) content, specifically 65% performance in provided that there is no stacking of the GO. 	[79]
16	2022	Taiwan	C. Hu et al.	Pebax-GO/PDMS/PSf	<ul style="list-style-type: none"> Membrane containing 1 wt% GO exhibited gas separation, achieving a CO₂ permeability of 54.5 GPU and a CO₂/N₂ selectivity of 36.9 at 35 °C and 0.1 MPa. MMMs containing 1 wt% GO loading enhanced CO₂ 208.9 GPU, achieving a CO₂/N₂ selectivity of 40 at a 35 °C and 0.7 MPa. 	[86]

continue of Table 1

17	2021	China	J. Wang et al.	Mg/DOBDC MOF@GO	<ul style="list-style-type: none"> • Mg/DOBDC MOF@GOw-30, incorporating 30 mL of GO, exhibited CO₂ adsorption 8.60 mmol g⁻¹ at 0.1 MPa and 25 °C. 	[82]
18	2021	China	Z. Shen et al.	B, N co-doped carbon nanomaterial (B/N-CN _s)	<ul style="list-style-type: none"> • B/N-CN_s demonstrates a capacity for selective capture of CO₂. • CO₂ absorption and CO₂/N₂ separation efficiency of B/N-CN_s attributed to the presence hierarchically porous architecture. 	[83]
19	2021	China	K. Xia et al.	Porous graphene materials (PGMs)	<ul style="list-style-type: none"> • Gas adsorption indicate the uptake of CO₂ and H₂ by PGMs is influenced by pore structure surface chemistry. 	[87]
20	2020	Spain	N. Politakos et al.	Graphene-Based Monolithic Nanostructures	<ul style="list-style-type: none"> • The selectivity of this monolith for capturing CO₂ in comparison to N₂ at 25 °C and is measured at 53. 	[84]
21	2020	Spain	N. Politakos et al.	Reduced Graphene Oxide/ Polymer Monolithic	<ul style="list-style-type: none"> • The integration of the polymer within the structures enhances the solvent resistance of the composites, attributed to the establishment of crosslinks establishment of crosslinks between the polymer and rGO. • The SSA and the DF were identified as factors in achieving elevated CO₂ capacity and selectivity for CO₂ over N₂. 	[85]
22	2020	UAE	M. Verghase et al.	UV-irradiated graphene oxide foam (UV-GOF)	<ul style="list-style-type: none"> • Performance of CO₂ adsorption was assessed based on several criteria, including capacity, selectivity, re-generability, kinetics, isosteric heat of sorption, and hydrophilicity. 	[88]
23	2020	China	M. Wang et al.	Penta-graphene	<ul style="list-style-type: none"> • The adsorbed CO₂ experienced a shift from physisorption to chemisorption with the parameter increasing from 0.025 to 0.030. 	[64]
24	2020	China	S. Shang et al.	CuBTC@GO	<ul style="list-style-type: none"> • CuBTC exhibited a CO₂ adsorption capacity of 8.02 mmol/g at 273 K and 1 bar. • CO₂/N₂ selectivity was achieved CuBTC@1%GO. 	[89]
25	2020	UK	D. Xia et al.	Reduced-graphene-oxide (rGO) aerogels	<ul style="list-style-type: none"> • Elevated heating rates exceeding 700 °C.min⁻¹, while leading to a decrease in energy consumption. • Evaluation of the CO₂ adsorption of MgAl- MMO/rGO hybrid aerogels is increased temperature and elevated CO₂ pressure. 	[90]
26	2020	Korea	J. Heo et al.	tertiary-amine-stabilized gold nanoparticles (Au NPs), graphene oxide (GO)	<ul style="list-style-type: none"> • The capacity CO₂ capture is in the design of a CO₂ capture membrane • The polar characteristics of polyelectrolytes facilitated capture of CO₂ by tertiary amines. 	[91]
27	2020	Greece	E. Thomou et al.	silylation of organically modified graphene oxide	<ul style="list-style-type: none"> • The porous heterostructure exhibiting highest surface was selected examination of its CO₂ adsorption. 	[94]
28	2019	Spain	Pruna et al.	Ethylenediamine-modified graphene oxide	<ul style="list-style-type: none"> • The CO₂ adsorption characteristics of modified aerogels were evaluated. 	[97]
29	2019	USA	F. Zhou et al.	Ultrathin, ethylenediamine-functionalized graphene oxide	<ul style="list-style-type: none"> • A performance in CO₂ separation was achieved, CO₂ permeance of 660 GPU and a CO₂/N₂ selectivity exceeding 500 at 75 °C. 	[92]
30	2019	Iran	Nazari-Kodahi et al.	Graphene Oxide/TiO ₂	<ul style="list-style-type: none"> • The GO/TiO₂ nanocomposite is designed for the selective adsorption of CO₂ over N₂, with an of CO₂ over N₂, with an emphasis on predicting its CO₂ adsorption capacity within binary gas mixtures of CO₂ and N₂. 	[98]

continue of Table 1

31	2018	China	G. Qin et al.	graphene-like C ₃ N	<ul style="list-style-type: none"> • The interaction between CO₂ and C₃N can be substantially enhanced through the application of electrochemical techniques. 	[99]
32	2018	China	Y. He et al.	graphene-carried -SO ₃ and Ag nanoparticles	<ul style="list-style-type: none"> • Ag@SGO at 0.25 g/L resulted CO₂ hydrate formation being time frame of 200 to 250 minutes. By the 1000-minute mark, the gas consumption had achieved a level of 7.62-0.16 mmol per mL of water. 	[93]
33	2018	Japan	G. Huang et al.	Pebax/Ionic liquid modified graphene oxide	<ul style="list-style-type: none"> • H₂, CO₂, O₂, N₂, CH₄) and mixed gases (CO₂/H₂, CO₂/N₂) the membranes was evaluated at 25 °C 4 bar. • An enhancement exceeding 90% in CO₂/N₂ selectivity and a 50% increase in CO₂ permeability have been observed (MMMs). 	[95]
34	2018	Pakistan	Sarfraz et al.	graphene oxide- and MOF-integrated Ultrason	<ul style="list-style-type: none"> • CO₂ permeability and CO₂/N₂ permselectivity as a result of the synergistic effects produced by the integrated nanofillers. 	[96]
35	2018	Korea	S. Park et al.	Transition-Metal-Porphyrin-like Graphene	<ul style="list-style-type: none"> • Sc- and V-functionalized porphyrin-like graphenes have the capability to selectively adsorb CO₂ from gas mixtures at low CO₂ pressures. 	[101]
36	2018	Italy	R. Rea et al.	PPO/Graphene Composites	<ul style="list-style-type: none"> • The findings indicate minor incorporations of graphene into polymers may improve permselectivity and reinforce their characteristics. 	[102]
37	2017	Singapore	P. Li et al.	Amorphous Carbon with Ultrafine MgO Nanocrystallites	<ul style="list-style-type: none"> • The enhanced rGO@MgO/C nanocomposite demonstrates an impressive capacity for CO₂ capture, achieving up to 31.5 wt% at a temperature of 27 °C and a pressure of 1 bar CO₂, as well as 22.5 wt% under conditions that simulate flue gas. 	[100]
38	2017	USA	F. Zhou et al.	Ultrathin graphene oxide-based hollow fiber membranes	<ul style="list-style-type: none"> • Layered GO-based hollow fiber membranes, characterized by a thickness of less than 20 nanometers, have been developed through a straightforward coating technique. 	[103]
39	2016	Australia	X. Tan et al.	Hexagonal boron nitride and graphene(h-BN)	<ul style="list-style-type: none"> • A considerable quantity of injected negative charges is across the h-BN strips of the P-BN/G, enabling the regulation of CO₂ capture and through the toggling states within the P-BN/G framework. 	[104]
40	2016	Saudi Arabia	M. Karunakaran et al.	Graphene oxide doped ionic liquid ultrathin	<ul style="list-style-type: none"> • GO/ionic liquid complex exhibit characteristics in terms of permeability, with a CO₂ flux of 37 GPU, and selectivity, achieving a CO₂/N₂ selectivity of 130. 	[105]

continue of Table 1

41	2016	China	Y. Dai et al.	Imidazole functionalized graphene oxide/PEBAX mixed	<ul style="list-style-type: none"> • The selectivity of CO₂ over N₂ reaches a value of 105.5, accompanied by a CO₂ permeability of 76.2 Barrer (where 1 Barrer is equivalent to 10⁻¹⁰ cm³(STP) cm cm⁻² s⁻¹ cmHg⁻¹) • The separation of CO₂ from N₂ in MMMs is efficient at lower temperature. 	[107]
42	2016	Australia	E. Haque et al.	Boron Functionalized Graphene Oxide-Organic Frameworks	<ul style="list-style-type: none"> • The measured SSA of the synthesized GOF is 506 m²/g, is approximately 11 times greater than the surface area of the original GO, recorded at 46 m²/g. 	[107]
43	2016	China	Y. Wang et al.	Graphene-Like Poly(triazine imide)	<ul style="list-style-type: none"> • PTI demonstrates a high efficacy in the separation of nitrogen (N₂) from CO₂ achieving a selectivity of 273 and a nitrogen permeance of 106 GPU. 	[109]
44	2016	China	G. Dong et al.	Graphene Oxide Nanosheets Based Novel Facilitated Transport	<ul style="list-style-type: none"> • The incorporation of GO has the potential to markedly enhance both the permeance of CO₂ and the selectivity of CO₂ over N₂. 	[108]
45	2016	China	F. Liu et al.	Nitrogen-Doped Graphene-Like MesoMacroporous Carbons	<ul style="list-style-type: none"> • The distinctive multi-layered architecture and the significant abundance of in GMCs substantially the exposure and accessibility of the immobilized nitrogen sites to CO₂. 	[111]
46	2016	Singapore	S. Chowdhury et al.	Three-dimensional (3D) crumpled graphene-based porous adsorbents	<ul style="list-style-type: none"> • The hierarchical porous graphene-based materials exhibit a rapid, stable, and reversible capacity for CO₂ absorption, achieving a high uptake of 2.45 mmol.g⁻¹ at a temperature of 25 °C and a pressure of 1 bar. 	[68]
47	2016	India	P. Bhanja et al.	imine-functionalized graphene oxide (IFGO)	<ul style="list-style-type: none"> • IFGO demonstrates a commendable CO₂ capacity of 8.10 mmol g⁻¹ at 273 K and 2.10 mmol g⁻¹ (9.24 wt%) at 298 K, both measured under 3 bar. 	[110]
48	2015	Sweden	G. S. Rao et al.	graphene-like ZnO monolayer	<ul style="list-style-type: none"> • A comprehensive set of calculations produced the optimal binding for the CO₂ gas on a ZnO monolayer. 	[112]
49	2015	China	F. Q. Liu et al.	Covalently-grafted Polyethyleneimine	<ul style="list-style-type: none"> • The materials produced exhibit surface areas, robust covalent between polyethyleneimine (PEI) and graphene, as well as thermal conductivity. 	[113]
					<ul style="list-style-type: none"> • The double-vacancy in graphene exhibits a stronger binding affinity for metal 	

continue of Table 1

50	2015	Australia	S. A. Tawfik et al.	metal-doped graphene	dopants compared to the single-vacancy. as each of the dopants—calcium (Ca), scandium (Sc), and yttrium (Y)-is capable of binding up to five molecules of carbon dioxide (CO ₂).	[114]
51	2015	Singapore	S. Chowdhury et al.	mesoporous TiO ₂ /graphene oxide	• The adsorption isotherms of pure components for CO ₂ were evaluated at temperatures of 0, 25, and 50 °C, with pressure conditions reaching up to 100 kPa.	[116]
52	2015	China	Y. Shen et al.	Novel Polyvinyl Amine/Chitosan/Graphene oxide	• The results from the gas separation experiments utilizing a CO ₂ /N ₂ (10:90 incorporation of (GO) may enhance the selectivity for CO ₂ over N ₂ .	[117]
53	2014	Singapore	G. K. Parshetti et al.	Plant derived porous graphene nanosheets	• PGLNS demonstrate as adsorbents for the capture of CO ₂ following combustion processes. At 25 °C and 1 bar, the maximum CO ₂ adsorption capacity reached 2.43 mmol g ⁻¹ , significantly surpassing that of other competing CO ₂ adsorbents.	[118]
54	2014	China	J. Shen et al.	Laminar Graphene Oxide	• The incorporation of molecular-sieving interlayer spaces and diffusion pathways in the GO has resulted in membranes that exhibit remarkable preferential CO ₂	[119]
55	2013	USA	A.Alhwaige et al.	Biobased chitosan hybrid aerogels with superior adsorption with graphene	• (BET) surface area experiences a significant enhancement, rising from 153 to 415 m ² /g upon the incorporation of 20 wt% GO into the chitosan adsorbent.	[120]
56	2012	Korea	V. Chandra et al.	N-doped carbon produced by chemical activation of polypyrrole functionalized graphene sheets	• N-doped porous carbon synthesized demonstrates a selective adsorption capacity for CO ₂ (4.3 mmol g ⁻¹) compared to N ₂ (0.27 mmol g ⁻¹) at 298 K.	[121]
56	2012	Korea	V. Chandra et al.	N-doped carbon produced by chemical activation of polypyrrole functionalized graphene sheets	• N-doped porous carbon synthesized demonstrates a selective adsorption capacity for CO ₂ (4.3 mmol g ⁻¹) compared to N ₂ (0.27 mmol g ⁻¹) at 298 K.	[121]
57	2011	Australia	Y. Jiao et al.	graphene-like boron nitride reaction pathway validated	• The identification of three stationary states and two transition states within the reaction pathway validated through a minimum energy pathway search.	[122]

groups and the graphene lattice, can introduce structural defects that compromise graphene’s intrinsic properties, such as its high surface area and electrical conductivity [127]. Furthermore, the harsh reaction conditions often required for covalent functionalization can lead to irreversible damage and make it difficult to control the degree and distribu-

tion of functional groups. Non-covalent functionalization, on the other hand, relies on weaker interactions like van der Waals forces, $\pi - \pi$ stacking, and hydrogen bonding to attach functional groups to graphene [128–130]. While this approach preserves graphene’s structural integrity, the weaker interactions can result in lower stability and a greater

tendency for functional groups to detach under operating conditions. Moreover, many functionalization methods utilize expensive reagents, complex procedures, and generate hazardous byproducts, hindering their scalability and economic viability for large-scale CO₂ capture applications [110, 131]. Future research should prioritize the development of sustainable and cost-effective functionalization techniques that minimize environmental impact and are amenable to industrial production. This includes exploring greener synthetic routes, utilizing bio-derived functional groups, and developing scalable deposition methods for uniform functionalization [132].

A deeper understanding of the CO₂ capture mechanisms at the molecular level is also crucial for optimizing functionalization strategies. While it is known that functional groups enhance CO₂ adsorption through various interactions, such as acid-base reactions, hydrogen bonding, and electrostatic interactions, the precise nature and contribution of each interaction are not fully elucidated [133–135]. Computational modeling and advanced spectroscopic techniques are needed to unravel the intricate details of CO₂ adsorption on functionalized graphene, including the binding energies, adsorption kinetics, and the influence of environmental factors such as temperature, pressure, and humidity [134–136]. This knowledge will enable the rational design of functional groups with enhanced CO₂ affinity and selectivity, leading to more efficient and targeted CO₂ capture materials [137, 138]. For instance, the incorporation of nitrogen-containing functional groups, such as amines and pyridines, has shown promise in enhancing CO₂ capture due to their basic nature and ability to form strong interactions with acidic CO₂ molecules [139–141]. However, further research is needed to optimize the type, density, and arrangement of these functional groups to maximize their CO₂ capture potential. Moreover, the synergistic effects of combining different functional groups should be explored to create multifunctional graphene-based materials with tailored CO₂ capture properties [142, 143].

In addition to the challenges associated with functionalization methods and mechanisms, practical applications of functionalized graphene for CO₂ capture face several hurdles. One major concern is the long-term stability of functionalized graphene under operating conditions. CO₂ capture processes often involve exposure to high temperatures, corrosive gases, and fluctuating humidity levels, which can degrade the functional groups and compromise the CO₂ capture performance [144–146]. Therefore, it is essential to develop strategies to enhance the stability of functionalized graphene, such as encapsulating the functional groups within protective layers, crosslinking the functional groups to form a robust network, or grafting the functional groups onto the graphene surface through strong covalent bonds. Furthermore, the scalability of functionalized graphene production is a critical factor for its widespread adoption. Current production methods often involve batch processes that are difficult to scale up and result in inconsistent product quality. Continuous manufacturing processes, such as chemical vapor deposition (CVD) and electrochemical exfoliation, offer promising routes for large-scale production of

functionalized graphene with controlled properties. However, further optimization of these processes is needed to reduce production costs and improve product uniformity [78, 106].

Opportunities abound in tailoring functionalized graphene for specific applications, such as flue gas treatment and direct air capture (DAC) [147]. Flue gas treatment involves capturing CO₂ from the exhaust streams of power plants and industrial facilities, where CO₂ concentrations are relatively high (typically 10 – 15%). Functionalized graphene can be designed to selectively capture CO₂ from flue gas mixtures containing other gases, such as nitrogen, oxygen, and water vapor [148]. Direct air capture, on the other hand, aims to capture CO₂ directly from the atmosphere, where CO₂ concentrations are much lower (around 400 ppm). This requires highly efficient and selective CO₂ capture materials that can operate under ambient conditions. Functionalized graphene can be engineered with ultra-high surface areas and tailored functional groups to capture CO₂ from dilute air streams. Furthermore, functionalized graphene can be integrated with other CO₂ capture technologies, such as absorption, adsorption, and membrane separation, to create hybrid systems with enhanced performance. For example, functionalized graphene can be incorporated into polymer membranes to improve their CO₂ permeability and selectivity [90, 149].

Overcoming these challenges will pave the way for the practical implementation of functionalized graphene as an efficient and sustainable solution for CO₂ capture. Future research should focus on developing scalable and cost-effective functionalization methods, gaining a deeper understanding of CO₂ capture mechanisms at the molecular level, enhancing the long-term stability of functionalized graphene, and tailoring functionalized graphene for specific applications. By addressing these key issues, functionalized graphene can play a significant role in mitigating climate change and transitioning to a low-carbon economy. The development of advanced characterization techniques, such as in-situ spectroscopy and microscopy, will be crucial for monitoring the performance of functionalized graphene under operating conditions and identifying degradation mechanisms. Collaboration between researchers, industry partners, and policymakers will be essential to accelerate the development and deployment of functionalized graphene-based CO₂ capture technologies. With continued innovation and investment, functionalized graphene has the potential to become a game-changing material for CO₂ capture, contributing to a cleaner and more sustainable future [150, 151].

A short survey of other techniques for CO₂ capture technology

Amine based-solvents for CO₂ capture technology: Opportunities and challenges

The increasing concentration of atmospheric CO₂ and its contribution to global climate change have intensified the urgent need for effective and economically viable CO₂ capture technologies [152, 153]. Among the various approaches, chemical absorption using amine-based solvents remains a leading technology due to its estab-

lished performance and amenability to retrofitting existing infrastructure. We examine novel amine formulations, including blends, sterically hindered amines, and phase-change solvents, evaluating their performance in terms of absorption capacity, reaction kinetics, energy efficiency, and resistance to degradation. Amine-based solvents are widely recognized as the preferred agents for CO₂ capture applications. The most frequently utilized amine solvents include diglycolamine (DGA) [154, 155], 2-amino-2-methylpropanol (AMP) [156, 157], methyldiethanolamine (MDEA) [158, 159], monoethanolamine (MEA) [160, 161], and piperazine [162, 163]. Although these solvents exhibit varying chemical and cost structures, they have all been empirically validated for their efficacy in CO₂ capture. However, a significant concern associated with the post-combustion carbon capture (PCCC) technique is the corrosion of equipment, which can be attributed to either the amine solvent itself or the CO₂-saturated amine solvent. Certain amines, such as MEA and its degradation products, are particularly noted for their corrosive properties. Consequently, recent research has concentrated on examining the corrosion behavior of carbon steel when exposed to either amine solvents or CO₂-laden amine solutions.

Amine-based CO₂ capture technology presents both significant opportunities and persistent challenges [23, 164]. The tunability of amine chemistry allows for the design of solvents tailored for enhanced performance, including faster absorption kinetics through sterically hindered amines or catalysts, improved CO₂ capacity to minimize circulation rates, and reduced regeneration energy via phase-change solvents and advanced stripping techniques [165, 166]. Computational methods are accelerating the discovery of novel amines with optimized properties [134, 167, 168]. Further opportunities lie in process intensification, such as employing advanced packing materials and integrating renewable energy for solvent regeneration. Addressing solvent degradation and emissions through robust amine development, solvent reclamation, and emission control strategies is also crucial. However, the high energy penalty of solvent regeneration remains a major obstacle, alongside challenges related to solvent degradation from flue gas contaminants, corrosion, solvent emissions, and the complexities of scaling up the technology. High viscosity in some promising solvents and limited long-term performance data also pose significant hurdles. Overcoming these challenges through sustained research and development is essential for realizing the full potential of amine-based CO₂ capture [169, 170].

Cryogenic and hydrate-based techniques for CO₂ capture technology: Opportunities and challenges

As the urgency to mitigate anthropogenic CO₂ emissions intensifies, innovative CO₂ capture technologies beyond traditional amine scrubbing are gaining increasing attention. Cryogenic and hydrate-based CO₂ capture methods offer potentially attractive alternatives for specific applications [171, 172]. Cryogenic separation, involving CO₂ condensation at low temperatures [173], can achieve high purity CO₂ streams, while hydrate formation, where CO₂ molecules are trapped within a water-based crystalline structure, of-

fers the potential for energy-efficient separation [174, 175]. This part examines the fundamental principles, recent advancements, and challenges associated with cryogenic and hydrate-based CO₂ capture techniques. Cryogenic separation technology operates on the principle of exploiting the differing phase transition characteristics of various components [176, 177]. This is achieved through a sequence of processes involving compression, cooling, and expansion, which facilitate the effective separation of these components. The technology of cryogenic separation is characterized by its relative simplicity, resulting in a CO₂ gas that exhibits higher purity and is more amenable to transportation [178]. In comparison to alternative separation methods, this approach is also more environmentally sustainable and non-corrosive [179]. It is also capable of eliminating various other harmful gases, such as sulfur oxides, mercury, and nitrogen oxides, among others. Cryogenic separation technology possesses a well-established industrial framework and can be readily scaled to meet industrial demands. Nevertheless, the challenges posed by the extremely low temperatures, significant energy requirements, and substantial capital expenditures associated with the equipment necessary for the CO₂ gas condensation process hinder its advancement. Zhang et al. introduced a hybrid system that integrates cryogenic separation for carbon capture with liquid air energy storage (CS-LAES), achieving a CO₂ capture efficiency of 99.97%. However, this system is associated with significant energy demands. This indicates that substantial advancements are necessary before cryogenic separation technology can be broadly implemented in industrial applications [180].

Gas hydrate is classified as a clathrate compound, characterized by a cage-like crystalline structure that emerges from the interaction of small gas molecules with water under specific temperature and pressure conditions [181]. The water molecules serve as the framework for these cages, forming intricate structures through hydrogen bonding. Within these cages, gas molecules are accommodated, engaging with the host water molecules via van der Waals forces, resulting in a relatively stable non-stoichiometric crystal formation. To date, three distinct types of hydrate crystal structures have been identified: type I, type II, and type H. The process of separating compound gas mixtures involves utilizing the varying degrees of difficulty with which different gases form hydrates, thereby facilitating effective separation [31]. The hydrate-based gas separation (HBGS) technology offers notable benefits, including a substantial capacity for gas storage and the ability to reversibly form and decompose hydrates. Consequently, this technology has emerged as a promising method for capturing CO₂ [183? –185]. In the process of capture, CO₂ molecules, characterized by their small size and non-polar nature, are particularly well-suited for occupying the larger cages within the hydrate structure [186]. When compared to other gases present in the mixture, the phase equilibrium pressure of CO₂ hydrate at ambient temperature is below 10 MPa, which leads to a considerably reduced formation pressure for CO₂ hydrate. This phenomenon enhances the affinity of CO₂ for occupying appropriate cages within the hydrate crystal lattice.

During the release phase, pure CO₂ gas can be extracted by dissociating the CO₂ hydrate cages, while the water is subsequently returned to its liquid state [187].

Mixed-matrix membranes (MMMs) techniques for CO₂ capture technology: Opportunities and challenges

Mixed-matrix membranes (MMMs) have emerged as a promising class of materials for CO₂ capture, aiming to surpass the limitations of conventional polymeric membranes [182]. The escalating urgency to mitigate greenhouse gas emissions has spurred extensive research into advanced separation technologies, with membrane separation offering a potentially energy-efficient and cost-effective alternative to traditional methods. MMMs, designed by incorporating porous fillers into a continuous polymer matrix, seek to combine the favorable processing characteristics of polymers with the superior separation performance of inorganic materials [188, 189]. This approach allows for the creation of tailored membranes with enhanced CO₂ permeability, selectivity, and mechanical stability, addressing key challenges in CO₂ capture from flue gas and other industrial sources. This work presents a comprehensive exploration of recent advances in MMMs for CO₂ capture, focusing on the influence of filler material, polymer matrix, and membrane fabrication techniques on separation performance. Following the seminal evaluation conducted by Okumus et al. [190] regarding the potential applications of mixed matrix membranes (MMMs), several significant review articles have emerged. These publications categorize MMMs into three distinct types: liquid-polymer [191, 192], solid-polymer [193], and solid-liquid polymer MMMs [194, 195]. In recent years, there has been a growing interest in the development of solid-polymer MMMs [196–203]. Solid fillers that utilize a polymer matrix in multifunctional materials (MMMs) can be categorized into conventional types, including carbon molecular sieves (CMSs), silicas, and zeolites, as

well as innovative types such as carbon nanotubes (CNTs), metal-organic frameworks (MOFs), graphene oxides (GO), spherical materials, layered materials, and delaminated materials [182]. The structural representations of several of these materials are illustrated in figure 32.

Mixed-matrix membranes (MMMs) hold considerable promise for revolutionizing CO₂ capture, offering opportunities to surpass the limitations of conventional polymeric membranes [40]. Their design, which strategically incorporates porous fillers within a continuous polymer matrix, aims to synergize the processability of polymers with the superior separation capabilities of inorganic materials [204]. This approach holds the potential to create membranes with tailored properties, notably enhanced CO₂ permeability, selectivity, and mechanical stability, addressing key challenges in capturing CO₂ from various industrial sources. However, the path to widespread adoption of MMMs is not without its challenges. Achieving uniform filler dispersion within the polymer matrix remains a critical hurdle, as filler agglomeration can lead to defects and reduced separation efficiency. Poor compatibility between the filler and polymer can also create interfacial voids, compromising selectivity and mechanical strength. Furthermore, increasing filler loading to enhance performance can lead to processing difficulties and embrittlement. Ensuring long-term stability under real-world conditions, along with scalable and cost-effective fabrication methods, are also key challenges that need to be addressed. Despite these obstacles, the potential benefits of MMMs in terms of energy efficiency, cost-effectiveness, and versatility make them a compelling area of research and development for advanced CO₂ capture technologies [95, 205].

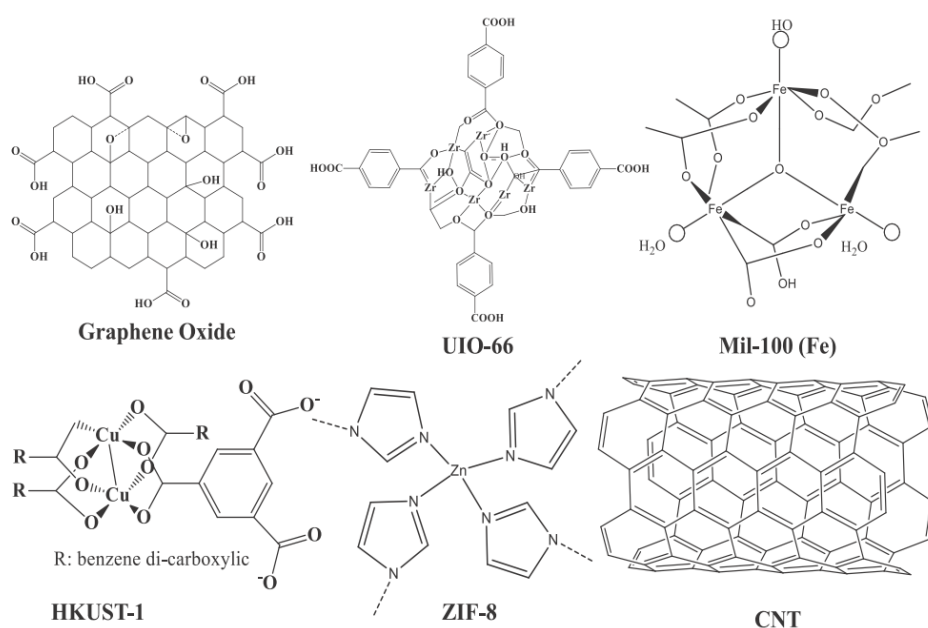


Figure 32. The chemical structure of graphene oxide, UIO-66, MIL-100 (Fe), HKUST-1, ZIF-8, and CNTs as fillers in MMMs for CO₂ capture technology [American Chemical Society, copyright 2023, with permission of open access] [182]

Deep eutectic solvents (DESs) techniques for CO₂ capture technology: Opportunities and challenges

The utilization of deep eutectic solvents (DESs) for CO₂ capture represents an innovative approach that employs an economical and eco-friendly solvent to effectively extract CO₂ from exhaust gases [206, 207]. DESs are classified as low-transition temperature mixtures (LTTMs), created by combining two or more solid and/or liquid substances in precise molar ratios, resulting in a mixture with a melting point that is lower than that of its constituent components [208]. A class of solvents suitable for an integrated capture–desorption–bio-fixation process includes DESs. One of the primary benefits of DESs is their ability to be functionalized or tailored to specific applications. In this context, carbon dioxide is sequestered within the eutectic structure created by hydrogen bonding interactions between the hydrogen bond acceptor (HBA) and the hydrogen bond donor (HBD), facilitated by weak physical interactions such as van der Waals forces. DESs are emerging as a promising class of solvents for CO₂ capture, presenting both significant opportunities and considerable challenges. Their key advantage lies in their tunable properties, low cost, and biodegradability, offering a greener alternative to traditional amine-based solvents. By carefully selecting the components of the eutectic mixture, DESs can be tailored to exhibit high CO₂ solubility and selectivity under specific operating conditions. However, the application of DESs for CO₂ capture is not without its difficulties. One major challenge is their relatively high viscosity, which can hinder mass transfer and increase energy consumption during the absorption and desorption processes. Furthermore, the long-term stability of DESs in the presence of moisture and other flue gas components needs to be thoroughly investigated to ensure reliable performance. The design and optimization of efficient CO₂ absorption processes using DESs require a deeper understanding of their thermodynamic and kinetic properties, as well as the development of appropriate process configurations. Despite these challenges, the potential benefits of DESs in terms of cost, environmental impact, and tunability make them a valuable area of research for next-generation CO₂ capture technologies. Further research is needed to overcome the viscosity limitations, improve stability, and optimize process design to fully realize the potential of DESs for efficient and sustainable CO₂ capture [209].

Metal organic frameworks (MOFs) techniques for CO₂ capture technology: Opportunities and challenges

The reticular chemistry associated with metal-organic frameworks (MOFs) has developed into a significant methodology for the synthesis of porous materials, enabling the meticulous design of their internal structures to tackle global energy and environmental challenges [24, 210]. Among these challenges, the capture and utilization of CO₂ emerge as significant issues that the domain of MOFs is particularly equipped to tackle [211]. The chemistry of MOFs has advanced to a stage where it is possible to methodically and logically adjust the relationship between the structure of the MOF and its targeted properties [212]. In the last

quarter-century, four significant advancements have positioned MOFs as viable contenders for applications related to CO₂. The initial aspect is the development and proliferation of reticular chemistry, which encompasses the design, functionalization, and structural modification of porous, crystalline, and extended solid materials. The application of these structural design concepts has enabled the utilization of MOFs in various elements of CO₂ capture. In the initial stages of research in this domain, MOFs characterized by extensive surface areas were employed for the purposes of capturing, concentrating, and ultimately storing and transporting CO₂. The subsequent development has involved leveraging the tunability of the internal pore environment of MOFs to improve their affinity for selective CO₂ capture from mixed gas systems under low-pressure conditions [213, 214].

The incorporation of amine groups within the MOF framework (Amine functionalized MOFs) has proven to be a highly effective strategy for enhancing CO₂ adsorption, particularly at low partial pressures relevant to post-combustion capture [215]. Recent efforts have focused on developing novel amine-functionalized MOFs with improved stability, CO₂ selectivity, and regeneration properties. Examples include: a) MOFs with covalently grafted amines [216, 217]; b) MOFs with encapsulated amines [218, 219]; c) MOFs with diamine linkers [220, 221]. The presence of water vapor in flue gas can significantly reduce the CO₂ capture performance of many MOFs (Water-Stable MOFs) [219, 222, 223]. Therefore, the development of water-stable MOFs is crucial for practical applications. Recent research has focused on: a) Synthesizing MOFs with hydrophobic building blocks [224]; b) Modifying MOFs with protective coatings [225, 226]; c) Designing MOFs with water-tolerant pore structures [227]. Combining MOFs with other materials (MOF Composites), such as polymers [228], carbon materials [229], or zeolites [230], can lead to synergistic effects and improved CO₂ capture performance. Examples include: a) Mixed-matrix membranes (MMMs) incorporating MOFs; b) MOF-carbon composites; c) MOF-zeolite composites.

Despite the significant progress in MOF-based CO₂ capture, several challenges remain: I) Cost: The high cost of some MOF materials and synthesis procedures can be a barrier to widespread adoption. Future research should focus on developing cost-effective MOF synthesis methods and exploring the use of inexpensive starting materials. II) Scalability: Scaling up the production of MOFs to meet the demands of large-scale CO₂ capture applications is a major challenge. Developing continuous and scalable MOF synthesis processes is crucial. III) Long-Term Stability: The long-term stability of MOFs under real-world conditions needs to be further investigated. Developing robust MOFs that can withstand exposure to moisture, contaminants, and harsh operating conditions is essential. IV) Process Integration: Integrating MOF-based CO₂ capture into existing industrial processes requires careful consideration of process design, energy consumption, and economic feasibility. Economic feasibility pertains to the evaluation of the cost-effectiveness of a proposed initiative or investment,

confirming its financial viability in relation to the available resources. Developing optimized process configurations and regeneration strategies is crucial. The development of novel materials, improved capture mechanisms, and optimized process integration strategies will pave the way for the successful deployment of MOFs for sustainable CO₂ capture. Further collaborative efforts between researchers, industry, and policymakers are needed to accelerate the transition from laboratory research to real-world applications [231, 232].

Application of ionic liquids (ILs) for CO₂ capture technology: Opportunities and challenges

Numerous ionic liquids (ILs) exhibit significant promise for CO₂ capture technologies [233]. These ILs can be categorized into two distinct molecular structures: (I) protic ionic liquids (PILs), which possess the ability to donate a proton, and (II) aprotic ionic liquids (AILs), which lack this proton-donating capability [234]. The initial investigations into CO₂ capture utilizing ILs primarily concentrate on the effectiveness of carbon dioxide uptake (UP_{CO₂}) through a diverse range of physically non-grafted ILs [235]. Studies have indicated that the interactions between the anionic component of the IL and CO₂ significantly influence UP_{CO₂}, particularly when contrasted with conventional solvents like toluene and n-hexane [13, 236–239]. Standard ILs, exemplified by [EMIM][Tf₂N], exhibited a notable capacity for carbon dioxide uptake across various operational conditions. In contrast, conventional molecular solvents displayed considerable carbon dioxide uptake primarily at elevated to moderate pressures. The field of ILs for CO₂ capture has witnessed significant advancements in recent years, with research efforts focused on improving CO₂ absorption capacity, selectivity, and process efficiency [240, 241].

A major focus has been on the development of functionalized ILs, where specific functional groups are incorporated into the IL structure to enhance CO₂ interactions. These functional groups can include amines, amino acids, and other CO₂-reactive moieties. In addition, amine-functionalized ILs exhibit enhanced CO₂ absorption capacity due to the chemical reaction between CO₂ and the amine group. Recent research has focused on optimizing the amine functionality and improving the stability and regeneration of these ILs. For example, studies have explored the use of sterically hindered amines to improve CO₂ desorption kinetics [242, 243]. Moreover, amino acid-functionalized ILs offer a biocompatible and environmentally friendly alternative to traditional amine-based solvents [244]. Recent studies have investigated the CO₂ absorption performance of various amino acid-functionalized ILs and their blends with other solvents [245, 246]. Furthermore, Task-Specific Ionic Liquids (TSILs) are designed with specific functional groups tailored for particular CO₂ capture applications [247–249]. This approach allows for fine-tuning of the IL properties to optimize CO₂ absorption and selectivity. The development of TSILs with high selectivity for CO₂ over N₂ is crucial for post-combustion CO₂ capture from flue gas. Recent research has focused on designing TSILs that exploit specific interactions between CO₂ and the IL, such as quadrupole

interactions or hydrogen bonding. Supported Ionic Liquid Membranes (SILMs) consist of a thin layer of IL supported on a porous membrane [250–252]. This configuration combines the advantages of ILs with the membrane separation technology, offering potential for high CO₂ flux and selectivity. Recent advances include: I) Developing novel membrane supports with high porosity and mechanical strength; II) Improving the long-term stability of SILMs; III) Exploring the use of functionalized ILs in SILMs.

A comparison viewpoint between presented technologies based on economic factors for CO₂ capture

Selecting the optimal CO₂ capture technology demands a comprehensive evaluation, weighing not just capture efficiency and scalability, but crucially, and the economic realities of implementation [253]. Functionalized graphene, while offering a tantalizing prospect due to its high surface area and tunable properties, faces hurdles regarding production costs and long-term durability in industrial environments. A rigorous economic analysis is essential to determine if its performance gains justify the investment. Amine-based solvents, a more established technology, benefit from a mature understanding of their performance characteristics; however, their energy-intensive regeneration process and potential for corrosion vulnerabilities necessitate a careful economic analysis to optimize operational expenses and mitigate potential long-term liabilities. Cryogenic and hydrate-based techniques, known for their potentially high CO₂ capture rates, are burdened by significant energy demands and complex infrastructure prerequisites, demanding a thorough economic analysis to assess their competitiveness against alternative methods [254]. Mixed-matrix membranes (MMMs) seek to capitalize on the combined advantages of polymers and inorganic materials, but the challenges associated with their fabrication and ensuring long-term performance stability necessitate a detailed economic analysis to ascertain their overall cost-effectiveness and reliability. Deep Eutectic Solvents (DESs) offer an attractive alternative, boasting low cost and tunable properties; however, their limited CO₂ capacity relative to other options and potential viscosity-related operational issues must be subjected to a rigorous economic analysis. Metal-Organic Frameworks (MOFs), lauded for their exceptional surface areas and design flexibility, face challenges related to their high synthesis costs and sensitivity to moisture, making a detailed economic analysis imperative to gauge their viability for large-scale deployment [255].

At present, amine-based solvents likely represent the most readily deployable solution for industrial CO₂ capture, leveraging existing infrastructure and operational expertise. However, technologies such as MOFs and advanced membrane systems hold considerable promise for the future. Continued research and development efforts focused on reducing costs and enhancing the stability of these emerging technologies could very well alter the landscape. Ultimately, a comprehensive lifecycle economic analysis, tailored to the specific requirements of each industrial application, is crucial for making informed decisions regarding the selection and implementation of the most sustainable and economi-

cally sound CO₂ capture technology.

A short review on practical successful CO₂ capture technology around the world

As the impacts of climate change increasingly threaten our environment, researchers and policymakers are urgently seeking strategies to mitigate our carbon emissions. One innovative approach gaining traction is carbon dioxide capture technology. This method entails the extraction of carbon emissions generated by industrial activities, followed by their transportation to designated storage sites where they are sequestered from the atmosphere. Various implementations of this technology have emerged worldwide, yielding notable success stories. In this section, we will examine several of the most effective CO₂ capture initiatives globally, analyze the factors contributing to their success or failure, and emphasize the opportunities for replicating these efforts. Here, some of these successful projects are as follow: I) Petra Nova Plant, Texas, USA: Petra Nova stands out as one of the most effective carbon capture initiatives worldwide, situated in Texas, United States. Initiated in 2017, this project represents a partnership between NRG Energy and JX Nippon Oil & Gas Exploration. II) Sleipner Project, North Sea: The Sleipner Project, located in the North Sea, represents the inaugural commercial-scale initiative for carbon capture. This project effectively captures carbon dioxide released during natural gas extraction and subsequently stores it beneath the seabed. Since its inception in 1996, the Sleipner Project has successfully sequestered over 25 million tonnes of CO₂. III) Gorgon Project, Australia: The Gorgon Project represents a substantial initiative in carbon capture technology, situated in Western Australia. This endeavor involves the extraction of carbon dioxide from natural gas production processes, subsequently sequestering it within subterranean reservoirs. Its importance lies in its ability to showcase the feasibility of implementing carbon capture solutions on a large scale, even in isolated regions. IV) Boundary Dam Power Station, Canada: The Boundary Dam Power Station, located in Saskatchewan, Canada, represents the inaugural commercial-scale initiative for carbon capture and storage associated with a coal-fired power facility. This pioneering project successfully captures 90% of the carbon dioxide emissions produced by the plant and subsequently sequesters them underground. V) Quest Project, Canada: The Quest Project, situated in proximity to Edmonton, Canada, is an initiative focused on carbon capture and storage. This project is designed to capture carbon dioxide emissions generated by a bitumen upgrading facility and subsequently sequester these emissions deep within the earth [37].

2. Conclusion

The pressing necessity to tackle the increasing levels of atmospheric CO₂ has driven the advancement of cutting-edge carbon capture technologies, with functionalized graphene emerging as a prominent option due to its remarkable characteristics. This review has underscored the notable progress made in utilizing functionalized graphene for CO₂ capture, highlighting its extensive surface area, robust

mechanical properties, and adjustable chemical functionalities. These qualities establish functionalized graphene as a flexible material that can significantly improve the output of CO₂ capture processes in various industrial settings. Investigating functionalization techniques has been essential for enhancing the yield of graphene-based materials. Recent research has shown that novel methods, including plasma treatment and the integration of metal-organic frameworks (MOFs), can greatly boost the CO₂ adsorption selectivity and capacity of functionalized graphene. The capacity to modify the surface chemistry of graphene with different functional groups has created new opportunities for enhancing its interaction with CO₂, thus improving its effectiveness in practical situations where other gases, such as nitrogen and water vapor, may be present. Furthermore, the combination of functionalized graphene with other advanced materials has yielded encouraging outcomes in improving CO₂ capture efficiency. Hybrid materials that merge the porous characteristics of MOFs with the conductive features of graphene have exhibited enhanced adsorption and regeneration capabilities. This collaborative strategy not only leverages the strengths of each component but also sets the stage for the creation of next-generation carbon capture technologies that are both effective and economically sustainable. Sustainability is a critical factor in the development of CO₂ capture technologies. As research advances, it is vital to assess both the environmental implications and the economic viability of functionalized graphene materials. Conducting life-cycle assessments and cost-benefit analyses will help ensure that the technologies created are not only efficient in lowering CO₂ emissions but also environmentally sound and economically viable. Furthermore, implementing strategies for the recycling and reuse of functionalized graphene can enhance sustainable practices in carbon capture. The shift from laboratory research to practical applications presents notable challenges. Pilot studies play a key role in evaluating the operational effectiveness of functionalized graphene across different industrial settings. Collaborative initiatives among researchers, engineers, and industry partners will be essential for scaling CO₂ capture technologies and incorporating them into current infrastructures. Such partnerships can lead to the creation of viable solutions that tackle the urgent issue of climate change while fostering a sustainable low-carbon economy. In summary, functionalized graphene holds significant promise for CO₂ capture, with the ability to greatly reduce greenhouse gas emissions. Ongoing research and innovation in this area are crucial for realizing the full potential of functionalized graphene and for formulating effective carbon capture strategies that support global decarbonization efforts. By concentrating on improvements in functionalization methods, enhancing CO₂ selectivity and sorption capacity, integrating with advanced materials, ensuring sustainability, and applying findings in real-world scenarios, the field can make meaningful strides in addressing one of the most pressing challenges of our era: climate change. The prospects for functionalized graphene in carbon dioxide capture are promising, and

through continued interdisciplinary collaboration, it has the potential to significantly contribute to a sustainable and low-carbon future.

Authors contributions

Authors have contributed equally in preparing and writing the manuscript.

Availability of data and materials

The data that support the findings of this study are available from the corresponding author, upon reasonable request.

Conflict of interests

The authors declare that they have no known competing financial interests or personal relationships that could have appeared to influence the work reported in this paper.

References

- [1] S. V. Ollinger, C. L. Goodale, K. Hayhoe, and J. P. Jenkins. *Mitigation and Adaptation Strategies for Global Change*, **13**(2008): 467–485.
DOI: <https://doi.org/10.1007/s11027-007-9128-z>.
- [2] Z. Xie, X. Zhang, Z. Zhang, and Z. Zhou. *Adv. Mater.*, **29**(2017): 1605891.
DOI: <https://doi.org/10.1002/adma.201605891>.
- [3] K. L. Kadam. *Energy Convers. Manage.*, **38**(1997):S505–S510.
DOI: [https://doi.org/10.1016/S0196-8904\(96\)00318-4](https://doi.org/10.1016/S0196-8904(96)00318-4).
- [4] C. Cao, H. Liu, Z. Hou, F. Mehmood, J. Liao, and W. Feng. *Energies*, **13**(2020):600.
- [5] P. Kelemen, S. M. Benson, H. Pilorge, P. Psarras, and J. Wilcox. *Frontiers in Climate*, **1**(2019).
DOI: <https://doi.org/10.3389/fclim.2019.00009>.
- [6] N. Mac Dowell, P. S. Fennell, N. Shah, and G. C. Maitland. *Nature Climate Change*, **7**(2017):243–249.
DOI: <https://doi.org/10.1038/nclimate3231>.
- [7] J. D. Figueroa, T. Fout, S. Plasynski, H. McIlvried, and R. D. Srivastava. *International Journal of Greenhouse Gas Control*, **2**(2008): 9–20.
DOI: [https://doi.org/10.1016/S1750-5836\(07\)00094-1](https://doi.org/10.1016/S1750-5836(07)00094-1).
- [8] B. Li, Y. Duan, D. Luebke, and B. Morreale. *Applied Energy*, **102**(2013):1439–1447.
DOI: <https://doi.org/10.1016/j.apenergy.2012.09.009>.
- [9] S. Valluri, V. Claremboux, and S. Kawatra. *Journal of Environmental Sciences*, **113**(2022):322–344.
DOI: <https://doi.org/10.1016/j.jes.2021.05.043>.
- [10] E. Alper and O. Yuksel Orhan. *Petroleum*, **3**(2017):109–126.
DOI: <https://doi.org/10.1016/j.petlm.2016.11.003>.
- [11] N. Li, L. Mo, and C. Unluer. *Journal of CO₂ Utilization*, **65**(2022): 102237.
DOI: <https://doi.org/10.1016/j.jcou.2022.102237>.
- [12] A. Gulzar, A. Gulzar, M. B. Ansari, F. He, S. Gai, and P. Yang. *Chemical Engineering Journal Advances*, **3**(2020):100013.
DOI: <https://doi.org/10.1016/j.cej.2020.100013>.
- [13] J. F. Brennecke and B. E. Gurkan. *The Journal of Physical Chemistry Letters*, **1**(2010):3459–3464.
DOI: <https://doi.org/10.1021/jz1014828>.
- [14] P. Bains, P. Psarras, and J. Wilcox. *Prog. Energy Combust. Sci.*, **63**(2017):146–172.
DOI: <https://doi.org/10.1016/j.pecs.2017.07.001>.
- [15] A. Stangeland. *International Journal of Greenhouse Gas Control*, **1**(2007):418–429.
DOI: [https://doi.org/10.1016/S1750-5836\(07\)00087-4](https://doi.org/10.1016/S1750-5836(07)00087-4).
- [16] O. Mohammadi, M. Golestanzadeh, and M. Abdouss. *New J. Chem.*, **41**(2017):11471–11497.
DOI: <https://doi.org/10.1039/C7NJ02515G>.
- [17] D. Ma, J. Deng, and Z. Zhang. *Atmos. Environ.*, **81**(2013):188–198.
DOI: <https://doi.org/10.1016/j.atmosenv.2013.09.012>.
- [18] V. Jimenez, A. Ramirez-Lucas, J. A. Diaz, P. Sanchez, and A. Romero. *Environ. Sci. Technol.*, **46**(2012):7407–7414.
DOI: <https://doi.org/10.1021/es2046553>.
- [19] S. Vasudevan, S. Farooq, I. A. Karimi, M. Saeys, M. C. G. Quah, and R. Agrawal. *Energy*, **103**(2016):709–714.
DOI: <https://doi.org/10.1016/j.energy.2016.02.154>.
- [20] A. Sodiq, Y. Abdullatif, B. Aissa, A. Ostovar, N. Nassar, M. El-Naas, and A. Amhamed. *Environmental Technology & Innovation*, **29**(2023):102991.
DOI: <https://doi.org/10.1016/j.eti.2022.102991>.
- [21] T. Lockwood. *Energy Procedia*, **114**(2017):2658–2670.
DOI: <https://doi.org/10.1016/j.egypro.2017.03.1850>.
- [22] D. J. Beerling, E. P. Kantzas, M. R. Lomas, R. M. Wade, P. and-Eufrasio, P. Renforth, B. Sarkar, M. G. Andrews, R. H. James, C. R. Pearce, J. F. Mercure, H. Pollitt, P. B. Holden, N. R. Edwards, M. Khanna, L. Koh, S. Quegan, N. F. Pidgeon, I. A. Janssens, J. Hansen, and S. A. Banwart. *Nature*, **583**(2020):242–248.
DOI: <https://doi.org/10.1038/s41586-020-2448-9>.
- [23] F. Meng, Y. Meng, T. Ju, S. Han, L. Lin, and J. Jiang. *Renewable and Sustainable Energy Reviews*, **168**(2022):112902.
DOI: <https://doi.org/10.1016/j.rser.2022.112902>.
- [24] S. A. Mazari, L. Ghalib, A. Sattar, M. M. Bozdar, A. Qayoom, I. Ahmed, A. Muhammad, R. Abro, A. Abdulkareem, S. Nizamuddin, H. Baloch, and N. M. Mubarak. *International Journal of Greenhouse Gas Control*, **96**(2020):103010.
DOI: <https://doi.org/10.1016/j.ijggc.2020.103010>.
- [25] A. Brunetti, E. Drioli, Y. M. Lee, and G. Barbieri. *J. Membr. Sci.*, **454**(2014):305–315.
DOI: <https://doi.org/10.1016/j.memsci.2013.12.037>.
- [26] W. D. Jones. *J. Am. Chem. Soc.*, **142**(2020):4955–4957.
DOI: <https://doi.org/10.1021/jacs.0c02356>.
- [27] M. Bui, M. Fajardy, and N. Mac Dowell. *Fuel*, **213**(2018):164–175.
DOI: <https://doi.org/10.1016/j.fuel.2017.10.100>.
- [28] S. Abuelgasim, W. Wang, and A. Abdalazeez. *Sci. Total Environ.*, **764**(2021):142892.
DOI: <https://doi.org/10.1016/j.scitotenv.2020.142892>.
- [29] C. Font-Palma, D. Cann, and C. Udemu. **7**(2021):58.
- [30] Y. T. Youns, A. K. Manshad, and J. A. Ali. *Fuel*, **349**(2023): 128680.
DOI: <https://doi.org/10.1016/j.fuel.2023.128680>.
- [31] L. Fu, Z. Ren, W. Si, Q. Ma, W. Huang, K. Liao, Z. Huang, Y. Wang, J. Li, and P. Xu. *Journal of CO₂ Utilization*, **66**(2022):102260.
DOI: <https://doi.org/10.1016/j.jcou.2022.102260>.
- [32] J. Pei, J. Chen, J. Wang, Z. Li, N. Li, and J. Kan. *Frontiers in Chemistry*, **12**(2024).
DOI: <https://doi.org/10.3389/fchem.2024.1448881>.
- [33] N. S. Sifat and Y. Haseli. *Energies*, **12**(2019):4143.
- [34] J. Yu, L. H. Xie, J.-R. Li, Y. Ma, J. M. Seminario, and P. B. Balbuena. *Chem. Rev.*, **117**(2017):9674–9754.
DOI: <https://doi.org/10.1021/acs.chemrev.6b00626>.

- [35] S. Kumar, R. Srivastava, and J. Koh. *Journal of CO₂ Utilization*, **41**(2020):101251. DOI: <https://doi.org/10.1016/j.jcou.2020.101251>.
- [36] P. Kumar and K. H. Kim. *Applied Energy*, **172**(2016):383–397. DOI: <https://doi.org/10.1016/j.apenergy.2016.03.095>.
- [37] P. Markewitz, W. Kuckshinrichs, W. Leitner, J. Linssen, P. Zapp, R. Bongartz, A. Schreiber, and T. E. Muller. *Energy Environ. Sci.*, **5**(2012):7281–7305. DOI: <https://doi.org/10.1039/C2EE03403D>.
- [38] M. Rezaei, A. Nezamzadeh-Ejhieh, and A. R. Massah. *Energy Fuels*, **38**(2024):8406–8436. DOI: <https://doi.org/10.1021/acs.energyfuels.4c00160>.
- [39] M. Rezaei, A. Nezamzadeh-Ejhieh, and A. R. Massah. *Ecotoxicol. Environ. Saf.*, **269**(2024):115927. DOI: <https://doi.org/10.1016/j.ecoenv.2024.115927>.
- [40] S. A. Ali, W. U. Mulk, A. U. Khan, H. S. Bhatti, M. Hadeed, J. Ahmad, K. Habib, S. N. Shah, and M. Younas. *Energy Fuels*, **38**(2024):18330–18366. DOI: <https://doi.org/10.1021/acs.energyfuels.3c02377>.
- [41] S. A. Ali, A. U. Khan, W. U. Mulk, H. Khan, S. Nasir Shah, A. Zahid, K. Habib, M. U. H. Shah, M. H. D. Othman, and S. Rahman. *Energy Fuels*, **37**(2023):15394–15428. DOI: <https://doi.org/10.1021/acs.energyfuels.3c02377>.
- [42] W. U. Mulk, S. A. Ali, S. N. Shah, M. U. H. Shah, Q. J. Zhang, M. Younas, A. Fatehizadeh, M. Sheikh, and M. Rezakazemi. *Journal of CO₂ Utilization*, **75**(2023):102555. DOI: <https://doi.org/10.1016/j.jcou.2023.102555>.
- [43] W. U. Mulk, M. U. Hassan Shah, S. N. Shah, Q. J. Zhang, A. L. Khan, M. Sheikh, M. Younas, and M. Rezakazemi. *Environ. Res.*, **237**(2023):116879. DOI: <https://doi.org/10.1016/j.envres.2023.116879>.
- [44] S. A. Ali, S. N. Shah, M. U. H. Shah, and M. Younas. *Chemosphere*, **311**(2023):136913. DOI: <https://doi.org/10.1016/j.chemosphere.2022.136913>.
- [45] S. A. Ali, W. U. Mulk, Z. Ullah, H. Khan, A. Zahid, M. U. H. Shah, and S. N. Shah. *Energies*, **15**(2022):9098. DOI: <https://doi.org/10.3390/en15090908>.
- [46] W. Wei and X. Qu. *Small*, **8**(2012):2138–2151. DOI: <https://doi.org/10.1002/sml.201200104>.
- [47] I. Craciun, M. F. and Khrapach, M. D. Barnes, and S. Russo. *J. Phys.: Condens. Matter*, **25**(2013):423201. DOI: <https://doi.org/10.1088/0953-8984/25/42/423201>.
- [48] C. Chung, Y. K. Kim, D. Shin, S. R. Ryoo, B. H. Hong, and D. H. Min. *Acc. Chem. Res.*, **46**(2013):2211–2224. DOI: <https://doi.org/10.1021/ar300159f>.
- [49] P. Avouris and C. Dimitrakopoulos. *Mater. Today*, **15**(2012):86–97. DOI: [https://doi.org/10.1016/S1369-7021\(12\)70044-5](https://doi.org/10.1016/S1369-7021(12)70044-5).
- [50] X. Wan, Y. Huang, and Y. Chen. *Acc. Chem. Res.*, **45**(2012):598–607. DOI: <https://doi.org/10.1021/ar200229q>.
- [51] R. Balasubramanian and S. Chowdhury. *J. Mater. Chem. A*, **3**(2015):21968–21989. DOI: <https://doi.org/10.1039/C5TA04822B>.
- [52] J. Li, M. Hou, Y. Chen, W. Cen, Y. Chu, and S. Yin. *Appl. Surf. Sci.*, **399**(2017):420–425. DOI: <https://doi.org/10.1016/j.apsusc.2016.11.157>.
- [53] L. An, S. Liu, L. Wang, J. Wu, Z. Wu, C. Ma, Q. Yu, and X. Hu. *Indust. Eng. Chem. Res.*, **58**(2019):3349–3358. DOI: <https://doi.org/10.1021/acs.iecr.8b06122>.
- [54] R. Navik, E. Wang, X. Ding, H. Yunyi, Y. Liu, and J. Li. *J. Energ. Chem.*, **100**(2025):653–664. DOI: <https://doi.org/10.1016/j.jechem.2024.09.019>.
- [55] A. Taheri Najafabadi. *Renewable and Sustainable Energy Reviews*, **41**(2015):1515–1545. DOI: <https://doi.org/10.1016/j.rser.2014.09.022>.
- [56] A. I. Osman, M. Hefny, M. I. A. Abdel Maksoud, A. M. Elgarahy, and D. W. Rooney. *Environ. Chem. Lett.*, **19**(2021):797–849. DOI: <https://doi.org/10.1007/s10311-020-01133-3>.
- [57] N. Hsan, P. K. Kumar, and S. J. Koh. *Journal of CO₂ Utilization*, **59**(2022):101958. DOI: <https://doi.org/10.1016/j.jcou.2022.101958>.
- [58] Y. Khadiri, A. Legrand, C. Volklinger, A. Anouar, S. Royer, A. El Kadib, and T. Loiseau. *J. Dhainaut, Materials Today Sustainability*, **28**(2024):100998. DOI: <https://doi.org/10.1016/j.mtsust.2024.100998>.
- [59] G. Mishra, A. Warda, and S. P. Shah. *Journal of Building Engineering*, **62**(2022):105356. DOI: <https://doi.org/10.1016/j.job.2022.105356>.
- [60] A. M. Varghese, K. S. K. Reddy, N. Bhorla, S. Singh, J. Pokhrel, and G. N. Karanikolos. *Chem. Eng. J.*, **420**(2021):129677. DOI: <https://doi.org/10.1016/j.cej.2021.129677>.
- [61] A. H. Berger and A. S. Bhowm. *Energy Procedia*, **4**(2011):562–567. DOI: <https://doi.org/10.1016/j.egypro.2011.01.089>.
- [62] S. Schaefer, V. Fierro, A. Szczurek, M. T. Izquierdo, and A. Celzard. *Int. J. Hydrogen Energy*, **41**(2016):17442–17452. DOI: <https://doi.org/10.1016/j.ijhydene.2016.07.262>.
- [63] J. Jin, Z. Wen, S. Li, and J. Huang. *Greenhouse Gases: Science and Technology*, **13**(2023):357–368. DOI: <https://doi.org/10.1002/ghg.2201>.
- [64] M. Wang, Z. Zhang, Y. Gong, S. Zhou, J. Wang, Z. Wang, S. Wei, W. Guo, and X. Lu. *Appl. Surf. Sci.*, **502**(2020):144067. DOI: <https://doi.org/10.1016/j.apsusc.2019.144067>.
- [65] N. Tit, K. Said, N. M. Mahmoud, S. Kouser, and Z. H. Yamani. *Appl. Surf. Sci.*, **394**(2017):219–230. DOI: <https://doi.org/10.1016/j.apsusc.2016.10.052>.
- [66] R. M. Firdaus, A. Desforges, M. Emo, A. R. Mohamed, and B. Vigolo. *Nanomaterials*, **11**(2021):2419. DOI: <https://doi.org/10.3390/nano11020419>.
- [67] F. Yang, Y. Jin, J. Liu, H. Zhu, R. Xu, F. Xiangli, G. Liu, and W. Jin. *Chin. J. Chem. Eng.*, **67**(2024):257–267. DOI: <https://doi.org/10.1016/j.cjche.2023.11.012>.
- [68] S. Chowdhury and R. Balasubramanian. *Indust. Eng. Chem. Res.*, **55**(2016):7906–7916. DOI: <https://doi.org/10.1021/acs.iecr.5b04052>.
- [69] B. Luan, B. Elmegeen, M. A. Kuroda, Z. Gu, G. Lin, and S. Zeng. *ACS Nano*, **16**(2022):6274–6281. DOI: <https://doi.org/10.1021/acsnano.2c00213>.
- [70] R. Kumar Jha, H. Bhunia, and S. Basu. *Chem. Eng. Sci.*, **285**(2024):119572. DOI: <https://doi.org/10.1016/j.ces.2023.119572>.
- [71] L. Zhang, Y. Zhao, H. Yu, L. Chen, X. Liu, A. Zhang, Z. Deng, and J. Z. Ou. *Chem. Eng. J.*, **494**(2024):153250. DOI: <https://doi.org/10.1016/j.cej.2024.153250>.
- [72] Z. Safaei, E. and Talebi and V. Ghafarinia. *Journal of the Taiwan Institute of Chemical Engineers*, (2024):105352. DOI: <https://doi.org/10.1016/j.jtice.2024.105352>.
- [73] S. Saha, G. Mohan Das, and G. Vadivel. *Colloids Surf. Physicochem. Eng. Aspects*, **687**(2024):133415. DOI: <https://doi.org/10.1016/j.colsurfa.2024.133415>.

- [74] I. Barbarin, M. Fidanchevska, N. Politakos, L. Serrano-Cantador, J. A. Cecilia, D. Martin, O. Sanz, and R. Tomovska. *Indust. Eng. Chem. Res.*, **63**(2024):7073–7087, . DOI: <https://doi.org/10.1021/acs.iecr.3c02989>.
- [75] B. Yao, Y. Wang, Z. Fang, Y. Hu, Z. Ye, and X. Peng. *Microporous Mesoporous Mater.*, **361**(2023):112758. DOI: <https://doi.org/10.1016/j.micromeso.2023.112758>.
- [76] A. I. Pruna, A. Carcel, A. Benedito, and E. Gimenez. *International Journal of Molecular Sciences*, **24**(2023):3865, .
- [77] S. Roy, B. Dasgupta Ghosh, K. Lim Goh, H. Jun Ahn, and Y. W. Chang. *Chem. Eng. J.*, **466**(2023):143326. DOI: <https://doi.org/10.1016/j.cej.2023.143326>.
- [78] I. Barbarin, N. Politakos, L. Serrano-Cantador, J. A. Cecilia, O. Sanz, and R. Tomovska. *Microporous Mesoporous Mater.*, **337**(2022):111907, . DOI: <https://doi.org/10.1016/j.micromeso.2022.111907>.
- [79] H. Zhao, D. Bahamon, M. Khaleel, and L. F. Vega. *Chem. Eng. J.*, **449**(2022):137884, . DOI: <https://doi.org/10.1016/j.cej.2022.137884>.
- [80] Z. J. Liu, W. H. Zhang, M. J. Yin, Y. H. Ren, and Q. F. An. *Sep. Purif. Technol.*, **312**(2023):123448, . DOI: <https://doi.org/10.1016/j.seppur.2023.123448>.
- [81] Z. Gu, Z. Cai, B. Elmegreen, M. Steiner, and B. Luan. *Chem. Eng. J.*, **474**(2023):145778. DOI: <https://doi.org/10.1016/j.cej.2023.145778>.
- [82] J. Wang, S. Cui, Z. Li, S. Wen, P. Ning, S. Lu, P. Lu, L. Huang, and Q. Wang. *Chem. Eng. J.*, **415**(2021):128859, . DOI: <https://doi.org/10.1016/j.cej.2021.128859>.
- [83] Z. Shen, Y. Song, C. Yin, X. Luo, Y. Wang, and X. Li. *Microporous Mesoporous Mater.*, **322**(2021):111158, . DOI: <https://doi.org/10.1016/j.micromeso.2021.111158>.
- [84] N. Politakos, I. Barbarin, L. S. Cantador, J. A. Cecilia, E. Mehravar, and R. Tomovska. *Indust. Eng. Chem. Res.*, **59**(2020):8612–8621, . DOI: <https://doi.org/10.1021/acs.iecr.9b06998>.
- [85] N. Politakos, I. Barbarin, T. Cordero-Lanzac, A. Gonzalez, R. Zangi, and R. Tomovska. *Polymers*, **12**(2020):936, .
- [86] C. C. Hu, H. H. Yeh, C. P. Hu, R. L. G. Lecaros, C. C. Cheng, W. S. Hung, H. A. Tsai, K. R. Lee, and J. Y. Lai. *Journal of the Taiwan Institute of Chemical Engineers*, **135**(2022):104379, . DOI: <https://doi.org/10.1016/j.jtice.2022.104379>.
- [87] K. Xia, R. Xiong, Y. Chen, D. Liu, Q. Tian, Q. Gao, B. Han, and C. Zhou. *Colloids Surf. Physicochem. Eng. Aspects*, **622**(2021):126640, . DOI: <https://doi.org/10.1016/j.colsurfa.2021.126640>.
- [88] A. M. Varghese, K. S. K. Reddy, S. Singh, and G. N. Karanikolos. *Chem. Eng. J.*, **386**(2020):124022, . DOI: <https://doi.org/10.1016/j.cej.2020.124022>.
- [89] S. Shang, Z. Tao, C. Yang, A. Hanif, L. Li, D. C. W. Tsang, Q. Gu, and J. Shang. *Chem. Eng. J.*, **393**(2020):124666. DOI: <https://doi.org/10.1016/j.cej.2020.124666>.
- [90] D. Xia, H. Li, J. Mannering, P. Huang, X. Zheng, A. Kulak, D. Baker, D. Iruretagoyena, and R. Menzel. *Adv. Funct. Mater.*, **30**(2020):2002788, . DOI: <https://doi.org/10.1002/adfm.202002788>.
- [91] J. Heo, M. Choi, D. Choi, H. Jeong, H. Y. Kim, H. Jeon, S. W. Kang, and J. Hong. *J. Membr. Sci.*, **601**(2020):117905. DOI: <https://doi.org/10.1016/j.memsci.2020.117905>.
- [92] F. Zhou, H. N. Tien, Q. Dong, W. L. Xu, H. Li, S. Li, and M. Yu. *J. Membr. Sci.*, **573**(2019):184–191, . DOI: <https://doi.org/10.1016/j.memsci.2018.11.080>.
- [93] Y. He and F. Wang. *J. Mater. Chem. A*, **6**(2018):22619–22625. DOI: <https://doi.org/10.1039/C8TA08785G>.
- [94] E. Thomou, E. K. Diamanti, A. Enotiadis, K. Spyrou, E. Mitsari, L. G. Boutsika, A. Sapalidis, E. Moreton Alfonsin, O. De Luca, and D. Gournis. *Frontiers in Chemistry*, **8**(2020):564838. DOI: <https://doi.org/10.3389/fchem.2020.564838>.
- [95] G. Huang, A. P. Isfahani, A. Muchtar, K. Sakurai, B. B. Shrestha, D. Qin, D. Yamaguchi, E. Sivaniah, and B. Ghalei. *J. Membr. Sci.*, **565**(2018):370–379. DOI: <https://doi.org/10.1016/j.memsci.2018.08.026>.
- [96] M. Sarfraz and M. Ba-Shammakh. *Polym. Bull.*, **75**(2018):5039–5059. DOI: <https://doi.org/10.1007/s00289-018-2301-6>.
- [97] A. Pruna, A. C. Carcel, A. Benedito, and E. Gimenez. *Appl. Surf. Sci.*, **487**(2019):228–235, . DOI: <https://doi.org/10.1016/j.apsusc.2019.05.098>.
- [98] S. Nazari Kudahi, A. Noorpoor, and N. M. Mahmoodi. *Iranian Journal of Chemistry and Chemical Engineering (IJCCE)*, **38**(2019):293–307.
- [99] G. Qin, Q. Cui, W. Wang, P. Li, A. Du, and Q. Sun. *Chemphyschem*, **19**(2018):2788–2795. DOI: <https://doi.org/10.1002/cphc.201800385>.
- [100] P. Li and H. C. Zeng. *Environ. Sci. Technol.*, **52**(2018):12998–13007. DOI: <https://doi.org/10.1021/acs.est.7b03308>.
- [101] S. Park, H. Bae, J. Ahn, H. Lee, and Y. Kwon. *ACS Omega*, **3**(2018):10554–10563, . DOI: <https://doi.org/10.1021/acsomega.8b01371>.
- [102] R. Rea, S. Ligi, M. Christian, V. Morandi, M. Giacinti Baschetti, and M. G. De Angelis. *Polymers*, **10**(2018):129.
- [103] F. Zhou, H. N. Tien, W. L. Xu, J. T. Chen, Q. Liu, E. Hicks, M. Fathizadeh, S. Li, and M. Yu. *Nature Communications*, **8**(2017):2017, . DOI: <https://doi.org/10.1038/s41467-017-02318-1>.
- [104] X. Tan, H. A. Tahini, and S. C. Smith. *Chem. Phys.*, **478**(2016):139–144. DOI: <https://doi.org/10.1016/j.chemphys.2016.04.001>.
- [105] M. Karunakaran, L. F. Villalobos, M. Kumar, R. Shevate, F. H. Akhtar, and K. V. Peinemann. *J. Mater. Chem. A*, **5**(2017):649–656. DOI: <https://doi.org/10.1039/C6TA08858A>.
- [106] Y. Dai, X. Ruan, Z. Yan, K. Yang, M. Yu, H. Li, W. Zhao, and G. He. *Sep. Purif. Technol.*, **166**(2016):171–180. DOI: <https://doi.org/10.1016/j.seppur.2016.04.038>.
- [107] E. Haque, M. M. Islam, E. Pourazadi, S. Sarkar, A. T. Harris, A. I. Minett, E. Yanmaz, S. M. Alshehri, Y. Ide, K. C. W. Wu, Y. V. Kaneti, Y. Yamauchi, and M. S. A. Hossain. *Chemistry – An Asian Journal*, **12**(2017):283–288. DOI: <https://doi.org/10.1002/asia.201601442>.
- [108] G. Dong, Y. Zhang, J. Hou, J. Shen, and V. Chen. *Indust. Eng. Chem. Res.*, **55**(2016):5403–5414. DOI: <https://doi.org/10.1021/acs.iecr.6b01005>.
- [109] Y. Wang, Q. Yang, C. Zhong, and J. Li. *J. Physic. Chem. C*, **120**(2016):28782–28788, . DOI: <https://doi.org/10.1021/acs.jpcc.6b08529>.
- [110] P. Bhanja, S. K. Das, A. K. Patra, and A. Bhaumik. *RSC Adv.*, **6**(2016):72055–72068. DOI: <https://doi.org/10.1039/C6RA13590K>.
- [111] F. Liu, K. Huang, S. Ding, and S. Dai. *J. Mater. Chem. A*, **4**(2016):14567–14571, . DOI: <https://doi.org/10.1039/C6TA06583J>.

- [112] G. S. Rao, T. Hussain, M. S. Islam, M. Sagynbaeva, D. Gupta, and P. Panigrahi. *R. Ahuja, Nanotechnology*, **27**(2016):015502, . DOI: <https://doi.org/10.1088/0957-4484/27/1/015502>.
- [113] F. Q. Liu, W. Li, J. Zhao, W. H. Li, D. M. Chen, L. S. Sun, L. Wang, and R. X. Li. *J. Mater. Chem. A*, **3**(2015):12252–12258, . DOI: <https://doi.org/10.1039/C5TA01536G>.
- [114] S. A. Tawfik, X. Y. Cui, S. P. Ringer, and C. Stampfl. *RSC Adv.*, **5**(2015):50975–50982. DOI: <https://doi.org/10.1039/C5RA09876A>.
- [115] J. Shen, G. Liu, K. Huang, W. Jin, K. R. Lee, and N. Xu. *Angew. Chem. Int. Ed.*, **54**(2015):578–582, . DOI: <https://doi.org/10.1002/anie.201409563>.
- [116] S. Chowdhury, G. K. Parshetti, and R. Balasubramanian. *Chem. Eng. J.*, **263**(2015):374–384. DOI: <https://doi.org/10.1016/j.cej.2014.11.037>.
- [117] Y. Shen, H. Wang, J. Liu, and Y. Zhang. *ACS Sustainable Chemistry & Engineering*, **3**(2015):1819–1829, . DOI: <https://doi.org/10.1021/acssuschemeng.5b00409>.
- [118] G. K. Parshetti and R. Chowdhury, S. Balasubramanian. *RSC Adv.*, **4**(2014):44634–44643. DOI: <https://doi.org/10.1039/C4RA05522E>.
- [119] J. Shen, G. Liu, K. Huang, W. Jin, K. R. Lee, and N. Xu. *Angew. Chem.*, **127**(2015):588–592, . DOI: <https://doi.org/10.1002/ange.201409563>.
- [120] A. A. Alhwaige, T. Agag, H. Ishida, and S. Qutubuddin. *RSC Adv.*, **3**(2013):16011–16020. DOI: <https://doi.org/10.1039/C3RA42022A>.
- [121] V. Chandra, S. U. Yu, S. H. Kim, Y. S. Yoon, D. Y. Kim, A. H. Kwon, M. Meyyappan, and K. S. Kim. *Chem. Commun.*, **48**(2012): 735–737. DOI: <https://doi.org/10.1039/C1CC15599G>.
- [122] Y. Jiao, A. Du, Z. Zhu, V. Rudolph, G. Q. Lu, and S. C. Smith. *Catal. Today*, **175**(2011):271–275. DOI: <https://doi.org/10.1016/j.cattod.2011.02.043>.
- [123] M. O. Aquatar, J. S. Mankar, U. Bhatia, S. S. Rayalu, and R. J. Kru- padam. *Journal of Environmental Chemical Engineering*, **9**(2021): 105839. DOI: <https://doi.org/10.1016/j.jece.2021.105839>.
- [124] A. H. Ruhaimi, C. N. C. Hitam, M. A. A. Aziz, N. H. A. Hamid, H. D. Setiabudi, and L. P. Teh. *Renewable and Sustainable Energy Reviews*, **167**(2022):112840. DOI: <https://doi.org/10.1016/j.rser.2022.112840>.
- [125] S. Chakraborty, R. Saha, and S. Saha. *Environ. Sci. Pollut. Res.*, **31**(2024):67633–67663. DOI: <https://doi.org/10.1007/s11356-023-30093-8>.
- [126] W. Yu, L. Sisi, Y. Haiyan, and L. Jie. *RSC Adv.*, **10**(2020):15328–15345, . DOI: <https://doi.org/10.1039/D0RA01068E>.
- [127] F. Banhart, J. Kotakoski, and A. V. Krashenninnikov. *ACS Nano*, **5**(2011):26–41. DOI: <https://doi.org/10.1021/nn102598m>.
- [128] V. Georgakilas, J. N. Tiwari, K. C. Kemp, J. A. Perman, A. B. Bourlinos, K. S. Kim, and R. Zboril. *Chem. Rev.*, **116**(2016):5464–5519. DOI: <https://doi.org/10.1021/acs.chemrev.5b00620>.
- [129] E. Y. Choi, T. H. Han, J. Hong, J. E. Kim, S. H. Lee, H. W. Kim, and S. O. Kim. *J. Mater. Chem.*, **20**(2010):1907–1912. DOI: <https://doi.org/10.1039/B919074K>.
- [130] J. A. Mann and W. R. Dichtel. *The Journal of Physical Chemistry Letters*, **4**(2013):2649–2657. DOI: <https://doi.org/10.1021/jz4010448>.
- [131] Z. Zhou, E. Davoudi, and B. Vaferi. *Journal of Environmental Chemical Engineering*, **9**(2021):106202, . DOI: <https://doi.org/10.1016/j.jece.2021.106202>.
- [132] Y. Liu, B. Sajjadi, W. Y. Chen, and R. Chatterjee. *Fuel*, **247**(2019): 10–18, . DOI: <https://doi.org/10.1016/j.fuel.2019.03.011>.
- [133] B. Yoon and G. A. Voth. *J. Am. Chem. Soc.*, **145**(2023):15663–15667. DOI: <https://doi.org/10.1021/jacs.3c03613>.
- [134] X. Yang, R. J. Rees, W. Conway, G. Puxty, Q. Yang, and D. A. Winkler. *Chem. Rev.*, **117**(2017):9524–9593, . DOI: <https://doi.org/10.1021/acs.chemrev.6b00662>.
- [135] K. Iida, D. Yokogawa, A. Ikeda, H. Sato, and S. Sakaki. *PCCP*, **11**(2009):8556–8559. DOI: <https://doi.org/10.1039/B906912G>.
- [136] X. E. Hu, Q. Yu, F. Barzagli, C. e. Li, M. Fan, K. A. M. Gasem, X. Zhang, E. Shiko, M. Tian, X. Luo, Z. Zeng, Y. Liu, and R. Zhang. *ACS Sustainable Chemistry & Engineering*, **8**(2020):6173–6193, . DOI: <https://doi.org/10.1021/acssuschemeng.9b07823>.
- [137] B. Li, Z. Zhang, Y. Li, K. Yao, Y. Zhu, Z. Deng, F. Yang, X. Zhou, G. Li, H. Wu, N. Nijem, Y. J. Chabal, Z. Lai, Y. Han, Z. Shi, S. Feng, and J. Li. *Angew. Chem. Int. Ed.*, **51**(2012):1412–1415, . DOI: <https://doi.org/10.1002/anie.201105966>.
- [138] M. Oschatz and M. Antonietti. *Energy Environ. Sci.*, **11**(2018): 57–70. DOI: <https://doi.org/10.1039/C7EE02110K>.
- [139] C. Zhang, W. Song, G. Sun, L. Xie, J. Wang, K. Li, C. Sun, H. Liu, C. E. Snape, and T. Drage. *Energy Fuels*, **27**(2013):4818–4823, . DOI: <https://doi.org/10.1021/ef400499k>.
- [140] S. Park, H. M. Lee, Y. S. Lee, S. An, J. Yang, and J. Kim. *ACS Applied Nano Materials*, **6**(2023):19611–19621, . DOI: <https://doi.org/10.1021/acsanm.3c02943>.
- [141] G. Lim, K. B. Lee, and H. C. Ham. *J. Physic. Chem. C*, **120**(2016): 8087–8095. DOI: <https://doi.org/10.1021/acs.jpcc.5b12090>.
- [142] N. Li, M. Almarri, X. I. Ma, and Q. f. Zha. *New Carbon Materials*, **26**(2011):470–478, . DOI: [https://doi.org/10.1016/S1872-5805\(11\)60093-0](https://doi.org/10.1016/S1872-5805(11)60093-0).
- [143] N. Li, J. Zhu, X. Ma, Q. Zha, and C. Song. *AIChE J.*, **59**(2013): 1236–1244, . DOI: <https://doi.org/10.1002/aic.13886>.
- [144] B. Ray, S. R. Churipard, and S. C. Peter. *J. Mater. Chem. A*, (): 26498–26527. DOI: <https://doi.org/10.1039/D1TA08862A>.
- [145] R. Barker, Y. Hua, and A. Neville. *Int. Mater. Rev.*, **62**(2017):1–31. DOI: <https://doi.org/10.1080/09506608.2016.1176306>.
- [146] Z. Xu, Z. Zhang, J. Huang, K. Yu, G. Zhong, F. Chen, X. Chen, W. Yang, and Y. Wang. *Construction and Building Materials*, **346**(2022):128399, . DOI: <https://doi.org/10.1016/j.conbuildmat.2022.128399>.
- [147] J. Ai, Z. Bacsik, K. Hallstenson, J. Yuan, A. Sugunan, and N. Hedin. *Chem. Eng. J.*, **506**(2025):159963. DOI: <https://doi.org/10.1016/j.cej.2025.159963>.
- [148] I. Nicotera, A. Enotiadis, and C. Simari. *Small*, **20**(2024):2401303. DOI: <https://doi.org/10.1002/sml.202401303>.
- [149] R. Lawal and M. M. Hossain. *Arabian Journal for Science and Engineering*, (2025). DOI: <https://doi.org/10.1007/s13369-025-09966-2>.

- [150] M. N. Naseer, A. A. Zaidi, K. Dutta, Y. A. Wahab, J. Jaafar, R. Nusrat, I. Ullah, and B. Kim. *Energy Reports*, **8**(2022):4252–4264. DOI: <https://doi.org/10.1016/j.egy.2022.02.301>.
- [151] F. Raganati and P. Ammendola. *Energy Fuels*, **38**(2024):13858–13905. DOI: <https://doi.org/10.1021/acs.energyfuels.4c02513>.
- [152] Z. L. Ooi, P. Y. Tan, L. S. Tan, and S. P. Yeap. *Chin. J. Chem. Eng.*, **28**(2020):1357–1367. DOI: <https://doi.org/10.1016/j.cjche.2020.02.029>.
- [153] D. Loachamin, J. Casierra, V. Calva, A. Palma-Cando, E. E. Avila, and M. Ricaurte. *ChemEngineering*, **8**(2024):129.
- [154] U. Zahid, F. N. Al Rowaili, M. K. Ayodeji, and U. Ahmed. *International Journal of Greenhouse Gas Control*, **57**(2017):42–51. DOI: <https://doi.org/10.1016/j.ijggc.2016.12.016>.
- [155] C. Yu, H. Ling, W. Cao, F. Deng, Y. Zhao, D. Cao, M. Tie, and X. Hu. *Chem. Eng. J.*, **495**(2024):153402, . DOI: <https://doi.org/10.1016/j.cej.2024.153402>.
- [156] M. Yu, S. Zhang, H. Wu, Z. Lian, M. Zhang, and Q. Zhong. *Indust. Eng. Chem. Res.*, **63**(2024):15735–15744, . DOI: <https://doi.org/10.1021/acs.iecr.4c01581>.
- [157] Z. Khoshraftar. *Sci. Rep.*, **15**(2025):1800. DOI: <https://doi.org/10.1038/s41598-025-86144-2>.
- [158] S. C. Tiwari, K. K. Pant, and S. Upadhyayula. *Indust. Eng. Chem. Res.*, **63**(2024):7578–7592. DOI: <https://doi.org/10.1021/acs.iecr.4c00192>.
- [159] Z. Wang, Z. Han, D. Liu, X. Yang, Z. Zhou, X. Wu, and S. Lu. *Sep. Purif. Technol.*, **357**(2025):130150, . DOI: <https://doi.org/10.1016/j.seppur.2024.130150>.
- [160] S. Zhou, Y. Zhu, H. Xi, Z. Hao, Z. Han, and C. Sun. *Chem. Eng. J.*, **485**(2024):149790, . DOI: <https://doi.org/10.1016/j.cej.2024.149790>.
- [161] L. Li, H. Yu, G. Puxty, S. Zhou, W. Conway, and P. Feron. *Indust. Eng. Chem. Res.*, **63**(2024):16019–16028, . DOI: <https://doi.org/10.1021/acs.iecr.4c02064>.
- [162] S. Jia, Y. Jiang, Y. Li, W. Chen, J. Huang, K. Wang, X. Q. Liu, and P. Cui. *Chem. Eng. J.*, **493**(2024):152561. DOI: <https://doi.org/10.1016/j.cej.2024.152561>.
- [163] B. J. Drewry, T. Mikoviny, A. Wisthaler, G. T. Rochelle, C. Stevens, and K. Erickson. *Indust. Eng. Chem. Res.*, (2025). DOI: <https://doi.org/10.1021/acs.iecr.4c03763>.
- [164] Z. Liang, K. Fu, R. Idem, and P. Tontiwachwuthikul. *Chin. J. Chem. Eng.*, **24**(2016):278–288. DOI: <https://doi.org/10.1016/j.cjche.2015.06.013>.
- [165] A. B. Rao, E. S. Rubin, D. W. Keith, and M. Granger Morgan. *Energy Policy*, **34**(2006):3765–3772, . DOI: <https://doi.org/10.1016/j.enpol.2005.08.004>.
- [166] N. Huser, O. Schmitz, and E. Y. Kenig. *Chem. Eng. Sci.*, **157**(2017):221–231. DOI: <https://doi.org/10.1016/j.ces.2016.06.027>.
- [167] M. Sharif, T. Han, T. Wang, X. Shi, M. Fang, D. Shuming, R. Meng, and X. Gao. *Chem. Eng. Res. Des.*, **204**(2024):524–535. DOI: <https://doi.org/10.1016/j.cherd.2024.03.005>.
- [168] W. Andreoni and F. Pietrucci. *J. Phys.: Condens. Matter*, **28**(2016):503003. DOI: <https://doi.org/10.1088/0953-8984/28/50/503003>.
- [169] L. B. Hamdy, C. Goel, J. A. Rudd, A. R. Barron, and E. Andreoli. *Materials Advances*, **2**(2021):5843–5880. DOI: <https://doi.org/10.1039/D1MA00360G>.
- [170] B. Dutcher, M. Fan, and A. G. Russell. *ACS Appl. Mater. Inter.*, **7**(2015):2137–2148. DOI: <https://doi.org/10.1021/am507465f>.
- [171] H. Dashti, L. Zhehao Yew, and X. Lou. *Journal of Natural Gas Science and Engineering*, **23**(2015):195–207. DOI: <https://doi.org/10.1016/j.jngse.2015.01.033>.
- [172] G. Pandey, T. Poothia, and A. Kumar. *Applied Energy*, **326**(2022):119900. DOI: <https://doi.org/10.1016/j.apenergy.2022.119900>.
- [173] G. Xu, L. Li, Y. Yang, L. Tian, T. Liu, and K. Zhang. *Energy*, **42**(2012):522–529, . DOI: <https://doi.org/10.1016/j.energy.2012.02.048>.
- [174] A. M. Yousef, W. M. El-Maghlany, Y. A. Eldrainy, and A. Attia. *Energy*, **156**(2018):328–351. DOI: <https://doi.org/10.1016/j.energy.2018.05.106>.
- [175] M. Shen, L. Tong, S. Yin, C. Liu, L. Wang, W. Feng, and Y. Ding. *Sep. Purif. Technol.*, **299**(2022):121734, . DOI: <https://doi.org/10.1016/j.seppur.2022.121734>.
- [176] X. b. Zhang, J. y. Chen, L. Yao, Y. h. Huang, X. j. Zhang, and L. m. Qiu. *Journal of Zhejiang University SCIENCE A*, **15**(2014):309–322, . DOI: <https://doi.org/10.1631/jzus.A1400063>.
- [177] K. Maqsood, A. Mullick, A. Ali, K. Kargupta, and S. Ganguly. *Rev. Chem. Eng.*, **30**(2014):453–477. DOI: <https://doi.org/10.1515/revce-2014-0009>.
- [178] A. F. Young, H. G. D. Villardi, L. S. Araujo, L. S. C. Raptopoulos, and M. S. Dutra. *Indust. Eng. Chem. Res.*, **60**(2021):14830–14844. DOI: <https://doi.org/10.1021/acs.iecr.1c02818>.
- [179] C. Song, Q. Liu, S. Deng, H. Li, and Y. Kitamura. *Renewable and Sustainable Energy Reviews*, **101**(2019):265–278. DOI: <https://doi.org/10.1016/j.rser.2018.11.018>.
- [180] L. Zhang, K. Ye, Y. Wang, W. Han, M. Xie, and L. Chen. *Energy*, **290**(2024):129867, . DOI: <https://doi.org/10.1016/j.energy.2023.129867>.
- [181] Y. Lee, H. Kim, W. Lee, D. W. Kang, J. W. Lee, and Y. H. Ahn. *Journal of Environmental Chemical Engineering*, **11**(2023):110933. DOI: <https://doi.org/10.1016/j.jece.2023.110933>.
- [182] A. Katare, S. Kumar, S. Kundu, S. Sharma, and L. M. Kundu. *B. Mandal, ACS Omega*, **8**(2023):17511–17522. DOI: <https://doi.org/10.1021/acsomega.3c01666>.
- [183] X. Lang, S. Fan, and Y. Wang. *Journal of Natural Gas Chemistry*, **19**(2010):203–209. DOI: [https://doi.org/10.1016/S1003-9953\(09\)60079-7](https://doi.org/10.1016/S1003-9953(09)60079-7).
- [184] P. Babu, P. Linga, R. Kumar, and P. Englezos. *Energy*, **85**(2015):261–279. DOI: <https://doi.org/10.1016/j.energy.2015.03.103>.
- [185] S. K. Viswanadhan, A. Singh, and H. P. Veluswamy. *Gas Science and Engineering*, **131**(2024):205465. DOI: <https://doi.org/10.1016/j.jgsce.2024.205465>.
- [186] J. He, Y. Liu, Z. Ma, S. Deng, R. Zhao, and L. Zhao. *Energy Procedia*, **105**(2017):4090–4097. DOI: <https://doi.org/10.1016/j.egypro.2017.03.867>.
- [187] A. Hassanpouryouzband, E. Joonaki, M. Vasheghani Farahani, S. Takeya, C. Ruppel, J. Yang, N. J. English, J. M. Schicks, K. Edlmann, H. Mehrabian, Z. M. Aman, and B. Tohidi. *Chem. Soc. Rev.*, **49**(2020):5225–5309. DOI: <https://doi.org/10.1039/C8CS00989A>.
- [188] S. Kanehashi and C. A. Scholes. *Frontiers of Chemical Science and Engineering*, **14**(2020):460–469. DOI: <https://doi.org/10.1007/s11705-019-1881-5>.

- [189] X. Li, Y. Cheng, H. Zhang, S. Wang, Z. Jiang, R. Guo, and H. Wu. *ACS Appl. Mater. Inter.*, **7**(2015):5528–5537, . DOI: <https://doi.org/10.1021/acsami.5b00106>.
- [190] T. Okumus, E. Gurkan and L. Yilmaz. *Sep. Sci. Technol.*, **29**(1994):2451–2473. DOI: <https://doi.org/10.1080/01496399408002203>.
- [191] M. T. Vu, R. Lin, H. Diao, Z. Zhu, S. K. Bhatia, and S. Smart. *J. Membr. Sci.*, **587**(2019):117157. DOI: <https://doi.org/10.1016/j.memsci.2019.05.081>.
- [192] H. Vinh-Thang and S. Kaliaguine. *Chem. Rev.*, **113**(2013):4980–5028. DOI: <https://doi.org/10.1021/cr3003888>.
- [193] R. Mahajan, R. Burns, M. Schaeffer, and W. J. Koros. *J. Appl. Polym. Sci.*, **86**(2002):881–890. DOI: <https://doi.org/10.1002/app.10998>.
- [194] Y. C. Hudiono, T. K. Carlisle, J. E. Bara, Y. Zhang, D. L. Gin, and R. D. Noble. *J. Membr. Sci.*, **350**(2010):117–123, . DOI: <https://doi.org/10.1016/j.memsci.2009.12.018>.
- [195] Y. C. Hudiono, T. K. Carlisle, A. L. LaFrate, D. L. Gin, and R. D. Noble. *J. Membr. Sci.*, **370**(2011):141–148, . DOI: <https://doi.org/10.1016/j.memsci.2011.01.012>.
- [196] M. Rezakazemi, A. Ebadi Amooghin, M. M. Montazer-Rahmati, A. F. Ismail, and T. Matsuura. *Prog. Polym. Sci.*, **39**(2014):817–861. DOI: <https://doi.org/10.1016/j.progpolymsci.2014.01.003>.
- [197] R. D. Noble. *J. Membr. Sci.*, **378**(2011):393–397. DOI: <https://doi.org/10.1016/j.memsci.2011.05.031>.
- [198] Y. Seo, Y. C. Jung, M. S. Park, and D. W. Kim. *J. Membr. Sci.*, **603**(2020):117995. DOI: <https://doi.org/10.1016/j.memsci.2020.117995>.
- [199] I. Pinnau and L. G. Toy. *J. Membr. Sci.*, **184**(2001):39–48. DOI: [https://doi.org/10.1016/S0376-7388\(00\)00603-7](https://doi.org/10.1016/S0376-7388(00)00603-7).
- [200] M. Das, A. Hazarika, N. Deka, and T. Jana. *ACS Applied Nano Materials*, **7**(2024):8081–8092. DOI: <https://doi.org/10.1021/acsanm.4c00560>.
- [201] B. Oh and Y. R. Kim. *Solid State Ionics*, **124**(1999):83–89. DOI: [https://doi.org/10.1016/S0167-2738\(99\)00129-0](https://doi.org/10.1016/S0167-2738(99)00129-0).
- [202] S. Leaper, A. Abdel-Karim, B. Faki, J. M. Luque-Alled, M. Alberto, S. M. Vijayaraghavan, A. Holmes, G. Szekeley, M. I. Badawy, N. Shokri, and P. Gorgojo. *J. Membr. Sci.*, **554**(2018):309–323. DOI: <https://doi.org/10.1016/j.memsci.2018.03.013>.
- [203] R. Castro-Munoz, V. Fila, and C. T. Dung. *Chem. Eng. Commun.*, **204**(2017):295–309. DOI: <https://doi.org/10.1080/00986445.2016.1273832>.
- [204] M. Alizamir, A. Keshavarz, F. Abdollahi, A. Khosravi, and S. Karagoz. *Sep. Purif. Technol.*, **325**(2023):124689. DOI: <https://doi.org/10.1016/j.seppur.2023.124689>.
- [205] S. Li, Y. J. Sun, Z. X. Wang, C. G. Jin, M. J. Yin, and Q. F. An. *Small*, **19**(2023):2208177, . DOI: <https://doi.org/10.1002/sml.202208177>.
- [206] C. Ma, S. Sarmad, J. P. Mikkola, and X. Ji. *Energy Procedia*, **142**(2017):3320–3325, . DOI: <https://doi.org/10.1016/j.egypro.2017.12.464>.
- [207] T. J. Trivedi, J. H. Lee, H. J. Lee, Y. K. Jeong, and J. W. Choi. *Green Chem.*, **18**(2016):2834–2842. DOI: <https://doi.org/10.1039/C5GC02319J>.
- [208] M. Francisco, A. van den Bruinhorst, and M. C. Kroon. *Angew. Chem. Int. Ed.*, **52**(2013):3074–3085. DOI: <https://doi.org/10.1002/anie.201207548>.
- [209] A. Krishnan, K. P. Gopinath, D. V. N. Vo, R. Malolan, V. M. Nagarajan, and J. Arun. *Environ. Chem. Lett.*, **18**(2020):2031–2054. DOI: <https://doi.org/10.1007/s10311-020-01057-y>.
- [210] C. A. Trickett, A. Helal, B. A. Al-Maythalony, Z. H. Yamani, K. E. Cordova, and O. M. Yaghi. *Nature Reviews Materials*, **2**(2017):17045. DOI: <https://doi.org/10.1038/natrevmats.2017.45>.
- [211] Y. Lin, C. Kong, Q. Zhang, and L. Chen. *Advanced Energy Materials*, **7**(2017):1601296, . DOI: <https://doi.org/10.1002/aenm.201601296>.
- [212] M. Vitillo, J. G. Savonnet, G. Ricchiardi, and S. Bordiga. *ChemSusChem*, **4**(2011):1281–1290. DOI: <https://doi.org/10.1002/cssc.201000458>.
- [213] Z. Xiang, S. Leng, and D. Cao. *J. Physic. Chem. C*, **116**(2012):10573–10579. DOI: <https://doi.org/10.1021/jp3018875>.
- [214] D. Wu, Q. Yang, C. Zhong, D. Liu, H. Huang, W. Zhang, and G. Maurin. *Langmuir*, **28**(2012):12094–12099. DOI: <https://doi.org/10.1021/la302223m>.
- [215] S. Gaikwad, Y. Kim, R. Gaikwad, and S. Han. *Journal of Environmental Chemical Engineering*, **9**(2021):105523. DOI: <https://doi.org/10.1016/j.jece.2021.105523>.
- [216] M. Yin, L. Wang, and S. Tang. *ACS Appl. Mater. Inter.*, **14**(2022):55674–55685. DOI: <https://doi.org/10.1021/acsami.2c18226>.
- [217] T. S. Nguyen, N. A. Dogan, H. Lim, and C. T. Yavuz. *Acc. Chem. Res.*, **56**(2023):2642–2652. DOI: <https://doi.org/10.1021/acs.accounts.3c00367>.
- [218] T. Wang, F. Liu, W. Tang, S. Xu, H. Dong, Z. Chen, and X. Gao. *Chem. Eng. J.*, **490**(2024):151426, . DOI: <https://doi.org/10.1016/j.cej.2024.151426>.
- [219] X. Shi, G. A. Lee, S. Liu, D. Kim, A. Alahmed, A. Jamal, L. Wang, and A. H. A. Park. *Mater. Today*, **65**(2023):207–226. DOI: <https://doi.org/10.1016/j.mattod.2023.03.004>.
- [220] J. Y. Yong, R. Y. Xie, Q. Huang, X. J. Zhang, B. Li, P. F. Xie, C. F. Wu, and L. Jiang. *Sep. Purif. Technol.*, **328**(2024):125018. DOI: <https://doi.org/10.1016/j.seppur.2023.125018>.
- [221] L. A. Darunte, K. S. Walton, D. S. Sholl, and C. W. Jones. *Current Opinion in Chemical Engineering*, **12**(2016):82–90. DOI: <https://doi.org/10.1016/j.coche.2016.03.002>.
- [222] P. Li, J. Chen, J. Zhang, and X. Wang. *Separation & Purification Reviews*, **44**(2015):19–27, . DOI: <https://doi.org/10.1080/15422119.2014.884507>.
- [223] H. Lin, Y. Yang, Y. C. Hsu, J. Zhang, C. Welton, I. Afolabi, M. Loo, and H. C. Zhou. *Adv. Mater.*, **36**(2024):2209073, . DOI: <https://doi.org/10.1002/adma.202209073>.
- [224] K. M. Gupta, Y. Chen, and J. Jiang. *J. Physic. Chem. C*, **117**(2013):5792–5799. DOI: <https://doi.org/10.1021/jp312404k>.
- [225] M. Kang, J. E. Kim, D. W. Kang, H. Y. Lee, D. Moon, and C. S. Hong. *J. Mater. Chem. A*, **7**(2019):8177–8183. DOI: <https://doi.org/10.1039/C8TA07965J>.
- [226] L. Xing, K. Wei, Y. Li, Z. Fang, Q. Li, T. Qi, S. An, S. Zhang, and L. Wang. *Environ. Sci. Technol.*, **55**(2021):11216–11224. DOI: <https://doi.org/10.1021/acs.est.1c02452>.
- [227] J. F. Kuringal, Y. Rachuri, A. S. Palakkal, R. S. Pillai, Y. Gu, Y. Choe, and D. W. Park. *ACS Appl. Mater. Inter.*, **11**(2019):41458–41471. DOI: <https://doi.org/10.1021/acsami.9b16834>.

- [228] J. Sun, Q. Li, G. Chen, J. Duan, G. Liu, and W. Jin. *Sep. Purif. Technol.*, **217**(2019):229–239, .
DOI: <https://doi.org/10.1016/j.seppur.2019.02.036>.
- [229] M. Ding, R. W. Flaig, H. L. Jiang, and O. M. Yaghi. *Chem. Soc. Rev.*, **48**(2019):2783–2828.
DOI: <https://doi.org/10.1039/C8CS00829A>.
- [230] D. Saha, Z. Bao, F. Jia, and S. Deng. *Environ. Sci. Technol.*, **44**(2010):1820–1826, .
DOI: <https://doi.org/10.1021/es9032309>.
- [231] H. Demir, G. O. Aksu, H. C. Gulbalkan, and S. Keskin. *Carbon Capture Science & Technology*, **2**(2022):100026.
DOI: <https://doi.org/10.1016/j.ccst.2021.100026>.
- [232] S. Bose, D. Sengupta, T. M. Rayder, X. Wang, K. O. Kirlikovali, A. K. Sekizkardes, T. Islamoglu, and O. K. Farha. *Adv. Funct. Mater.*, **34**(2024):2307478.
DOI: <https://doi.org/10.1002/adfm.202307478>.
- [233] M. Hasib-ur Rahman, M. Siaj, and F. Larachi. *Chemical Engineering and Processing: Process Intensification*, **49**(2010):313–322.
DOI: <https://doi.org/10.1016/j.cep.2010.03.008>.
- [234] F. Karadas, M. Atilhan, and S. Aparicio. *Energy Fuels*, **24**(2010):5817–5828.
DOI: <https://doi.org/10.1021/ef1011337>.
- [235] M. Ramdin, T. W. de Loos, and T. J. H. Vlught. *Indust. Eng. Chem. Res.*, **51**(2012):8149–8177.
DOI: <https://doi.org/10.1021/ie3003705>.
- [236] W. Jiang, X. Li, G. Gao, F. Wu, C. Luo, and L. Zhang. *Chem. Eng. J.*, **455**(2022):136767.
DOI: <https://doi.org/10.1016/j.cej.2022.136767>.
- [237] W. Faisal Elmobarak, F. Almomani, M. Tawalbeh, A. Al-Othman, R. Martis, and K. Rasool. *Fuel*, **344**(2023):128102.
DOI: <https://doi.org/10.1016/j.fuel.2023.128102>.
- [238] D. Hospital-Benito, J. Lemus, C. Moya, R. Santiago, and J. Palomar. *Chem. Eng. J.*, **390**(2020):124509.
DOI: <https://doi.org/10.1016/j.cej.2020.124509>.
- [239] X. Zhang, X. Zhang, H. Dong, Z. Zhao, S. Zhang, and Y. Huang. *Energy Environ. Sci.*, **5**(2012):6668–6681, .
DOI: <https://doi.org/10.1039/C2EE21152A>.
- [240] R. Zhang, Q. Ke, Z. Zhang, B. Zhou, G. Cui, and H. Lu. *International Journal of Molecular Sciences*, **23**(2022):11401, .
- [241] J. Sun, Y. Sato, Y. Sakai, and Y. Kansha. *Journal of Cleaner Production*, **414**(2023):137695, .
DOI: <https://doi.org/10.1016/j.jclepro.2023.137695>.
- [242] K. Wang, Z. Zhang, S. Wang, L. Jiang, H. Li, and C. Wang. *ChemSusChem*, **17**(2024):e202301951, .
DOI: <https://doi.org/10.1002/cssc.202301951>.
- [243] Y. Zhao, X. Wang, Z. Li, H. Wang, Y. Zhao, and J. Qiu. *J. Physic. Chem. B*, **128**(2024):1079–1090, .
DOI: <https://doi.org/10.1021/acs.jpccb.3c06510>.
- [244] J. Yang, D. Gao, H. Zhang, and Q. Yi. *Fuel*, **366**(2024):131351, .
DOI: <https://doi.org/10.1016/j.fuel.2024.131351>.
- [245] H. Karim, S. Sardar, H. Bibi, F. Perveen, M. Arfan, and A. Mumtaz. *J. Mol. Liq.*, **405**(2024):125079.
DOI: <https://doi.org/10.1016/j.molliq.2024.125079>.
- [246] A. R. Shaikh, A. Grillo, M. C. D'Alterio, J. J. Pajski, S. I. Amran, H. Karim, M. Chawla, G. Talarico, A. Poater, and L. Cavallo. *J. Mol. Liq.*, **24**(2025):127084.
DOI: <https://doi.org/10.1016/j.molliq.2025.127084>.
- [247] Z. Lei, C. Dai, J. Hallett, and M. Shiflett. *Chem. Rev.*, **124**(2024):7533–7535.
DOI: <https://doi.org/10.1021/acs.chemrev.4c00291>.
- [248] X. Yang, C. Zhu, T. Fu, and Y. Ma. *Int. J. Heat Mass Transfer*, **222**(2024):125210, .
DOI: <https://doi.org/10.1016/j.ijheatmasstransfer.2024.125210>.
- [249] S. Hussain, H. Dong, H. Duan, X. Ji, H. M. Asif, W. Liu, and X. Zhang. *Langmuir*, **40**(2024):8636–8644.
DOI: <https://doi.org/10.1021/acs.langmuir.4c00412>.
- [250] I. Roppolo, M. Zanatta, G. Colucci, R. Scipione, J. M. Cameron, G. N. Newton, V. Sans, and A. Chiappone. *React. Funct. Polym.*, **202**(2024):105962.
DOI: <https://doi.org/10.1016/j.reactfunctpolym.2024.105962>.
- [251] M. Zhang, R. Semiat, and X. He. *Sep. Purif. Technol.*, **345**(2024):127281, .
DOI: <https://doi.org/10.1016/j.seppur.2024.127281>.
- [252] Y. R. Xue, C. Liu, H. C. Yang, H. Q. Liang, C. Zhang, and Z. K. Xu. *Small*, **20**(2024):2310092.
DOI: <https://doi.org/10.1002/smll.202310092>.
- [253] Z. Turakulov, A. Kamolov, A. Norkobilov, M. Variny, Diaz-Sainz, G. L. Gomez-Coma, and M. Fallanza. *J. Chem. Technol. Biotechnol.*, **99**(2024):1291–1307.
DOI: <https://doi.org/10.1002/jctb.7606>.
- [254] P. Wang, Z. Liu, Z. Pan, J. Gonzalez-Arias, L. Shang, Y. Wang, and Z. Zhang. *Sep. Purif. Technol.*, **346**(2024):127252, .
DOI: <https://doi.org/10.1016/j.seppur.2024.127252>.
- [255] N. MacDowell, N. Florin, A. Buchard, J. Hallett, A. Galindo, G. Jackson, C. S. Adjiman, C. K. Williams, N. Shah, and P. Fennell. *Energy Environ. Sci.*, **3**(2010):1645–1669.
DOI: <https://doi.org/10.1039/C004106H>.

Abbreviations

Carbon Dioxide	(CO ₂)
Metal-Organic Frameworks	(MOFs)
Carbon Capture and Storage	(CCS)
Carbon Capture, Utilization, and Storage	(CCUS)
Direct Air Capture	(DAC)
Enhanced Rock Weathering	(ERW)
Bioenergy with Carbon Capture and Storage	(BECCS)
Cryogenic Carbon Capture	(CCC)
Graphene Oxide	(GO)
Wrinkled Graphene	(WG)
Ethylenediamine	(EDA)
Reduced Graphene Oxide	(rGO)
Carbon Nanotubes	(CNT)
Poly(AmidoAmine)	(PAMAM)
Grand Canonical Monte Carlo	(GCMC)
Temperature Swing Adsorption	(TSA)
Poly(dimethylsiloxane)	(PDMS)
3-(Aminopropyl)triethoxysilane	(APTES)
Boron and Nitrogen co-Doped Carbon Nano-material	(B/N-CNs)
Porous Graphene Materials	(PGMs)
UV-irradiated graphene oxide foam	(UV-GOF)
Single-Layered Graphene Oxide	(SLGO)
Attenuated Total Reflectance-Fourier Transform Infrared Spectroscopy	(ATR-FTIR)
Ideal Adsorbed Solution Theory	(IAST)
Adsorption Performance Indicator	(API)
Pressure Swing Adsorption	(PSA)
Sodium Dodecyl Sulfate	(SDS)
Mixed Matrix Membranes	(MMMs)
hexagonal Boron Nitride	(h-BN)
in-plane h-BN/graphene	(P-BN/G)
glass Transition Temperature	(T _g)
Density Functional Theory	(DFT)
Molecular Dynamics	(MD)
Hyperbranched Polyethylenimine	(HPEI)
Chemical Vapor Deposition	(CVD)
diglycolamine	(DGA)
2-amino-2-methylpropanol	(AMP)
Methyldiethanolamine	(MDEA)
Monoethanolamine	(MEA)
Post-Combustion Carbon Capture	(PCCC)
Hydrate-Based Gas Separation	(HBGS)
Low-Transition Temperature Mixtures	(LTTMs)
Deep Eutectic Solvents	(DESS)
Task-Specific Ionic Liquids	(TSILs)